UNIVERSITY OF SOUTHAMPTON

SCHOOL OF OCEAN AND EARTH SCIENCE

Lab-on-a-chip technology for *in situ* molecular analysis of marine microorganisms

by

Christos-Moritz Loukas

Thesis for the degree of doctor of Biology / Bioelectronics

March 2016

UNIVERSITY OF SOUTHAMPTON

ABSTRACT

In situ monitoring of ocean biology is typically done in the form of sample collection during ship based cruises or other field expeditions, and sample analysis either on-board the ship or in a laboratory at a later time. However such expeditions can be expensive, labour intensive, and only follow pre-defined courses and locations. Alternative methods are used and in development in an effort to provide flexibility and reduced costs. Molecular methods are valuable tools in ecological studies, offering high specificity, reliability and excellent limits of detection. Techniques including polymerase chain reaction (PCR) and nucleic acid sequence based amplification (NASBA) are now routinely used for the monitoring of microorganisms in water (e.g. pathogens, biotoxins and viruses). The use of these techniques, however, is time consuming, costly, and requires substantial training and specially adapted laboratories, making them impractical in many field applications or where infrastructure is limited.

Recent advances in microfluidic research have demonstrated that molecular techniques (e.g. qPCR, NASBA) can be applied on lab-on-a-chip (LOC) systems for the *in situ* detection of target organisms or biomarkers in natural waters. Microfluidic devices (i.e. LOC systems) can automatically perform multiple laboratory functions on a single integrated and compact chip. NASBA is particularly attractive for LOC applications targeting RNA, because it is an isothermal amplification assay and does not require complex microfluidic systems. A NASBA assay, targeting toxic microalgae *Karenia brevis*, has been successfully automated using a LOC-based, bench-top sensor "LabCardReader" here at the National Oceanography Centre of Southampton (NOCS).

The purpose of this work has been to develop and optimise a fully automated molecular assay on a novel lab-on-a-chip system, which performs RNA-based amplification, for the detection and quantification of marine microorganisms. This PhD provides significant developments in the field of lab-on-chip technology, as well as *in situ* sample collection and processing for harmful algal bloom (HAB) monitoring. This thesis reports on (1) the optimisation of an internal control (IC) NASBA assay for the detection and quantification of microorganisms while examining the validity of the technique under varying physiological states and growth conditions; (2) the long-term preservation and storage of NASBA reaction components; (3) the development of a fully automated, fully preserved, lab-on-a-chip-based IC-NASBA protocol for real-time detection and quantification of microorganisms; (4) the development of a simple, rapid, and reliable sample collection and concentration method, aimed for *in situ* application and compatibility with nucleic acid analysis techniques.

FACULTY OF OCEAN AND EARTH SCIENCE

Ocean Technology and Engineering

Thesis for the degree of Doctor of Philosophy

Lab-on-a-chip technology for *in situ* molecular analysis of marine microorganisms

Christos-Moritz Loukas

Table of Contents

List of Tables

List of Figures

DECLARATION OF AUTHORSHIP

I, Christos-Moritz Loukas

declare that this thesis and the work presented in it are my own and has been generated by me as the result of my own original research.

Lab-on-a-chip technology for *in situ* molecular analysis of marine microorganisms

I confirm that:

1. This work was done wholly or mainly while in candidature for a research degree at the University of Southampton;
2. Where any part of this thesis has previously been submitted for a degree or any other qualification at this University or any other institution, this has been clearly stated;
3. Where I have consulted the published work of others, this is always clearly attributed;
4. Where I have quoted from the work of others, the source is always given. With the exception of such quotations, this thesis is entirely my own work;
5. I have acknowledged all main sources of help;
6. Where the thesis is based on work done by myself jointly with others, I have made clear exactly what was done by others and what I have contributed myself;
7. Parts of this work have been published as:
    - "*Real-time isothermal RNA amplification of toxic marine microalgae using preserved reagents on an integrated microfluidic platform*" by M.-N. Tsaloglou, F. Laouenan, C.-M. Loukas, L. G. Monsalve, C. Thanner, H. Morgan, J. M. Ruano-López and M. C. Mowlem. (*published in Analyst* **2013,** *138*, (2), 593-602)

Signed: .....

Date: .....

Dedication

I would like to dedicate this PhD first and foremost to Gerlinde Winter (geb. Weiler), who inspired me to follow this path in academia and carry out the degree.

"Einen Teil unseres Lebens durften wir gemeinsam gehen"

I would also like to dedicate this PhD to Werner Winter, Alexandra Winter, Georgios Loukas, Timothy Loukas, Richard Winter, and Irina Winter. I wouldn't be the person I am today without them, as they have consistently encouraged and supported me over the course of my life, granting me the drive to follow my dreams and motivating me to strive for greatness.

Acknowledgements

I would like to express my great thanks to my primary supervisor, Professor Matthew Mowlem, and to my secondary supervisors, Doctor Nicolas Green, Doctor Maria-Nefeli Tsaloglou, and Professor Debora Iglesias-Rodriguez for their guidance, encouragement, and support during my PhD. Funding and support by EU FP7 LABONFOIL project 224306 and the Natural Environmental Research Council.

Definitions and Abbreviations

This nomenclature is in alphabetical order and includes the page number where the abbreviations are first referenced:

AMV-RT
avian myoblastosis virus reverse transcriptase.....9

BIP
backward inner primer.....12

C
cytosine.....8

CFP
Christos-Moritz Loukas.....22

CML
Christos-Moritz Loukas.....29

COC
cyclo-olefin copolymer.....26

CT
Christine Thanner.....29

Ct
threshold cycle.....39

cDNA
complementary DNA.....8

DGGE
denaturing gradient gel electrophoresis.....14

DNA
deoxyribonucleic acid.....4

DNase
deoxyribonuclease.....9

dNTP
deoxynucleotide.....7

DSP
diarrheic shellfish poisoning.....22

E. coli
Escherichia coli.....26

ESP
Environmental Sample Processor.....26

FIP
forward inner primer.....12

FISH
fluorescence *in situ* hybridisation.....15

FL
Florian Laouenan.....29

G
guanine.....8

HAB
harmful algal bloom.....22

HDA
helicase-dependent amplification.....2

IC
internal control.....2

K. brevis
Karenia brevis.....3

K. mikimotoi
Karenia mikimotoi.....29

LAMP
loop-mediated isothermal amplification.....2

LOC
lab-on-a-chip.....2

MNT
Maria-Nefeli Tsaloglou.....29

mRNA
messenger RNA.....4

NASBA
nucleic acid sequence-based amplification.....2

NG
Nicolas Green.....29

NSP
neurotoxic shellfish poisoning.....22

PCR
polymerase chain reaction.....2

PDMS
Polydimethylsiloxane 26

PKS
polyketide synthesis.....48

PMMA
poly(methyl methacrylate).....26

Chapter 1: Introduction

Chapter 1

Marine biology is an interdisciplinary study of life in the world's oceans, estuaries, and inland seas (Thakur et al. 2008). Over the years, it has witnessed significant growth in the application of molecular techniques and as a result, new fields of investigation have opened, and previous studies have been re-evaluated (Burton 1996). Thus, the discipline of marine molecular biology has emerged, and is constantly evolving while trying to solve problems regarding the exploration of marine organisms for human health and welfare purposes (Thakur et al. 2008). The aim of this PhD is to provide innovations leading to the development of a biological sensor, and in particular to optimise the biosensor assay for use in a "Lab-on-a-Chip" (LOC) format. This will incorporate work on four major fronts: (1) the optimisation of an internal control (IC) nucleic acid sequence based amplification (NASBA) assay for the detection and quantification of microorganisms while examining the validity of the technique under varying physiological states and growth conditions (see Chapter 2:); (2) the long-term preservation and storage of NASBA reaction components (see Chapter 3:); (3) the development of a fully automated, fully preserved, lab-on-a-chip-based IC-NASBA protocol for real-time detection and quantification of microorganisms (see Chapter 4:); (4) the development of a simple, rapid, and reliable sample collection and concentration method, aimed for *in situ* application and compatibility with nucleic acid analysis techniques (see Chapter 5:).

Regarding the first objective (IC-NASBA optimisation), an appropriate molecular tool was chosen and optimised for the detection of potentially harmful marine microorganisms. Requirements for the method included reliability, sensitivity, and specificity. NASBA (see section 1.1.2.2) met the above requirements and was preferred amongst other molecular techniques for reasons that will be discussed further in this thesis. These include low temperature operation (maximum 65^{o}C), compared to equivalent techniques, and no need for thermal cycling which greatly eases the engineering challenge when converting to LOC. In addition NASBA primer design is significantly simpler compared to other molecular techniques, such as loop-mediated isothermal amplification (LAMP; see section 1.1.2.4), and does not require additional reverse transcription steps for RNA amplification, contrary to polymerase chain reaction (PCR; see section 1.1.2.1) and helicase-dependent amplification (HDA; see section 1.1.2.3) methods. To transform this otherwise qualitative assay to a method that enables quantitation, an internal control (IC) was added and optimised (IC-NASBA), with a few variations to what has been described in literature; namely IC RNA addition was integrated in a sample RNA extraction protocol. This provided real-time calibration of the assay, which is otherwise variable in time, in response to sample matrices, and with reagent and extraction buffer batch. Subsequently, a series of experiments were undertaken to assess the reliability of IC-NASBA, which tested the potential effects of different growth conditions on phytoplankton cultures (Chapter 2).

Preservation of reagents, and enzymes form another significant section in the development of the biological sensor. This work is reported in detail within Chapter 3 of this thesis. The product of the European LABONFOIL project[1], named "LabCardReader" (see section 4.2.7), and future devices in development at Southampton are intended to perform IC-NASBA in an automated fashion, while requiring minimal input from its user. However, reagents are easily affected by environmental factors and tend to be prone to degradation when unprotected and exposed to temperatures over 4°C. NASBA reagents and enzymes are currently purchased as lyophilised spheres, and in order for them to become functional, they need to be rehydrated into a solution that has a one-hour lifetime. Therefore, if field deployable automated devices are to be used over long time periods this limitation must be overcome. One tactic is to prepare and preserve reagents in advance of deployment, e.g. by lyophilisation or storage in gels on chip. Both approaches were developed in this project.

As indicated by the thesis title, the main aim of this PhD was to develop and optimise LOC technology, for the detection and quantification of marine microorganisms. Chapter 4 presents a fully automated IC-NASBA assay on a novel LOC system, the LabCardReader, for the detection and quantification of toxic microalgae. The LabCardReader, performed real-time IC-NASBA on *Karenia brevis* (*K. brevis*) using preserved reagents and enzymes on disposable plastic cartridges. The presented method provided simple, rapid, precise and accurate detection and quantification of microbial RNA, making the LabCardReader a viable option for in-field monitoring of HABs, and otherwise toxic or harmful microorganisms.

Harmful microorganisms, such as the toxic marine dinoflagellate *K. brevis*, are capable of having adverse effects on human health starting from concentrations as little as 5 cells mL^{-1} (Bricelj et al. 2012). This is at odds with the volume of fluid typically analysed by LOC devices (typically a few microlitres). Reliable *in situ* detection of low cell concentrations with potential LOC-based detectors may therefore require robust collection methods, and pre-concentration of sample material. This motivated the development of a filtration system which concentrates cells from several litres of environmental seawater into a single filter, while removing unwanted particles that may interfere with sensor functionality. The results of this study are presented in Chapter 5.

[1] The LABONFOIL project was funded by the European Commission and aimed to develop low-cost LOC technologies, without compromising time response, sensitivity, and simplicity of use. The project was co-ordinated by Ikerlan (Mondragon, Spain), and the Sensors Group at the National Oceanography Centre of Southampton was in charge of development for environmental applications; other applications included human health and food testing. A significant portion of the development was done in the form of this PhD. For more information on the LABONFOIL project, visit www.labonfoil.eu

To provide the necessary background for this multidisciplinary development of a biological sensor system, it is important to examine: some of the molecular tools used in marine biology; preservation methods for molecular assays used for marine applications; and microfluidic nucleic acid analysers and their incorporation in marine molecular biology. A literature review on the state-of-art follows in the next section.

1.1 Molecular tools and applications

Following sample collection and concentration (a topic covered in Chapter 5:), molecular tools applied to nucleic acids for environmental applications have 3 key steps: 1) cell lysis and nucleic acid extraction; 2) amplification; and 3) detection. Steps 2 and 3 are frequently performed synchronously. Detection includes analysis of amount of amplified product (amplicon) and more detailed analysis such as separation and fingerprinting analysis techniques. These steps are reviewed below together with reviews of clone library technologies (used to amplify and store nucleic acids), microarrays (a multiplexed detection method) and long term reagent storage (essential for field deployed biosensors).

1.1.1 Cell lysis and nucleic acid extraction

The strength of many molecular assays is ultimately affected by the quality (purity and stability) and amount of nucleic acids extracted from the target sample (Simister et al. 2011). The first step in achieving this, the breaking down of a cell (lysis), is typically achieved via mechanical, chemical or enzymatic approaches, or a combination of those, which ultimately lead to, depending on the cellular characteristics of the target organism, a plethora of nucleic acid extraction and purification techniques have been developed. These techniques refer to the processes followed for the acquisition of genetic material from within the cell, and include breaking of cell walls (lysis), removal of contaminants (washing), and re-suspension/collection of target material (elution). Extraction of deoxyribonucleic acid (DNA) and ribonucleic acid (RNA) is largely similar for many methods, but due to the approach of this PhD and the nature of the chosen amplification method (i.e. NASBA) this section will focus on cell lysis and RNA extraction.

Cells contain several types of RNA, including mRNA, rRNA, tRNA, snRNA[2] (Alberts et al. 2013; Stewart et al. 1977) and additional non-coding RNAs, each having its own function and role

[2] Messenger RNA (mRNA) determines the sequence of amino acids in polypeptide chains, and is regarded as a carrier of information from the genome. Ribosomal RNA (rRNA) is a component of each ribosome subunit, when combined with a variety of proteins, and is thus involved in protein production. Transfer RNA (tRNA) plays a vital role in protein synthesis, as it is responsible for the acceptance and transfer of amino acids.

throughout the life of the cell. Out of the above, mRNA plays a central role in the flow of information leading to protein production from DNA (Moore 2005; Muller-McNicoll and Neugebauer 2013) and therefore it is commonly targeted during amplification techniques in molecular biology. The acquisition of total RNA from cellular targets is often troublesome due to a variety of factors, such as the chemical instability of mRNA which is susceptible to enzymatic degradation by a family of enzymes, collectively termed ribonucleases (RNases); RNases are typically present in cells, contributing to RNA processing and degradation, and persist in the environment (Bonnin and Bouloc 2015; Costa et al. 2004).

Nucleic acids are polar, due to oxygen and nitrogen atoms in the backbone acting as hydrogen-bond acceptors, making them soluble in water; water molecules form hydration shells with the nucleic acids through dipole-dipole interactions, separating groups of nucleic acids from one another and allowing to remain suspended in solution (Chuprina et al. 1991). Precipitation out of solution is achievable when introducing a solvent of a lower dielectric constant[3] than water, which will increase the attraction between cations and the negatively charged nucleic acids (Flock et al. 1996). The salvation shells surrounding the nucleic acid chains cease to exist, neutralising them, and rendering them out of solution in the form of precipitants.

In the following, a few RNA extraction methods will be reviewed, including the "Boom" extraction technique, the commercial RNeasy extraction kit, and Trizol®-based extraction. RNA destined for molecular analysis typically follows a form or variation of the Boom nucleic acid extraction technique (Berensmeier 2006; Boom et al. 1990; Hofmann and Mader 2015; Valledor et al. 2014). It typically involves a chaotropic agent[4], such as guanidinium thiocyanate, as well as lipases[5] and detergent[6] for the lysis and nuclease-inactivation of samples. Due to its strong ionic strength, the chaotrope in turn induces binding of the negatively charged nucleic acids to negatively charged silica (Boom et al. 1990; Valledor et al. 2014), typically on magnetic beads (Berensmeier 2006; Hofmann and Mader 2015), or glass particles (Melzak et al. 1996) with the formation of salt bridges; when the chaotropic salt is at sufficient concentration, and optimal pH levels are achieved in the presence of buffers, the existing hydration shells surrounding the nucleic acids are

---

Small nuclear RNA (snRNA) is found within the cellular nucleus and is primarily associated with precursors of other RNA species.

[3] The dielectric constant (ε) of a solvent refers to its relative permittivity, as a measure of its polarity and its ability to insulate charges within it and from itself and another solute.

[4] Chaotropic agents are molecules that disrupt the hydrogen bonding network between molecules, reducing the stability of the native state of proteins and enzymes. They are typically used in molecular biology to destroy the three-dimensional structure of proteins and inhibit RNases.

[5] Lipases are enzymes that catalyse the hydrolysis of fats and lipids, effectively breaking them down.

[6] Detergents are typically used to lyse cells, as they disrupt cell membranes by breaking associations between proteins and lipids, and release intracellular material in a soluble form.

disrupted by the chaotrope, allowing positively charged ions to link the negatively charged nucleic acid backbone with the negatively charged chosen adsorption material (i.e. form salt bridges). Washing buffers are subsequently employed in order to remove remaining unbound molecules including proteins, salts and cellular debris that would otherwise interfere with the assay. These buffers have a high salt concentration, and thus the previously formed salt bridges are maintained. The bridges are finally broken through the application of a low-salt aqueous buffer, allowing the nucleic acids to be eluted and then stored or analysed according to personal preference.

Commercial RNA extraction kits and reagents are often employed in research involving nucleic acid analysis. **The RNeasy Mini Kit** (QIAGEN, Hilden, Germany), for instance, is a licensed product which allows users to rapidly purify high-quality total RNA from cells, tissues, and yeast. Similarly to the Boom extraction technique, this method utilises a high-salt buffer, containing guanidine thiocyanate, for lysis and RNase inactivation. Ethanol (70%) is subsequently added to instigate binding of RNA molecules to a silica matrix, as it increases attraction between phosphate groups of the RNA backbone and positive ions derived from the salt, thus leading to the formation of strong ionic bonds between them and precipitation of nucleic acids, while other molecules are washed away. Elution of the bound molecules is achieved with the addition of water, which cancels the ethanol-provided binding conditions. **TRIzol®-based RNA extraction** (Thermo Fisher Scientific, Inc.) utilises a buffer containing phenol and guanidine isothiocyanate to perform cell lysis. It dissolves cell components, and inactivates RNases (thus protecting any RNA molecules). Under acidic conditions and with the addition of chloroform, the solution can be separated into an organic and an aqueous phase; RNA remains exclusively in the latter, whereas DNA and proteins are situated in the inter phase and the organic phase (Simms et al. 1993). The nucleic acid molecules can finally be recovered via precipitation techniques in the aqueous phase, once this has been separated from the other phases, for example by ethanol or isopropanol precipitation (Tan and Yiap 2009).

1.1.2 Nucleic acid amplification methods

This section aims to provide the reader with a better insight of some molecular tools commonly used for nucleic acid amplifications. These include the widespread thermocycling-based PCR, as well as a number of isothermal amplification methods, such as NASBA, HDA, and LAMP. These methods were examined and considered for integration in the LOC platform presented in this thesis, and NASBA was ultimately chosen as the preferred assay.

1.1.2.1 **Polymerase chain reaction**

Polymerase chain reaction (PCR) (Fykse et al. 2012; Henson and French 1993; Zehr et al. 2008) is a powerful method for qualitative and quantitative nucleic acid analysis (Figure 1). It is performed on a single or double stranded DNA template, and for the reaction process to take place, two oligonucleotide primers, a heat-stable polymerase (usually Taq polymerase), metal ion co-factors, and deoxynucleotides (dNTPs) are needed (Kubista et al. 2009).

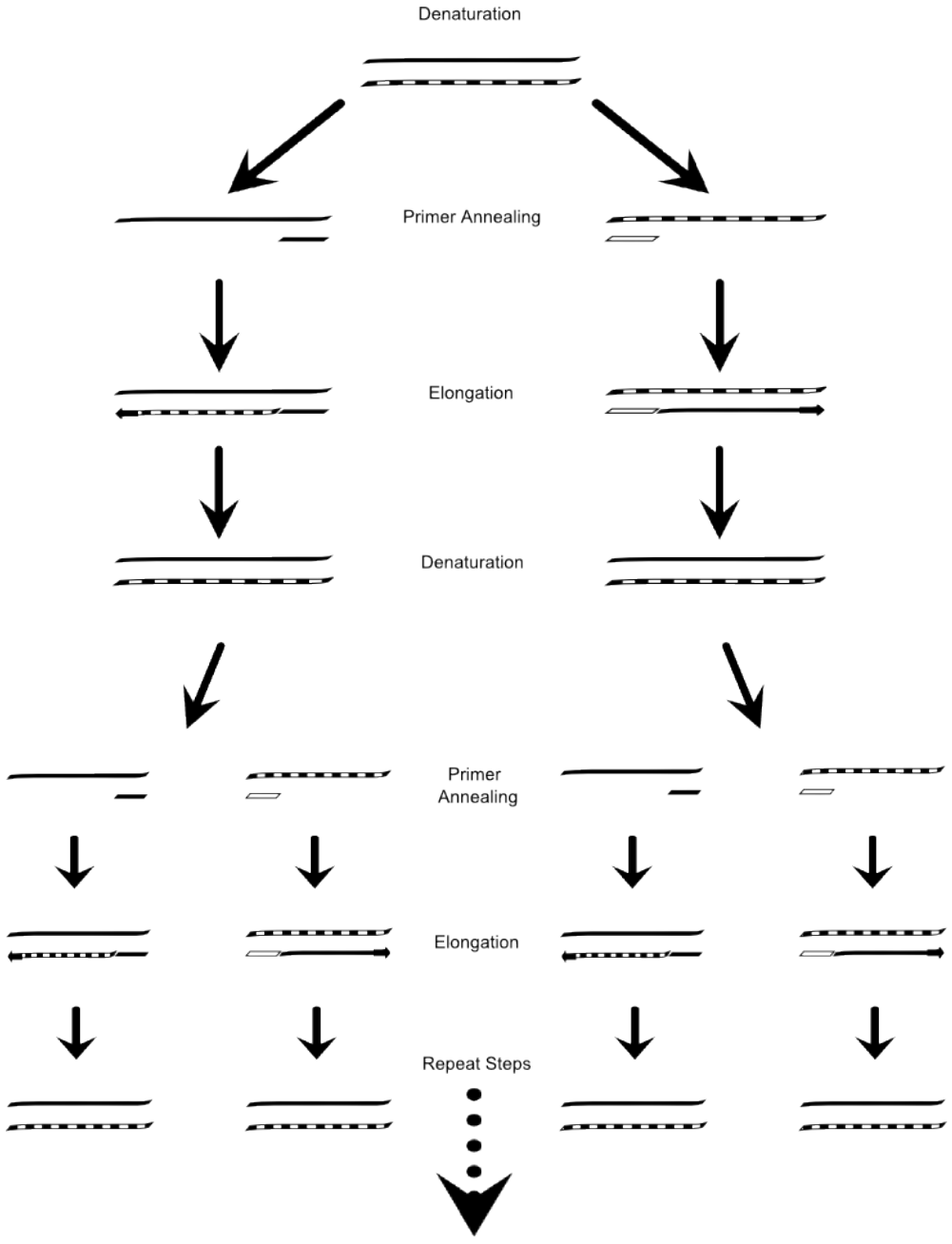

Figure 1 Schematic representation of the different stages during PCR amplification. The cyclic process starts with temperature-induced denaturation of the double-stranded DNA sequence. Primer annealing occurs at a lower temperature followed by primer elongation, which is catalyzed by Taq polymerase. The process is repeated, leading to the doubling of the product at the end of each cycle.

It involves temperature cycling which is divided into three major steps: denaturation of double stranded DNA at high temperature (typically 95°C), primer annealing at a lower temperature (dependent on the primer sequence and resulting base pairing), and primer extension (at a temperature that it optimal for the activity of the polymerase) (Schochetman et al. 1988). In the denaturation step the hydrogen bonds that hold together the duplex DNA strands are broken via heating. The temperature increase required generally depends on the sequence of the target template, but usually ranges between 95°C and 100°C, guanine-cytosine (G-C) rich sequences typically requiring a higher temperature. Once the denaturation step is complete, the PCR mixture is cooled to permit primer annealing to the 5' and 3' side of the target template. The annealing temperature varies, as it should be a few degrees below the melting temperature of the chosen primers. After this stage, Taq polymerase catalyses primer elongation and a complimentary strand of the DNA template is formed. This product is termed the amplicon. The recommended temperature for optimal polymerase efficiency is approximately 72°C, but elongation during PCR has been reportedly performed at 60°C as well (De Regge et al. 2012; Holland et al. 1991; Kubista et al. 2009). The process is repeated by cycling the temperature sequentially through that required for denaturation, annealing and elongation. The number of DNA strands is, in theory, doubled at the end of each cycle, and typically repeated 20-40 times. PCR can also be applied for RNA amplification, with the addition of an initial reverse transcription step (Cheung et al. 2010; De Regge et al. 2012; Delaney et al. 2011). A complementary DNA (cDNA) copy of the original RNA target is produced through the employment of reverse transcriptase, and will then be used for the cyclic PCR reaction.

Real-time monitoring of PCR, also known as quantitative PCR (qPCR), can be achieved with the use of interchelating dyes or more sophisticated reporting methods such as Taqman probes, DNA-binding dyes, and molecular beacons (Arya et al. 2005; Heid et al. 1996); the strength of the generated fluorescent signal is proportional to the amount of product formed (Arya et al. 2005). PCR has also been further developed to detect and quantify RNA with the incorporation of a reverse transcription step (RT-PCR) (De Regge et al. 2012; Weis et al. 1992). The most common enzymes employed in this procedure are avian myeloblastosis virus reverse transcriptase, and Moloby murine leukaemia virus reverse transcriptase (Brooks et al. 1995). The target RNA template is transcribed into cDNA, and can be either stored for future analysis, or used for a PCR assay as previously described. PCR is a simple, yet powerful method and possesses high sensitivity and specificity, and it is capable of detecting and amplifying as little as a single target molecule in a complex mixture (Henson and French 1993). The preference of PCR as a molecular tool is also related to the relatively low cost of reagents and primer synthesis. Nonetheless, it suffers from

drawbacks, such as high energy consumption as a result of the large temperature variation required during the procedure, and the increased risk of contamination when multiple reagent addition steps are required. PCR is also prone to nuclease degradation, from deoxyribonucleases (DNases). Furthermore, reverse transcriptase PCR is accompanied by sensitivity, reproducibility and RNA-related issues, making it in some cases unreliable (Bustin 2000). For instance, efficiency of the reverse transcription and PCR steps may show significant variation during each run, even if the same sample source is analyzed (Ferre 1992).

1.1.2.2 **Nucleic acid sequence-based amplification**

Nucleic acid sequence-based amplification (NASBA) is an isothermal (41°C) transcription-based RNA amplification system, and has been used for clinical, environmental, and food testing applications. NASBA was first developed by Compton (Compton 1991), incorporates two target specific primers and is catalyzed by an enzyme mixture containing T7 RNA polymerase, avian myoblastosis virus reverse transcriptase (AMV-RT), as well as ribonuclease H (RNaseH) (Walker et al. 2005).

The reaction initiates with the attachment of a primer which encompasses a promoter binding site for T7 RNA polymerase (an enzyme which catalyses RNA formation from a DNA template), in an inverted (antisense) orientation, to the target RNA molecule (Figure 2). The AMV-RT then elongates the primer resulting in the formation of a RNA/cDNA hybrid; AMV-RT is an RNA-directed DNA polymerase, which can synthesize a complementary DNA strand initiated from a primer using RNA or single-stranded DNA as a template. RNaseH, which only degrades RNA in an RNA/DNA duplex, recognises the hybridised molecule and degrades the RNA chain, leaving only the single-stranded cDNA. The second primer then anneals to the cDNA and a double stranded, transcription-active DNA sequence is catalysed by AMV-RT. T7 RNA polymerase can then recognise the promoter sequence in its 3'-5' (sense) orientation, and produces multiple RNA copies, complementary (antisense) to the original target molecule. At this point, NASBA enters a cyclic phase. The second primer binds to the antisense RNA product, followed by elongation with AMV-RT and resulting to the formation of a RNA/cDNA hybrid. RNaseH then degrades the RNA chain, allowing the first primer to bind to the single stranded cDNA. The primer is elongated via AMV-RT activity, and a double stranded DNA sequence is formed once again, containing a T7 RNA polymerase binding site. T7 RNA polymerase recognises the site, proceeds to produce more antisense RNA copies, and the cycle is repeated. Real-time detection or RNA amplification can be achieved when incorporating **molecular beacons**: nucleic acid probes which emit a fluorescent signal upon hybridization with their targets (X. Fang et al. 2002; Leone et al. 1998; Sidoti et al. 2012; Tyagi and Kramer 1996). Molecular beacons consist of a sequence complementary to the

target molecule, embedded within two unrelated, complementary arm sequences which have a fluorophore and a quencher attached to their ends. The stem formed by the hybridization of the arm sequences naturally keeps the fluorophore in close proximity to the quencher, causing fluorescence energy to be absorbed by the latter. When a target molecule is present, the probe hybridizes with the target which causes it to unfold thus allowing the fluorophore to move away from its quencher, and a greatly increased fluorescent signal is emitted. Consequently, the fluorescence of the solution is linearly related to the concentration of the target present at each point in time.

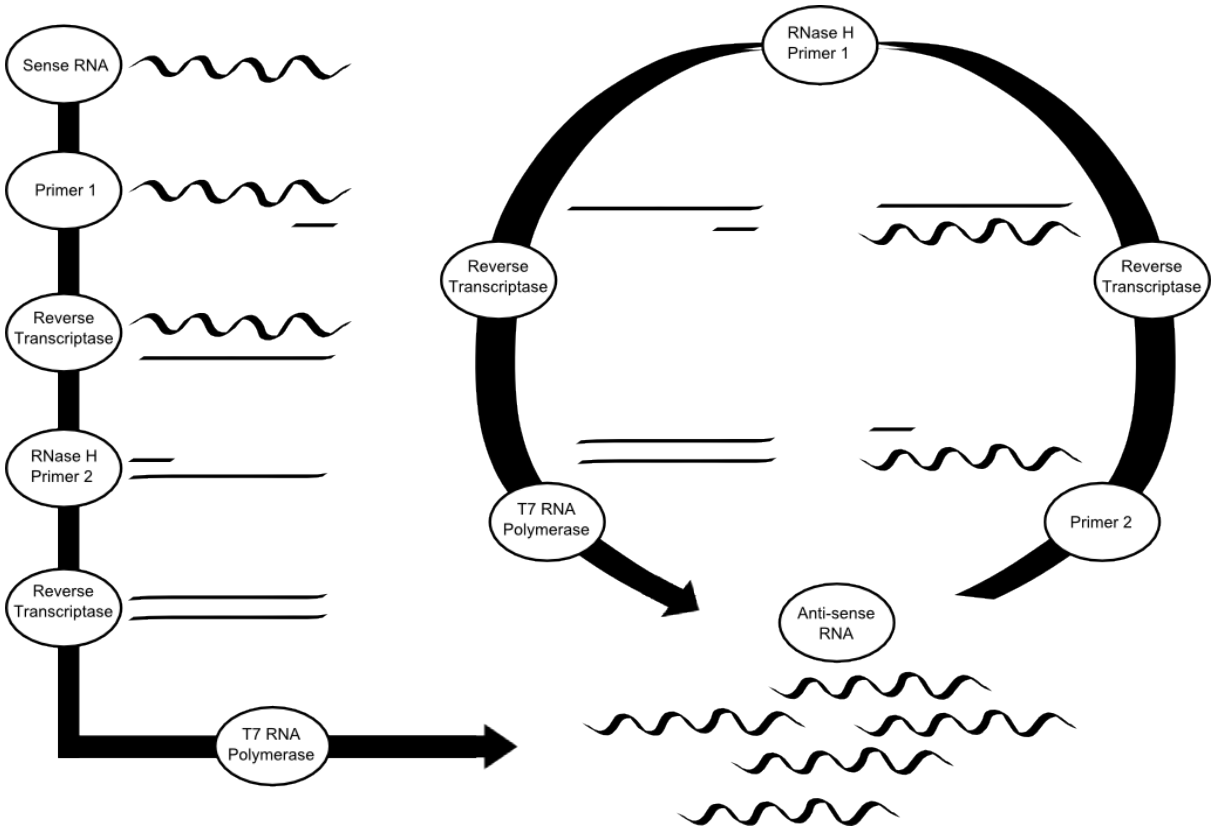

Figure 2 Schematic representation of NASBA amplification. The straight arrow represents the initiation phase and the circular arrow represents the cyclic phase. The activities of reverse transcriptase, RNase H, T7 RNA polymerase, and primer binding are indicated. The sequence of the T7 RNA polymerase product amplified in the cyclic phase, is complementary to that of the target nucleic acid.

Due to the nature of the NASBA cyclic and non-cyclic phase and the requirements of the three incorporated enzymes, results often show significant variability, rendering them unquantifiable. This is to be expected, as each separate enzyme has its own kinetic parameters, and samples extracted from different sources may introduce inhibitors, affecting overall reaction kinetics (Patterson et al. 2005). The introduction of an internal control (IC) overcomes this issue (Casper et al. 2004; Patterson et al. 2005; Ulrich et al. 2010); a synthetic IC RNA molecule, of known concentration is amplified in tandem with the target “wild-type” RNA, allowing for direct

comparison and estimation of original target RNA concentration. IC-NASBA can thus be used for the detection and quantification of microorganisms, as an alternative to qPCR, by targeting a conservatively expressed gene.

NASBA has also been successfully applied for the amplification of DNA on a variety of targets, including hepatitis B virus, herpes simplex virus and methicillin resistant *Staphylococcus aureus* (Deiman et al. 2008). In this case, the target DNA is digested with a restriction enzyme prior to amplification; restriction enzymes, also known as restriction endonucleases, are enzymes which cut DNA molecules at or near specific nucleotide sequences (restriction sites). The first primer is designed so that binding with the target sequence will take place directly upstream of the digestion. Once this stage is completed, the remaining NASBA enzymes are added to the mixture (i.e. AMV-RT, RNaseH, T7 RNA polymerase), and the previously described NASBA non-cyclic and cyclic phases ensue. The reaction unfolds in a similar fashion to RNA NASBA, albeit with a single stranded DNA molecule to begin with, and a series of single stranded RNA amplicons are generated.

NASBA is suitable for analyzing a range of nucleic acids, including mRNA, rRNA, ssDNA (Leone et al. 1998) and apart from high specificity it offers a number of other advantages. For instance, like other isothermal approaches (such as HDA or LAMP; see 1.1.2.3; 1.1.2.4) NASBA does not involve thermocycling (unlike PCR), it also offers direct amplification of RNA, without the need of additional reverse transcription steps (Leone et al. 1998; Walker et al. 2005). Furthermore, the amplification of RNA or DNA products is bi-exponential, and results can be acquired within 90 minutes of process initiation (Leone et al. 1998). The main disadvantage of NASBA rises from the integrity of RNA samples, which can be compromised through exposure to nucleases. Finally, due to the thermolabile nature of enzymes used, the reaction must not exceed 42°C, otherwise the characterising bi-exponential shape of the amplification curve may change as a result of enzyme degradation or inactivation (Deiman et al. 2002; Walker et al. 2005). This could be potentially avoided with the use of thermo-stable enzyme alternatives (Deiman et al. 2002; Sugiyama et al. 2009), which would also shorten the set up time of NASBA by omitting the secondary, separate, primer annealing step.

1.1.2.3 **Helicase-dependent amplification**

Other than NASBA, there are more isothermal nucleic acid amplification techniques. DNA has been successfully amplified under isothermal conditions (37°C) while employing helicase-dependent amplification (HDA) (Eckert et al. 2014; Faron et al. 2015; Motré et al. 2011; Vincent et al. 2004). The reaction starts with the separation of the DNA double helix through DNA helicase activity. This class of enzymes unwinds double stranded DNA molecules by separating base pairs,

while using nucleoside hydrolysis as an energy source, and is stimulated by single-stranded DNA-binding proteins (LeBowitz and McMacken 1986). Two target-specific primers subsequently bind to the separated DNA strands, followed by DNA-polymerase-dependent elongation. The newly formed molecules are separated once more by DNA helicases, thus allowing for another round of primer binding and extension. The pattern is repeated and a continuous chain of reactions will unfold, leading to exponential amplification of the target sequence. HDA follows a simple reaction scheme, similar to PCR, while remaining a true isothermal reaction by excluding the need for thermocycling. However, it requires an additional reverse transcription step for RNA amplification, contrary to NASBA.

1.1.2.4 **Loop-mediated isothermal amplification**

Loop-mediated isothermal amplification (LAMP) is another nucleic acid amplification method that does not require thermocycling (Notomi et al. 2000; Notomi et al. 2015). It consists of three major stages, including a starting material producing step, a cycling amplification step, and an elongation and recycling step. LAMP employs four target-specific primers that recognise six distinct sequences of the desired DNA molecule, and are separated into inner and outer primers. The inner primers contain sequences for the sense and antisense sequence of the target DNA, as they are involved in both the first and later stages of LAMP, and are referred to as forward inner primer (FIP) and backward inner primer (BIP).

The reaction initiates with the employment of all four primers and DNA polymerase, while incubated at 65°C. As illustrated on Figure 3 (Notomi et al. 2000) FIP hybridizes to F2c and a complementary strand is synthesised. One of the outer primers subsequently hybridizes to F3c and strand displacement DNA synthesis takes place, thus releasing a FIP-linked complementary strand. In a similar fashion, BIP and the remaining outer primer initiate complementary DNA synthesis and displacement DNA synthesis at B2c and B3c accordingly. A dumb-bell DNA structure is formed, which is converted to a stem-loop DNA through self-primed synthesis; this finalizes the LAMP starting material producing step. During the LAMP cycling step, FIP hybridizes to the loop of the stem-loop molecule and induces strand displacement DNA synthesis. This leads to the generation of an intermediate one gapped stem-loop DNA with an inverted copy of the target sequence in the stem, as well as a loop formed at the opposite end through the BIP sequence.

Self-primed strand displacement DNA synthesis takes place, which forms a complementary structure of the original stem-loop DNA as well as a gap repaired stem-loop DNA with a stem elongated to twice as long, including a loop at the opposite end. Both of them provide a template for the strand displacement reaction in the following cycles, induced by BIP. A part of this reaction is designated as the elongation and recycling step of LAMP, and leads to 3-fold amplification of

the target sequence for every half cycle. The final products of LAMP include a combination of stem-loop DNA molecules with varying lengths, and structures characterized by multiple loops, as a result of annealing between alternately inverted repeats of the target sequence in the same strand.

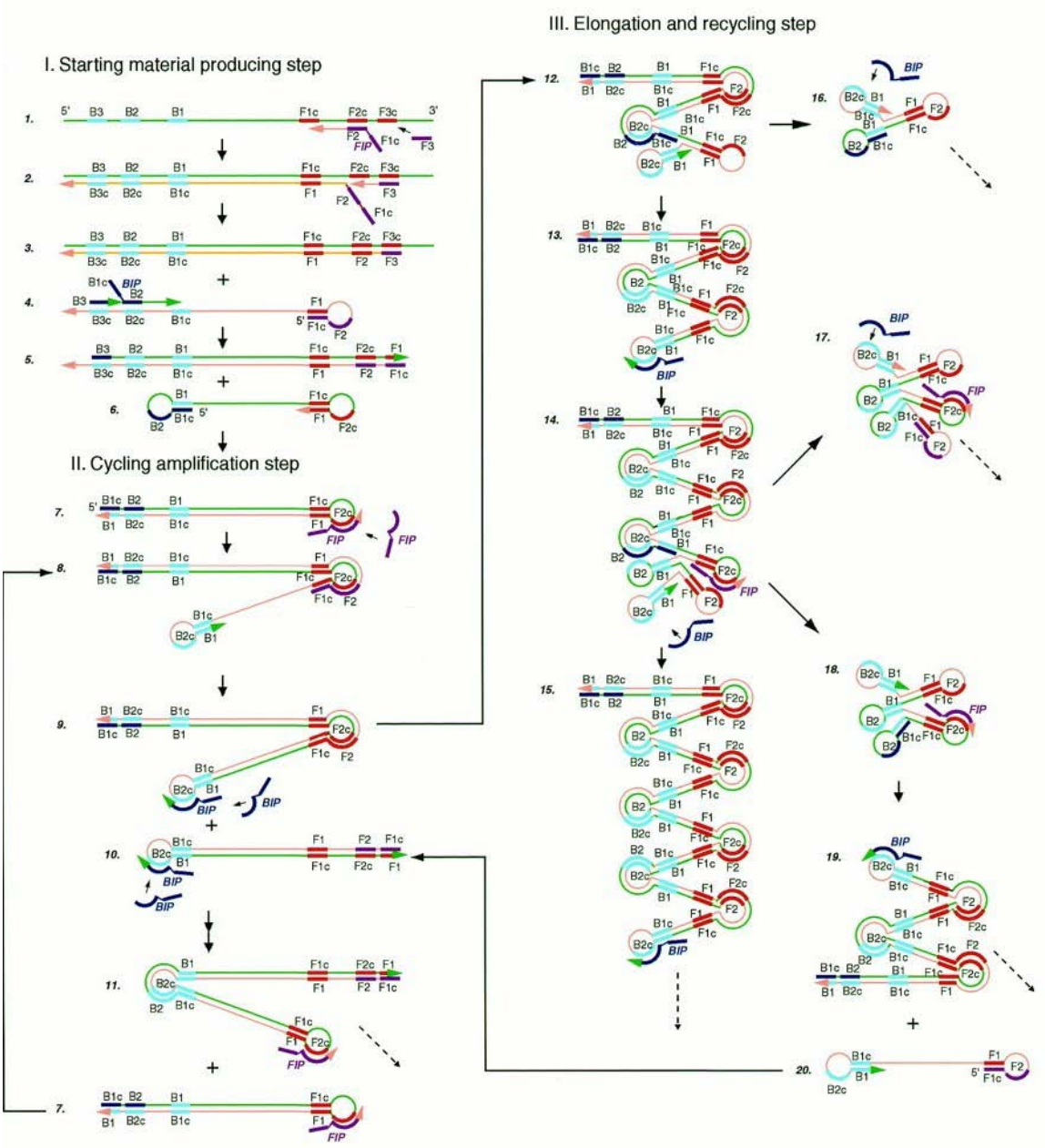

Figure 3 Schematic representation of three major amplification steps in LAMP amplification: (I) Starting material producing step (II) Cycling amplification step (III) Elongation and recycling step. (Notomi et al. 2000)

Despite its novelty and high specificity, thanks to the use of four target-specific primers, LAMP was found to be effective only when the assay template was pure (Deguo et al. 2008). A study on foodborn *Salmonella* species detection in raw milk concluded that LAMP methods are limited by the presence of inhibitors, and have lower sensitivity compared to PCR. NASBA kinetics, in

comparison, may also be partially affected by inhibitors, but the assay's quantitative attributes are not diminished thanks to the incorporation of an IC, and has a significantly simpler design while maintaining sensitivity (only two primers and a target-specific beacon).

1.1.3 Fingerprinting techniques

Profiles of the genetic diversity in marine microbial communities can be acquired through the separation of DNA fragments of the same length in polyacrylamide gels containing a linear gradient of DNA denaturants or a linear temperature gradient. This can be achieved with denaturing gradient gel electrophoresis (DGGE) and temperature gradient gel electrophoresis (TGGE); two related techniques which have been used for genetic fingerprinting on a variety of targets such as bacterial communities (Nubel et al. 1996) zooplanktonic organisms (Dooms et al. 2007) and seagrass communities (Medina-Pons et al. 2008).

A "target gene" will be initially identified and serve as a molecular marker. Genes encoding ribosomal RNA, like 16S rRNA, are frequently used for this purpose because they encompass distinct and highly conserved sequence domains, combined with more variable regions (Olsen et al. 1986). Target gene fragments of identical size are amplified (usually with PCR) and, once inserted in a gel, they migrate according to their denaturing points, which depend on their G-C content (Gadanho and Sampaio 2004). During DGGE, DNA fragments will encounter increasing concentrations of chemical denaturants; a mixture of urea and formaldehyde (Muyzer and Smalla 1998). Once they encounter a threshold denaturant concentration, fragments will lose their double-helical structure and turn into partially melted molecules, at which time migration along the polyacrylamide gel will be significantly reduced. Thus a pattern of bands will be formed, reflecting the variation between DNA fragments as well as their nature (i.e. molecules with an earlier melting point would contain more G-C pairs). TGGE follows a similar logic but, instead of denaturant concentration domains, it involves a linear thermal gradient. Visualisation of DNA bands during DGGE and TGGE can be achieved with the use of stains which work as fluorescent or colourimetric tags and bind to nucleic acids (preferably double stranded) such as ethidium bromide, SYBR Green I, and silver staining (Muyzer and Smalla 1998; Muyzer 1999).

The pattern of bands (fingerprints) generated with DGGE and TGGE can subsequently be used in a variety of ways. Even without sequencing, fingerprints can give information regarding ecosystem complexity. Fingerprint similarity can be assessed to infer ecological differences between communities or treatments, as well as changes within a community (Gadanho and Sampaio 2004; Jing et al. 2010; Medina-Pons et al. 2008; Muyzer 1999). In addition, DGGE and TGGE can be applied to examine intra-species heterogeneity, pathogens, or xenobiotic degraders (Muyzer and

Smalla 1998; Nubel et al. 1996). Nevertheless there are certain limitations associated with DGGE and TGGE. For instance, the separated fragments can be no longer than 500 base pairs thus limiting the total phylogenetic information that can be acquired (Muyzer and Smalla 1998). Furthermore the techniques are not always capable of separating DNA molecules that differ in only a small number of nucleotides, and may struggle to depict results when a large number of different fragments are analyzed simultaneously (Muyzer and Smalla 1998; Vallaeys et al. 1997).

Restriction fragment length polymorphism (RFLP) is another fingerprinting method that has been applied for the analysis of marine groups, including bacterial (Scala and Kerkhof 2000), nematode (M. H. Lee et al. 2009), fungal (Klamer et al. 2002) and archaeal genes (Luna et al. 2009). RFLP has also been employed in the study of functional genes involved in nitrogen fixation and methane oxidation (Schütte et al. 2008) and it is generally described as a rapid technique and more sensitive, when compared to DGGE (Moeseneder et al. 1999).

During RFLP the target genetic material is initially amplified with PCR, and the products are digested by one or more restriction enzymes. The fragments created differ in length depending on species origin, and can therefore be separated via horizontal or vertical gel electrophoresis. As a result a series of bands are formed, representing the diversity of the microbial isolates or communities, and visualization of these bands is usually achieved through fluorescent labelling with dyes such as ethidium bromide (Moeseneder et al. 1999). During terminal-restriction fragment length polymorphism, which is a widely used, modified version of RFLP, target genes are amplified with the employment of primers labelled with a fluorescence dye (Luna et al. 2009; Schütte et al. 2008)

The applications of RFLP are similar to those of DGGE and TGGE; therefore it can be used for the detection of certain marine organisms or pathogens, and for studying the changes in complexity of marine communities over time or under different treatments. However, due to the nature of the process, it is bound to share the same problems associated with the chosen amplification method for the target sequences. Moreover, as encountered in other fingerprinting techniques, RFLP does not reflect the abundance of a detected organism and thus only enables qualitative analysis.

Fluorescence *in situ* hybridisation (FISH) is a molecular labelling technique that is applied to whole cells. It has been described as precise, non-destructive and rapid method, and it is widely applied when monitoring micro-organisms in complex ecosystems (Gan et al. 2010; Zhang et al. 2010). FISH may initiate with immobilization, or fixation, of the target specimen (cells) by applying precipitating (e.g. ethanol, methanol) and cross-linking agents (e.g. aldehydes) either on their own or as a mixture (Moter and Göbel 2000). The cells are then prepared, often with the employment

of pre-treatment steps; for instance, glass slides are often treated with coating agents, in order to improve permeabilisation, Gram-positive cells may require additional treatment with lysozyme, and mycolic acid-containing organisms or complexes may need mild acid hydrolysis (Moter and Göbel 2000; Schonhuber et al. 1997; Schuppler et al. 1998). The pre-treatment process is followed by introduction of the probe into the cell where it hybridizes with the target. Appropriate probes are designed to detect specific DNA and RNA sequences. This is accomplished with 30 minutes and labelling may persist for up to several hours (Moter and Göbel 2000) while in dark humid conditions and at temperatures between 37°C and 50°C. Probes for FISH are selected by taking into account specificity, sensitivity, and tissue penetration and are usually between 15 and 30 base pairs long. They are typically labelled with one or more fluorescent dyes (e.g. FITC, FluoX, TRITC, Texas Red, Cy3 or Cy5) which are attached either at the 3'-end or both ends of the molecule (Moter and Göbel 2000; Spear et al. 1999). Once the hybridisation stage is finished, the sample undergoes washing steps in order to remove unbound probes, and is then ready for visualisation and documentation via conventional epifluorescence microscopy or cytometry (Moter and Göbel 2000).

The ability of FISH to give a detailed picture of microenvironments without the need of nucleic acid extraction and selective amplification procedures makes it a useful tool when studying microbial diversity in environmental samples, as well as the changes in community structure over a period of time or throughout different treatments. Furthermore it can be applied for the detection of endo-symbiotic microorganisms and pathogens (Kjeldsen et al. 2010; Q. Wu et al. 2010). Nevertheless, FISH frequently suffers from low signal intensity of the detected microbes as a consequence of either insufficient probe penetration or low target sequence content (Moter and Göbel 2000; Stoecker et al. 2010). Cell permeability can also be a challenging aspect of the FISH technique; extended application of enzymes that facilitate probe penetration may cause lysis and loss of whole cells, whereas fixation conditions may influence the degree of probe permeability as well (Wendeberg 2010). Consequently, its highly destructive nature may make FISH less favourable for observing structural aspects of microbes as part of a community, such as biofilms. Finally, the accuracy and reliability of the technique largely depends on the degree of specificity of the employed probes (Mallmann et al. 2010). Therefore FISH should not be seen as a stand-alone molecular tool, but it is nonetheless a powerful and useful tool to incorporate into appropriate microbiological studies.

1.1.4 Clone libraries

One of the most common approaches to examine marine diversity is the creation of clone libraries. Cloning involves shearing of genomic DNA from a chosen microbial community or

assemblage into small fragments, which will then be ligated into a vector, taken up by a host and screened after cultivation (Zehr et al. 2008). When studying microbial communities, clone libraries can be applied to phylogenetic screening, species identification, and determination of inter or intra-species similarity (Nocker et al. 2007). They can also be used when studying a specific organism, by screening its whole genome and, as a consequence, they may lead to the discovery of novel genes, and regulatory sequences (López-Legentil et al. 2010).

There are two different sequence isolation approaches from target cells; one entails dividing the total sample DNA into fragments and cloning everything, thus leading to the production of a clone library, whereas the other involves target specific amplification prior to selectively cloning it (Primrose 1998). The cloning itself is generally split into four major stages: 1) DNA fragment management and preparation, 2) incorporation of fragments into a vector, 3) introduction of vector into an appropriate host, and 4) selection or screening of products after cultivation. During the first step of cloning, a series of DNA fragments are formed either via restriction endonuclease digestion or mechanical shearing, but specific fragments may also be produced through cDNA synthesis, and PCR amplification. The fragments are then ligated into a cloning vector; a DNA molecule is replicated inside a cell, usually in the form of a bacterial plasmid or a modified virus (Clark 2005). This is achieved with the employment of DNA ligase, an enzyme which normally operates during DNA replication and catalyses the formation of phosphodiester bonds, thus connecting fragments of the lagging strand whenever two molecules are touching each other end to end (Clark 2005). The host destined to contain the vector is finally selected and cultured in order to produce multiple clones containing copies of the original target nucleic acid molecules (Shepherd et al. 1994). Several types of clone libraries can be produced such as RNA interference clones (Root et al. 2006), genomic clones (Shepherd et al. 1994), open reading frame clones (Kitagawa et al. 2006), and cDNA expressed sequence tag clones (Yu et al. 2008).

Information derived from clone libraries, however, may be misleading and may not accurately represent the studied communities, due to the combination of issues associated with sample collection, cell lysis, nucleic acid extraction and amplification, as well as the cloning procedure. This is especially evident when reverse transcription is involved in the generation of clone libraries due to sensitivity, reproducibility and RNA integrity concerns (Bustin 2000). Moreover, the process is time consuming and therefore may be less preferable compared to other molecular approaches when studying community structure and composition. Therefore a balance needs to be found between number of clones sequenced and the amount of time and costs involved. Nonetheless, clone libraries can be viewed as a complementary tool, capable of providing a more extensive view on marine community structure and dynamics (Medina-Pons et al. 2009).

1.1.5 Microarrays

Microarrays consist of different oligonucleotides or affinity reagents immobilised on a rigid substrate. Advances in microarray technology have provided new tools for the study of gene expression, phylogenetic classification, ecological studies, and the detection of a variety of organisms in marine environments (Gonzalez et al. 2004; Humbert et al. 2010; Maerkl 2011). Currently two types of microarrays are being used and developed; one is based on DNA probes for the detection of DNA or RNA molecules (Peplies et al. 2004), whereas the other is protein-based, and is consequently used for protein identification (Kodadek 2001). Furthermore, depending on their purpose of use, microarrays may be divided into four categories: 1) whole genome arrays, 2) community genome arrays, 3) phylogenetic arrays, and 4) functional gene arrays (Zehr et al. 2008).

DNA microarrays consist of sets of oligonucleotide probes typically immobilised on rigid surfaces, such as glass or plastic. This is achieved either via stepwise chemical synthesis of the probes on the chosen material by employing microfabrication techniques (e.g. photolithography) (Nuwaysir et al. 2002) or through DNA/RNA microdeposition with the application of spotter equipment (Frank 2002). Each probe is complementary to a gene or RNA molecule of interest and as a result, if the desired nucleotide chain is present in the sample, hybridisation events will occur. Less abundant species may possibly be left undetected due to low gene or protein concentration; roughly 10^7 cells are needed in order to achieve sufficient hybridization (L. Wu et al. 2008). Therefore, signal magnification and amplification of the target nucleic acid molecules, either before or after the binding event, may be needed for the method to work. Once the hybridisation process is completed, the microarray experiment is followed by detection and visualisation of results (L. Wu et al. 2008).

Protein microarrays are grids either containing numerous different affinity reagents (protein-detection arrays) or a variety of purified proteins, protein domains, or functional peptides (protein function arrays) (Kodadek 2001). Protein function arrays are constructed by immobilising thousands of native proteins in a defined pattern (Kodadek 2001). This is achieved through proteins being spotted onto chemically derivatised glass slides, while retaining their activity and functionality (MacBeath and Schreiber 2000). The proteins can therefore interact with other proteins, enzymes, or small molecules present in solution. Protein function arrays tend to be employed for molecular interaction studies, and screening of interacting molecules (Berrade et al. 2011). Protein-detecting arrays, on the other hand, have an analogous function to DNA microarrays, as they employ protein capture reagents such as antibodies (MacBeath 2002) that recognise and bind to specific target proteins from a complex mixture. They are usually employed

for protein profiling purposes, including protein quantification, and evaluation of post-translational modifications (Berrade et al. 2011).

Microarrays may contain tens of thousands of different probes per square centimetre (Templin et al. 2002) and can potentially detect hundreds of proteins, transcribed genes, genes or species simultaneously while differentiating them from each other (Kochzius et al. 2008). However, the creation of microarray requires prior knowledge of the target genes or proteins, resulting in extensive and time consuming research when new organisms or qualities are involved (MacBeath 2002). One may argue that this is the case for primer and beacon based molecular techniques, but microarrays are designed for the detection of a significant number of targets, thus making this particular disadvantage more prominent.

1.2 Long-term preservation of reagents for molecular assays

Long-term preservation of reagents, nucleic acids, proteins, and tissue can be of significant importance in several fields of research including biomedical application, pharmaceuticals, environmental analysis, and the overall development of *in-situ* lab-on-a-chip devices. Samples are traditionally frozen (-20^{o}C to -190^{o}C) or stored under cool temperature conditions (4^{o}C), rendering them difficult to transport over long distances and making them entirely depended on freezer/fridge maintenance, power supply and space. Dry reagent preservation is an attractive storage solution, as it provides great portability and protects target biochemicals, by making them more robust against temperature fluctuations and other environmental conditions that may promote degradation (Carpenter et al. 1997; van Dam et al. 2013).

Lyophilisation, a preservation method based on sample dehydration, has been widely used for the preservation of various forms of biological tissues, as well as stabilisation of biological molecules, such as purified collagen, fibronectin, and enzymes (Freytes et al. 2008) and it is a common method for the formation of solid protein pharmaceuticals (Fox 1995; Kasper and Friess 2011; W. Wang 2000). It has only recently been applied on miniaturised polymer-based devices for the storage of reagents for single target immunoassays, PCR, and recombinase polymerase amplification (Ahlford et al. 2010; Lutz et al. 2010; Mauk et al. 2015; Tanaka et al. 2014; Yoon and Kim 2012).

During lyophilisation, samples are dehydrated under vacuum conditions, down to 0.04 mBar (Kadoya et al. 2010) and may be exposed at low temperatures beforehand, usually between -80°C and -55°C (W. Wang 2000). In this case, the dehydration process is divided into two steps; the first phase consists of removing the frozen water from the sample, whereas a secondary drying process removes non-frozen 'bound' water (Arakawa et al. 2001; W. Wang 2000). Freeze drying,

however, generates a variety of stresses, such as the formation of ice crystals, potential changes in pH, and structure alterations of proteins, all of which are capable of affecting the lyophilised samples' properties (Freytes et al. 2008; W. Wang 2000). Different proteins are characterised by varying degrees of tolerance to the aforementioned stresses (Hsu et al. 1995; Koseki et al. 1990; W. Wang 2000) and therefore the effectiveness of lyophilisation largely depends on the nature and properties of the target sample. In addition, the damaging properties of freeze-drying may be inhibited with the incorporation of other substances during the reaction. The stabilisation properties of trehalose (α-D-glucopyranosyl α-D-glucopyranoside) (Figure 4) are commonly applied in industry for the preservation of proteins, food and biosystems (Patist and Zoerb 2005). Being a non-reducing disaccharide, trehalose does not undergo the protein-damaging Maillard reaction, and retains a glassy state, granting it high viscosity and low mobility, up to 106°C. During the lyophilisation process, water is substituted with sugar molecules whilst drying, and the proteins are therefore protected from degradation and crystallisation.

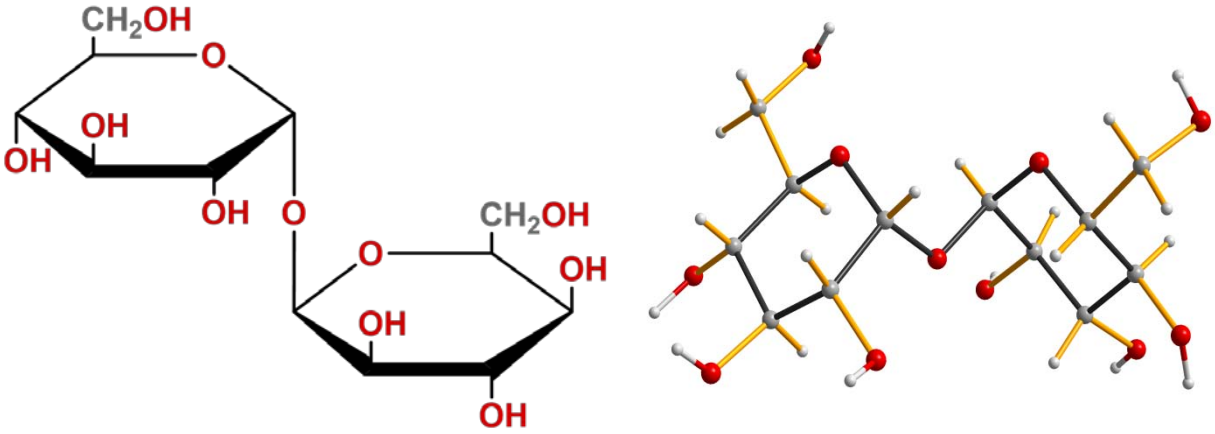

Figure 4 Structural diagram (left) and 3d ball-and-stick model (right) of trehalose.

The properties of disaccharides such as trehalose and sucrose have also been used for the storage and reconstitution of reagents, following simple dehydration (Stevens et al. 2008). This technique follows the premise of anhydrobiosis, a function used by some organisms to survive under almost complete dehydration (Crowe et al. 1998). The disaccharides stabilise and protect membranes and proteins in the dehydrated state via hydrogen bonding; the interactions between the –OH groups of the two disaccharides and water molecules are closely similar in energy and configuration (Franks and Auffret 2008) and will therefore form hydrogen bonds with proteins in solution, protecting their tertiary structure and overall physical state (Arakawa et al. 2001; Crowe et al. 1998). Furthermore, sucrose and trehalose undergo a transition during the preservation process, forming a glassy solid which potentially provides additional protection from external stress (Crowe et al. 1998). Nevertheless, the addition of sugars may affect molecular reaction kinetics, due to increased viscosity, and overall assay signal strength (Stevens et al. 2008).

Preservation of reagents and molecular assay components via gelification can be a useful alternative to the aforementioned dry-reagent storage techniques. A method of gelification was originally developed in the late 90s, in order to form a stable matrix for long-distance shipping and fieldwork-use of complex molecular reagents (Madejon et al. 2005).

Gelification involves the reaction of several chemical components at room temperature to form a protective, jelly-like medium. This can be achieved via desiccation and under the presence of a gelator, consisting of stabilising agents and disaccharides. The former prevent reactions between carboxyl and carbonyl groups with amine and phosphate groups, whereas the latter preserve the macromolecular structure of proteins during the dehydration process. This novel gelification technology has been patented and outlined by Biotools as part of the European LABONFOIL project (Rosado et al. 2002), and has been successfully applied to preserve reagents on-chip for PCR (Sun et al. 2013) and NASBA (Tsaloglou et al. 2013) assays.

This gelification technique can be regarded as a low-energy and cost-effective method of reagent preservation; sample preparation can take place at room temperature, without the need for dedicated manufacturing equipment or pressure and temperature adjustments. Nevertheless, vacuum-induced dehydration at elevated temperatures can accelerate the process, and gelification can be achieved in less than 30 minutes.

Other than gelification or lyophilisation, more preservation options exist in molecular biology, through the employment of liquid solvents. Amyl acetate, for instance, has been applied to remove water from samples, in order to preserve anatomical dissections (Saunders and Rice 1944); this is achieved through hydrolysis of primary amyl acetate, due to the presence of water, leading to the production of an amyl alcohol (Polanyi and Szabo 1934). Tissue preservation has also been achieved with the use of ethanol, acetone, chloroform, and liquid nitrogen (Astrid et al. 2015; Thakuria et al. 2009) as well as formalin solvents (Jeon et al. 2010; Lou et al. 2014).

Amongst them, ethanol is relatively easy to use, and has been described as the most frequently applied medium for tissue preservation (Nagy 2010). Methylated ethanol, in particular, has been used as a reliable and cost-effective RNA-fixative for sampling insects in remote areas (Astrid et al. 2015). Ethanol is often contained in buffers, and depending on its concentration, it may have some unwanted effects; high ethanol concentrations may lead to rigidness and shrinking of the target organic material, whereas water-diluted ethanol can cause DNA degradation (Nagy 2010). Finally, in comparison to other molecular stabilisation methods, it appears that liquid solvents are preferred for long-term preservation of tissue samples instead of molecular reagents.

1.3 Harmful algal blooms and dinoflagellate toxicity

Algal blooms are a natural worldwide phenomenon, resulting from rapid accumulation of algal populations in marine and freshwater systems. They form the basis of production in marine food webs and are often recognised from distinct water discoloration, caused by the pigments of associated algae (Davidson et al. 2011; Smythe-Wright et al. 2010). Some algal blooms are classed as harmful due to their negative effects on humans, marine mammals, fish, and the overall marine ecosystem. Their harmful impact can be attributed either to high biomass or the production of biotoxins (Anderson et al. 2002; Anderson et al. 2012a); the latter is of particular concern due to toxin accumulation in seafood, which can lead to human food poisoning from fish and shellfish consumption.

Harmful algal blooms (HABs) have been studied over recent decades as they have a significant impact on the global economy and public health (Backer et al. 2015; Hoagland et al. 2002). In the United States alone, they annually affect expenses in public health ($20 million), commercial fisheries ($18 million) and recreational tourism ($7 million), while monitoring and management costs account for another $2 million (Hoagland et al. 2002). HAB-associated species can be found among several phytoplankton groups, including diatoms, dictyochophyceae, dinoflagellates, haptophytes, raphidophyceae, and cyanobacteria; among them, dinoflagellates make up the majority of toxin producing microalgae and were even thought to be the only HAB species until the 1980s (Arff and Martin-Miguez 2016). As of 2012, there have been 2,377 described dinoflagellate species, 80 of which are listed as toxin producers (Arff and Martin-Miguez 2016; Gómez 2012). Their associated toxins are responsible for ciguatera fish poisoning (CFP), neurotoxic shellfish poisoning (NSP), diarrheic shellfish poisoning (DSP), paralytic shellfish poisoning (PSP), respirational irritation, and asthma-like symtoms (among others) in humans, as well as animal mortalities (Ferrante et al. 2013; Fleming et al. 2011; Hallett et al. 2015; Pierce and Henry 2008; D.-Z. Wang 2008).

The cosmopolitan dinoflagellate genus *Dinophysis* accounts for more than 120 marine species (Jensen and Daugbjerg 2009), including 12 species connected with DSP and gastrointestinal outbreaks on a global scale and at cell densities as low as 1-2 x 10^2 cells L^{-1} (Reguera et al. 2012; Yasumoto et al. 1985). They are reported to be a source of lipophilic toxins, such as okadaic acid, dinophysistoxins, and pectenotoxins (Arff and Martin-Miguez 2016; Fabro et al. 2016; Reguera et al. 2012; Yasumoto et al. 1985). The toxins are thermostable polyethers which inhibit protein phosphatase enzyme systems, causing significant changes in smooth muscle contraction (Pierce and Kirkpatrick 2001). *Dinophysis* and their associated harmful effects are becoming a common occurrence in European waters, with cell concentrations systematically surpassing regulatory

levels, and thus raising concerns for human health, the shellfish industry, and marine harvesting areas alike (Arff and Martin-Miguez 2016; Grattan et al. 2016; Hallegraeff 2010).

Lingulodinium polyedrum, *Gonyaulax spinifera*, and *Protoceratium reticulatumi* are also known to produce a group of lipophilic toxins, named yessotoxins (Miles et al. 2005; Paz et al. 2004; D.-Z. Wang 2008). Yessotoxins are disulfated polycyclic ether compounds associated with DSP and PSP toxic episodes (Miles et al. 2005; Murata et al. 1987; Paz et al. 2004; Tubaro et al. 1998). They act as potent neurotoxins, and have been demonstrated to interact with calcium channels of human lymphocytes, causing slight non-capacitative Ca^{2+} entry and inhibiting Ca^{2+}entry produced by emptying of internal calcium stores (de la Rosa et al. 2001; Miles et al. 2005; Paz et al. 2004). The first instance of yessotoxin-induced poisoning was recorded in Japan, in 1986, followed by events in Norway, Italy, Spain, Canada, Chile, Russia, and New Zealand (Miles et al. 2005; Murata et al. 1987; Paz et al. 2004; Paz et al. 2008).

Out of 33 species of *Alexandrium*, 14 are listed as toxin producers and connected with PSP events and red tides worldwide (Anderson 1998; Anderson et al. 2012b; Anderson et al. 2012a; Arff and Martin-Miguez 2016). Among them, *Alexandrium catenella*, *Alexandrium fundyense*, and *Alexandrium tamarense* are responsible for the majority of these poisoning, through the production of saxitoxins and derivatives (Anderson et al. 2012b). Saxitoxin is potentially the most toxic PSP-inducing toxin (D.-Z. Wang 2008) and acts by blocking neuronal transmission as the toxin binds to voltage-gated Na^{+} channels (Andrinolo et al. 1999). Four of the other 11 toxic *Alexandrium* species produce fast-acting micro-cyclic imines, such as spirolides and goniodomins (Arff and Martin-Miguez 2016; Suikkanen et al. 2013). Spirolid toxicity has been attributed to either binding of the toxin to muscarinic acetylcholine receptors, or antagonist interactions with nicotinic acetylcholine receptors, whereas goniodomins induce conformational changes of actin, thus affecting cytoskeletal reorganisation (Rasmussen et al. 2016). Nevertheless it can be difficult to determine the potential harm of *Alexandrium* blooms, as some species may consist of both toxic and non-toxic strain variations; for instance, populations of the aforementioned *Alexandrium tamarense* in Northern Ireland and Scotland have been documented to contain both toxic and non-toxic versions of the species (Anderson et al. 2012b; Anderson et al. 2012a).

Karenia brevis, formerly known as *Gymnodinium breve* and *Ptychodiscus brevis*, is another toxic marine dinoflagellate associated with HABs (Magaña et al. 2003) and the formation of red tides (López-Legentil et al. 2010). It has recurrently plagued the Gulf of Mexico, especially along the west Florida shelf, for over a century (Lekan and Tomas 2010; Vargo et al. 2008). *K. brevis* is known to produce brevetoxins, lipid soluble polyethers which cause depolarisation in affected cells by opening sodium ion channels in cell membranes, leading to uncontrollable influx of Na^{+}

into the cell (Errera and Campbell 2011; D.-Z. Wang 2008). Brevetoxins are responsible for fish and mammal mortality as well as NSP in humans, and can accumulate in the food web through trophic transfer (Fleming et al. 2011; Landsberg et al. 2009). Brevetoxin concentrations were quantified from the south-west Florida coast over the lifetime of a bloom, corresponding with *K. brevis* cell counts by microscopy (Pierce and Henry 2008). The results indicated that toxin levels were sufficient to cause fish kills, NSP events, as well as respiratory irritation, despite *K. brevis* counts diminishing to below detectable levels. Increasingly recurrent HABs (Kudela et al. 2010) make toxic species like *K. brevis,* important targets of environmental research, and thus sensitive, rapid and informative detection methods are needed to determine mechanisms of bloom formation for HAB management.

1.4 Microfluidic devices and biological sensors

In-situ monitoring of ocean biology is typically done in the form of sample collection during organized cruises, and sample analysis either on-board the research ship or in a laboratory at a later time. However, such research expeditions can be expensive, labour intensive, and only cover a fraction of the oceans, as they follow pre-defined courses and locations. This leads to significant under-sampling of the oceans and, consequently, alternative monitoring methods are used in an effort to fill the gaps. Remote sensing, for instance, is a cost-effective approach for estimating phytoplankton biomass, by determining chlorophyll concentration on satellite images (Blondeau-Patissier et al. 2014; Carvalho et al. 2010). Autonomous underwater vehicles implement *in situ* and deployable sensors for the analysis of biological samples, and may be useful for getting a more complete picture of ocean biology (Schofield et al. 2013). Nevertheless, microfluidic biosensors and lab-on-chip technologies will play an important part in the future of ocean monitoring; this is particularly evident when looking at projects such as the European LABONFOIL and “The Ocean of Tomorrow” initiative, both funded by the European Commission, which invested in the development of microfluidic devices for the molecular sensing of phytoplankton, among others.

Microfluidics have been defined as the science and technology of systems that manipulate small volumes of fluids, using channels with dimensions ranging from tens to hundreds of micrometers (Whitesides 2006). It is considered a heavily interdisciplinary field, as the development of microfluidic devices and sensors requires the combined involvement of engineers, physicists, chemists, and biologists. Handheld analysers for the detection of marine microorganisms in environmental samples have been developed for some time now (Casper et al. 2007), and the application of biological sensors in the field of oceanography is a concept that has been analysed to some extent (Zehr et al. 2008). Microfluidic systems, both within and outside the field of

oceanography, have been designed for numerous purposes such as molecule separation (Brody and Yager 1997) genotyping (Rich et al. 2011) and for the performance of various biochemical and molecular assays (Lin et al. 2009). They have also been employed to monitor cell growth (J.-H. Lee et al. 2008) detect water-borne pathogens (Yamahara et al. 2015; Zhao et al. 2012) and observe a range of cellular functions (Dimov et al. 2011; Tsopela et al. 2016).

1.4.1 Microfluidic and LOC design considerations

Microfluidic and LOC systems can provide a range of benefits over traditional methods in specialised laboratories (Tsaloglou 2016). Operation is significantly simplified, as sample processing and analysis is done automatically and without the need for specialised or highly trained personnel. Furthermore, microfluidic devices offer precisely controlled and reduced reagent consumption, thus decreasing expenses and chemical waste. They are also designed to be small in size and often portable; when coupled with the targeted low-power usage during operation, they have the potential of becoming excellent and powerful tools for *in situ* studies and environmental monitoring. Finally, LOC systems can be designed to run multiple reactions in parallel, allowing for faster results, improved replication, and the simultaneous study and comparison of a variety of parameters.

Nevertheless, microfluidic devices are more complex than traditional laboratory test tubes and microtitre plates, making fluid manipulation and reagent integration particularly challenging. Commercialisation of microfluidic systems is often hindered due to difficulties associated with the consistent, reproducible, and low-cost incorporation of multiple reagents on a single platform and across numerous devices (Hitzbleck and Delamarche 2013). On-chip reagent handling requires precise manipulation of only a few micro- or nano-litres at a time, while avoiding cross-contamination with other reagents across the platform. Furthermore, fluid control must be done in a manner so that the microfluidic device is simple to use, without the need for additional external instrumentation or user handling. Other issues include complicated cell loading, channel blockage by air bubbles (Jowhar et al. 2010) and evaporation of liquids (Velve-Casquillas et al. 2010); these attributes are likely to induce changes in reagent concentrations and osmolality and therefore affect the integrity of biochemical analyses. Finally, all reagents must be appropriately stored on the microfluidic platform, and with an acceptable lifetime, rendering the platform portable and suitable for *in situ* measurements, without relying on freezer/fridge availability. On-chip reagent storage is preferably done in powder form (Whitesides 2006), but gelification (Sun et al. 2013; Tsaloglou et al. 2013) and dehydration under disaccharide presence (Stevens et al. 2008) have been recently demonstrated as additional non-liquid alternatives.

Microfluidic chips are typically fabricated using optically clear material, such as polymer substrates (Hoek et al. 2010; Hoffmann et al. 2010; Milani et al. 2015; Sun et al. 2013; Tsaloglou et al. 2013), glass (Jellema et al. 2009) or a combination of the two (W.-F. Fang and Lee 2015; Millet et al. 2007). The type of chosen material will largely depend on the conducted on-chip application, to avoid compatibility issues. For instance, polydimethylsiloxane (PDMS) is a commonly employed polymer in lab-based microfluidic systems, but may cause unwanted biomolecule absorption or adsorption, due to its affinity for small hydrophobic molecules and porosity (Velve-Casquillas et al. 2010), and has poor chemical resistance to organic solvents (Rolland et al. 2004). In comparison, poly(methyl methacrylate) (PMMA) and cyclo-olefin copolymer (COC) are chemically robust, biocompatible, and optically clear thermopolymers (Ogilvie et al. 2010).

Naturally, the level of complexity when designing microfluidic devices depends on the incorporated assay. For example, the integration of NASBA in LOC platforms may be more favourable compared to thermocycling-based methods, such as PCR, since most of the assay is performed at 41°C, and has been successfully demonstrated in the past for *Escherichia coli* (*E. coli*) (Dimov et al. 2008) and *K. brevis* (Casper et al. 2007; Tsaloglou et al. 2013). Overall, biological sensors use molecular tools for the detection and quantification of marine microorganisms by targeting nucleic acids, proteins, and lipids associated with a species or a wider group (Tsaloglou 2016). As such, a number of systems have been developed for *in situ* phytoplankton detection using antibody- and probe-binding techniques, or nucleic acid amplification based methods.

1.4.2 Environmental Sample Processor

The Environmental Sample Processor (ESP), an autonomous deployable system, has been used for the detection of marine microorganisms by carrying out real-time DNA and antibody-based tests (Doucette et al. 2009; Scholin et al. 2006). The system consists of a core sample processor, analytical and sampling modules, and uses custom designed reaction chambers to support a variety of filters and absorptive media, to allow for protocol adjustments. A rotating carousel, weighting 27 kg, in conjunction with a robotic arm, two clamps, three syringe pumps, and a CCD camera, automate sample collection and then process samples under atmospheric pressure (Scholin et al. 2006). More recently, the ESP was redeveloped with a reinforced casing to conduct qPCR in the deep sea for *in situ* identification of aerobic methanotrophs (Ussler III et al. 2013), and was also used for qPCR-based detection of faecal indicators and harmful algae (Yamahara et al. 2015). The ESP has also been deployed for automated *in situ* sampling of heterotrophic bacteria and archaea, to perform whole-genome transcriptome profiling (Ottesen et al. 2014) and in relation to diurnal rhythm oscillations in terms of transcription, metabolic activity, and behavior.

Evidently, this type of biological sensor provides significant flexibility with the integration of molecular assays, and allows for *in situ* analyses well below the ocean surface. However, the system is bulky, heavy, and requires a range of personnel to handle; smaller microfluidic systems will offer superior portability and only a single user for operation purposes.

1.4.3 NASBA handheld analyser

In the other end of the spectrum, a handheld analyser has been developed for successful environmental detection of *K. brevis*, when combined with field nucleic acid extraction protocols (Casper et al. 2007). RNA was extracted using a modified version of a commercially available kit (Qiagen RNeasy Mini Kit), and subsequently amplified and detected real-time by a portable NASBA incubator system with two-channel fluorescence detection. Even though the analyzer is an improvement over ESP-type systems when it comes to portability, it appears to restrict users in other departments. Thermal control is achieved using an infrared light source with a temperature deviation of ±5^{o}C, potentially limiting reaction accuracy and the use of thermocycling-based molecular methods. Furthermore, the sensor does not appear to store or preserve NASBA reagents and enzymes, further limiting its usefulness for *in situ* applications.

1.4.4 *In situ* point-of-care analysers

Handheld or otherwise portable microfluidic analysers have also been developed for point-of-care (POC) diagnostics. For example, the “Fraunhofer ivD-platform” is a LOC system designed to adapt to a variety of biochemical assay types for POC applications, and can be transported from the laboratory to the point-of-need (Schumacher et al. 2012). It addresses topics such as personalized medicine or companion diagnostics, while using a low-cost and self-contained cartridge with integrated reagents, microfluidic actuators and various sensors. The Fraunhofer ivD-platform combines fully automated instrumentation with a user-friendly interface which initiates the assay protocol, data acquisition and data analysis. Despite its portability, however, the system cannot be considered a true handheld analyser and appears to be still in its testing stages. By contrast, a cellphone-based handheld analyser was recently developed (Berg et al. 2015) and uses a colorimetric microplate reader for viral detection via enzyme-linked immunosorbent assays. More specifically, a 96-well plate is inserted and illuminated by a 3D-printed opto-mechanical smartphone attachment; the smartphone camera then captures any transmitted light, and results are analysed with a pre-installed phone app. It is presented as a cost-effective, extremely portable platform, which could assist POC applications in resource-poor environments and field-settings. Nevertheless, the analyser does not provide the flexibility required to run other biochemical assay types, and does not appear to address long-term reagent storage.

1.4.5 IISA-Gene system

The IISA-Gene system is an *in situ* biological analyzer capable of detecting gene fragments and analysing microbial activities in ocean environments (Fukuba et al. 2011b; Fukuba et al. 2011a). It uses a microfluidic device as its core element, whose components are immersed in fluorinated oil, to perform sample collection, along with nucleic acid extraction, and subsequent molecular analysis in an ambient environment. The microfluidic device is connected to a control unit, enclosed in a pressure vessel, and operated remotely using a personal computer. The IISA-Gene can be deployed at extreme depths and offers high assay adaptability, similar to the ESP system albeit more compact in size, and its most recent iteration can collect up to 128 samples simultaneously, but suffers from relatively small sample collection (0.5 mL per hour) (Okamura et al. 2013; Tsaloglou 2016). The small sample collection process may affect the systems precision and could be particularly problematic for the detection of less abundant species.

1.4.6 LOC system with automated sampling

In situ systems for molecular-based sensing have also been developed for waterborne pathogen detection (Delattre et al. 2012; Kwon et al. 2010; Ligler et al. 2007; Tsaloglou 2016). One such example is a field analyser, designed to sample and detect *E. coli* in a variety of fresh water sources (Kwon et al. 2010). An automatic sampling system was constructed by connecting adjustable drip emitters to a pressurised water pipe, performing at flow rates equal to 0.4-2.0 L h^{-1}. Samples would then be analysed, via light scattering detection of particle immunoagglutination, with antibody-conjugated submicron particles stored for up to four weeks via lyophilisation. Even though the system has not been implemented for algal detection, it could be adapted for phytoplankton analysis and marine microbial studies, as long as it can be connected to a pressurised pipe network.

As of yet, no true LOC microfluidic device has been developed to incorporate all the desired requirements for molecular-based *in situ* detection of marine microorganisms and HABs. This thesis presents a novel LOC, bench-top sensor for the detection and quantification of toxic microalgae *K. brevis*, using a fully automated NASBA protocol with preserved reaction components. The system combines assay flexibility (Sun et al. 2013; Tsaloglou et al. 2013) with portability, and is capable of achieving rapid, accurate, and precise *in situ* molecular analysis of marine microorganisms when combined with a novel, customised sample collection system-protocol.

1.5 Contributions

Due to the multidisciplinary nature of the PhD and the overall project, cooperation and teamwork have been essential. Thus, a number of co-workers have contributed to the achievement of aims and objectives presented in this thesis.

- Prof Matt Mowlem secured funding
- Prof Matt Mowlem, Dr Nicolas Green, Dr Maria-Nefeli Tsaloglou, and Prof Debora Iglesias-Rodriguez supervised this PhD
- Experimental contributors: Christos-Moritz Loukas (CML), Dr Nicolas Green (NG), Florian Laouenan (FL), Dr Maria-Nefeli Tsaloglou (MNT), and Christine Thanner (CT)

MNT modified and optimised NASBA assays for *Karenia brevis*, *Karenia mikimotoi* (*K. mikimotoi*), and *Tetraselmis suecica* species. CML maintained all cultures, prepared all media, and assisted with modification and optimisation of *Karenia brevis* NASBA assay. All data presented in this thesis has been collected in experiments performed primarily by CML: (1) Chapter 2 experiments were entirely performed by CML; (2) Chapter 3 experiments were entirely performed by CML; (3) Chapter 4 LabCardReader experiments were performed by CML in collaboration with FL; (4) Chapter 5 sample filtration/collection was performed by CML in collaboration with NG; (5) Appendix A EVG501 bonder experiments were performed by CML in collaboration with CT; (6) Appendix B experiments were performed by MNT in collaboration with CML and FL; (7) Appendix C data analysis was entirely performed by CML.

Chapter 2: Effect of growth conditions on transcription of gene *rbcL* for toxic microalga *Karenia brevis*

2.1 Introduction

2.1.1 The toxicity of *Karenia brevis* and their detection

Harmful algal blooms (HABs) have been studied over recent decades as they have a significant impact on the global economy and public health (Backer et al. 2015; Hoagland et al. 2002). In the United States alone, they annually affect expenses in public health ($20 million), commercial fisheries ($18 million) and recreational tourism ($7 million), while monitoring and management costs account for another $2 million (Hoagland et al. 2002). *Karenia brevis*, formerly known as *Gymnodinium breve* and *Ptychodiscus brevis*, is a toxic marine dinoflagellate associated with harmful algal blooms (HABs) (Magaña et al. 2003) and the formation of red tides (López-Legentil et al. 2010). It has recurrently plagued the Gulf of Mexico, especially along the West Florida shelf, for over a century (Lekan and Tomas 2010; Vargo et al. 2008).

K. brevis is known to produce brevetoxins, lipid soluble polyethers which cause depolarisation in affected cells by opening sodium ion channels in cell membranes, leading to uncontrollable influx of Na^+ into the cell (Errera and Campbell 2011; D.-Z. Wang 2008). Brevetoxins are responsible for fish and mammal mortality as well as neurotoxic shellfish poisoning (NSP) in humans, and can accumulate in the food web through trophic transfer (Fleming et al. 2011; Landsberg et al. 2009). Increasingly recurrent HABs (Kudela et al. 2010) make toxic species like *K. brevis,* important targets of environmental research. Thus, sensitive, rapid and informative detection methods are needed to determine mechanisms of bloom formation for HAB management.

Brevetoxin concentrations have been quantified from the south-west Florida coast over the lifetime of a bloom, corresponding with *K. brevis* cell counts by microscopy (Pierce and Henry 2008). The results indicated that toxin levels were sufficient to cause fish kills, NSP events, as well as respiratory irritation, despite *K. brevis* counts diminishing to below detectable levels. Limits of detection by microscopy are typically 1000 cells L^{-1} (LeGresley and McDermott 2010), abundances which are not currently a cause for regulatory action (classified as the lowest level *K. brevis* bloom state, 'present' by the Florida Fish and Wildlife Conservation Commission[7]) (FWRI 2015). Coupled with the difficulty of distinguishing *K. brevis* from morphologically similar organisms (Haywood et al. 2004), cell counts by microscopy are not the best determinant of HAB formation or environmental brevetoxin toxicity, and more sensitive indicators are needed. Cellular release of brevetoxin upon cell lysis in dying populations might represent a major source of environmental

[7] Classification of *K.brevis* blooms is as follows: not present (0-1,000 cells L^{-1}); very low (>1,000-10,000 cells L^{-1}); low (>10,000-100,000 cells L^{-1}); medium (>100,000-1,000,000 cells L^{-1}); high (>1,000,000 cells L^{-1})

brevetoxin (Pierce and Henry 2008), and as *K. brevis* toxicity is induced by cell stress it may therefore not always be directly correlated to cell abundances (Errera and Campbell 2011; Hardison et al. 2013; Hardison et al. 2014). A quantitative method to gauge the physiological state of *K. brevis* at concentrations typical of marine waters would provide a more sensitive measure for environmental monitoring and management.

The recurring harmful algal blooms, in conjunction with the hazardous effects of the brevetoxin, make *K. brevis* an important target of environmental research, and rapid detection methods are consequently needed. Molecular techniques, which are known for their sensitivity and specificity, have been successfully applied to identify *K. brevis* amongst other species while targeting the ribulose-1,5-bisphosphate carboxylase/oxygenase (RuBisCO) large-subunit gene (*rbcL*) (Gray et al. 2003). RuBisCO is a key enzyme mediating CO_2 fixation via the Calvin-Benson Cycle in photosynthetic organisms. *rbcL* is a conserved gene often used to construct microbial phylogenies, with enough diversity to deliver clade-level resolution of eukaryotic species (Spreitzer and Salvucci 2002). What remains unknown is if the transcription of gene *rbcL* is adequately conserved to allow quantification of microorganisms using RNA-based amplification techniques under varying growth and physiological conditions. Since RNA detection serves as a better indicator of physiologically active organisms when compared to DNA, quantification using RNA-based amplification methods, such as IC-NASBA, would provide measurements that are more accurate for monitoring purposes.

2.1.2 The effect of chemistry on cell growth and physiology

K. brevis growth largely depends on the availability of nutrients within their environmental surroundings. Naturally, as microalgal populations are continuously transported via currents along the water column they will inevitably experience a variety of chemical conditions. Phosphorous (P) and nitrogen (N) sources are generally considered vital for the maintenance of phytoplankton blooms, and this is the case for *K. brevis* (Vargo et al. 2008). Amongst the two, it is suggested that N is most often the limiting factor for cell growth and bloom formation in marine environments (Ren et al. 2009). Nevertheless co-limitation of N and P is commonly observed and, as a result, the dinoflagellate has developed mechanisms to utilise organic P and N whenever concentrations of inorganic equivalents are as low as 0.025-0.24 µM and 0.02-0.2 µM, respectively (Vargo et al. 2008).

Trace metals are also considered essential for phytoplankton growth as they are connected with various cellular processes and the production of bioactive compounds. Zinc for instance is a cofactor in all 6 functional classes of enzymes, and involved in pan-metabolic biochemical

processes, such as the synthesis or degradation of major metabolites (Vallee and Auld 1990). Whereas some species plastocyanin content is affected by copper levels (Peers and Price 2006). Iron may be one of the more important metals involved in microalgal metabolism as it is employed for electron transport during photosynthesis, detoxification of reactive oxygen species, chlorophyll synthesis, and the reduction of nitrate (Sunda and Huntsman 1995). Trace metals may be of even greater significance for toxic species, as they are shown to influence toxin production; the addition of copper to *Ostreopsis siamensis* or selenium to *Protoceratium reticulatum* cultures, led to increased production of palytoxin-related compounds and yessotoxin, respectively (Rhodes et al. 2006).

Vitamins are organic micronutrients, some of which have specific metabolic purposes whereas others have more extensive roles (A. G. Smith et al. 2007). Despite the ability of microalgae to biosynthesise vitamins, many groups require an exogenous source: they exhibit vitamin auxotrophy (Croft et al. 2006). Many studies focused on species-specific requirements of different combinations of vitamins B_{12}, thiamine, and biotin, all of which are often obligate requirements for culture growth (Croft et al. 2006). Vitamin B_{12}, for instance, is associated with the metabolism of amino acids, deoxyriboses, and the reduction of carbon fragments (E. L. Smith 1956) whereas biotin is universally required as a cofactor in various carboxylase enzymes, which are essential for eukaryotic cell metabolism, and catalyzes the metabolism of amino acids, cholesterol, and fatty acids (Streit and Entcheva 2003). Thiamine is also involved in intermediary carbon and amino acid metabolism and, similarly to the aforementioned vitamins, it is essential for all organisms (Croft et al. 2006).

2.1.3 The choice of growth media for phycology

Studies on the cultivation of marine algae in various media evolved after successful laboratory attempts to grow diatoms in the early 1890's (Provasoli et al. 1957). This facilitated research on phytoplankton physiology to a significant extent, and eventually it became easier to culture cells to desired concentrations. Due to advancements in medium preparation methods, it is now possible to grow many phytoplankton species under laboratory conditions (Price et al. 1989).

The half strength version of the "f" enrichment (f/2 media), along with the addition of vitamins and chelating substances, is perhaps one of the most widely used medium recipes (Price et al. 1989). L1 and L2 media can be employed for selective enrichment studies, as well as general enrichment purposes when adequately diluted (Hallegraeff et al. 2003). After numerous modifications, Aquil* has become a well-characterized type of artificial seawater and is used to culture a variety of coastal and oceanic phytoplankton species (Sunda et al. 2005). NH-15 is

another artificial medium that is commonly used in dinoflagellate studies ontains additional sulphide and "vitamin 8" enrichments (Gates and Wilson 1960; Lekan and Tomas 2010). Please see the materials and methods section for a complete list of media components.

2.1.4 The employment of nucleic acid sequence-based amplification for environmental analysis

Molecular techniques, which are known for their sensitivity and specificity, have been successfully applied to identify *K. brevis* amongst other species, targeting gene *rbcL* (Gray et al. 2003). RuBisCO is a key enzyme mediating CO_2 fixation via the Calvin-Benson Cycle in photosynthetic organisms. *rbcL* is a conserved gene often used to construct microbial phylogenies, with enough diversity to deliver clade-level resolution of eukaryotic species (Spreitzer and Salvucci 2002) and it is not typically regulated by circadian rhythms in dinoflagellates (Casper et al. 2004; van Dolah et al. 2007). These characteristics make it an excellent target for quantification of viable *K. brevis* through molecular assay analysis (Casper et al. 2004; Casper et al. 2005; Casper et al. 2007).

Previous developments resulted in a robust quantitative and sensitive assay targeting *K. brevis* *rbcL* transcripts and determined a clear log-linear relationship between cell number and *rbcL* transcript abundances from 1-1000 cells (Patterson et al. 2005). Under most stresses, *rbcL* transcription per cell remains stable, but with high variation between replicates when measured semi-quantitatively (Casper et al. 2005). Further, *rbcL* transcription has a 1.1:1 (log-log; $R^2 = 0.89$) relationship with cell counts in environmental samples for concentrations above 1000 cells L^{-1}, indicating the utility of *rbcL* transcript quantification as a proxy for high *K. brevis* cell abundances. In the present study, we grew *K. brevis* using different growth media to impose variation in cell physiology and quantified *rbcL* transcription during growth stages to evaluate whether cell physiological state and potentially cell stress impact the relationship between *rbcL* transcription and cell abundance. If *rbcL* transcription was unaffected, the robustness and reliability of the technique for quantification purposes would be reinforced; however it would also strengthen claims of *K. brevis* bloom toxicity not being directly correlated with cell concentration, and raise concerns over how HABs should be monitored to avoid associated damage.

The aim of this study was to determine whether transcription of RuBisCO *rbcL* gene of *K. brevis* is affected by varying growth conditions, induced by differences in environmental chemistry. Thus, the effect of culture medium on *K. brevis* growth was examined, followed by the effect of the varying growth conditions on *rbcL* transcription and normalised *rbcL* transcription per cell. In order to investigate the difference in growth conditions, *K. brevis* was cultured in three media of varying composition. Two of them followed the L1 enrichment; however one treatment used

natural seawater for the enrichment, whereas the second L1 enrichment was added to artificial Aquil* seawater. NH-15 artificial seawater was employed for the third and final treatment in the experiment, which encompasses a larger array of vitamins and an additional sulphide mixture.

2.2 Materials and Methods

2.2.1 Experimental conditions

Karenia brevis strain CCMP2228 was employed as a model organism for the purpose of this study. The strain was obtained from the Provasoli-Guillard National Center for Culture of Marine Phytoplankton, and was originally isolated from the Gulf of Mexico, Sarasota Bay as a non-axenic culture. The strain was maintained in L1 Aquil* medium in the exponential phase of the growth curve and bellow 32,000 cells ml^{-1} until the initiation of any experimental procedures; this ensured that cultures were exponentially growing and nutrient-replete. All cultures were maintained, without shaking at 19±1 °C on a 12:12 hour light:dark cycle, under cool fluorescent light (85-95 µmol photons m^{-2} s^{-1}; measured with a LI-189 light meter LI-COR®, Lincoln, USA). Prior to the experiment, aliquots of *K. brevis* were grown in each testing media for a minimum of three generations as part of the pre-acclimation procedure. Once the required concentrations were reached, cells were gently inoculated into the experimental flasks (400-500 cells mL^{-1} final concentration).

2.2.2 Culture media

Triplicate cultures of *K. brevis* were grown in three different medium compositions: L1 Aquil*, L1 Solent SW and NH-15 media. L1 medium contains 882.5 µM $NaNO_3$, 36.2 µM NaH_2PO_4.H2O, 909 nM $MnCl_2.4H_20$, 80 nM $ZnSO_4.7H_2O$, 50 nM $CoCl_2.6H_2O$, 10 nM $CuSO_4.5H_2O$, 82.2 nM $Na_2MoO_4.2H_2O$, 10 nM H_2SeO_3, 10 nM $NiSO_4.7H_2O$, 10 nM NH_4VO_3, 10 nM K_2CrO_4, 11.7 µM $FeCl_3.6H_2O$, 11.7 µM $Na_2EDTA.2H_2O$, 2.1 nM biotin, 0.37 nM B_{12} cyanocobalamin, 296.5 nM thiamin HCl. The enrichment was added to natural seawater (L1 Solent SW), which originated from Solent Waters in the United Kingdom, and Aquil artificial seawater (L1 Aquil*) which comprised of 420 mM NaCl, 9.4 mM KCl, 55 mM $MgCl_2.6H_2O$, 10.5 mM $CaCl_2.2H_2O$, 28.8 mM Na_2SO_4, 2.38 mM $NaHCO_3$, 840 µM KBr, 63.8 µM $SrCl_2.6H_2O$, 71.4 mM NaF, 200 nM KI, 485 µM H_3BO_3 at pH 8.4.

NH-15 (Baden and Mende 1978) consists of 411 mM NaCl, 22.1 mM $MgCl_2.6H_2O$, 24.3 mM $MgSO_4.7H_20$, 6.3 mM $CaCl_2$, 8.1 mM KCl, 935 nM $MnCl_2.4H_2O$, 1.1 µM $ZrOCl_2$, 5.2 µM TiO_2, 24.3 µM H_3BO_3, 8.8 µM Na_2SiO_3, 388 nM H_2SeO_3, 360 nM $BaCl_2$, 513 nM NH_4VO_3, 283 nM K_2CrO_4, 5.2

µM $FeCl_3.6H_2O$, 99 µM KNO_3, 57 µM K_2HPO_4, 18.7 µM NH_4Cl, 11.9 µM $NaHCO_3$, 3.1 µM $Na_2S.9H_2O$, 3.7 µM KH_2PO_4, 984 nM $MgCl_2.6H_2O$, 27.8 µM inositol, 31.7 µM thymine, 17.9 µM choline chloride, 8.3 µM orotic acid, 32.6 µM thiamin HCl, 4.1 µM nicotinic acid, 1.2 µM pyridoxine, 415 nM pyridoxamine diHCl, 365 nM *para*-aminobenzoic acid, 454 nM putrescine, 66 nM riboflavin, 28 nM folic acid, 11 nM biotin, 0.55 nM B_{12} (cyanocobalamin), 3.3 mM Tris, 26.9 µM EDTA, at pH 8.4. All chemicals were of highest purity and of molecular biology grade (Sigma Aldrich, UK).

Each culture was sampled inside a laminar flow hood every two days, starting from day 0, for a total of 14 days. Samples were collected as 1 mL triplicates for cell counts and 1 mL triplicates for RNA extraction. Cell counts were performed on a Sedgewick Rafter Counting Chamber (Fisher Scientific, UK) with the use of an inverted microscope, following initial cell fixation and staining with Lugol's iodine (Sigma Aldrich, UK).

2.2.3 Internal Control (IC) RNA synthesis

The IC RNA employed in this experiment followed the same sequence as the wildtype RNA molecule of the *rbcL* gene, with a length of 87 bp. The beacon binding site however was replaced with an enterovirus sequence, which could be recognised by a second molecular beacon within our NASBA assay.

Synthesis of the IC RNA followed previously described protocols (Casper et al. 2005; Patterson et al. 2005; Tsaloglou et al. 2013) and thus a DNA template (Eurofins MWG Operon, UK) was designed containing a T3 RNA polymerase promoter at the 5' end of the sequence. The DNA template was employed for the transcription of IC RNA over the course of 2 hours at 37°C, which was then purified (RNeasy kit, Qiagen, Netherlands) and quantified (Ribogreen RNA quantification kit, Invitrogen, UK) before storage at -20°C (Tsaloglou et al. 2013).

2.2.4 RNA extraction and NASBA analysis

RNA extraction from sampled cells was achieved through the employment of three custom buffers (Table 1). Cell lysis was performed with the incubation of 1 mL sample in 1 mL Buffer A for 10 minutes, followed by the addition of an internal control (IC) at 800 copies per sample, and 50 µL magnetic bead stock (bioMérieux, UK, Limited); mixing via vortexing took place after each step. After a further 10 minute wait, samples were centrifuged, and the supernatant was removed mechanically with the use of pipettes. The remaining beads were then washed twice with 500 µL Buffer B, while magnetically attached and mixed on a NucliSENS® miniMAG® for 30 seconds at a time. RNA was eluted from the beads using 50 µL of Buffer C, followed by shaking on an

Eppendorf thermomixer at 60°C, 1200 rpm, for 5 minutes, and removal of the supernatant. All extracted RNA was stored at -20°C until the initiation of NASBA® analysis. All chemicals were molecular biology grade (Sigma Aldrich, UK).

Custom RNA extraction Buffers		
Custom Buffer A	**Custom Buffer B**	**Custom Buffer C**
1% Triton X-100	0.15M LiCl	0.01M Tris pH 7.5
4M GuSCN	1mM EDTA	
0.5M LiCl	0.01M Tris pH 7.5	
0.01M EDTA		
0.1M Tris pH 7.5		

Table 1 Custom RNA extraction buffer composition. Buffers A, B, and C were used for lysis, washing, and elution steps, respectively.

The magnitude of transcription of a gene, or simply the amount of a specific RNA sequence, can be estimated via nucleic acid sequence based amplification (NASBA®). NASBA® is an isothermal (41°C) RNA amplification system, which is catalyzed by an enzyme mixture containing T7 RNA polymerase, avian myoblastosis virus reverse transcriptase, as well as RNaseH (Deiman et al. 2002; Walker et al. 2005). It incorporates two target-specific oligonucleotide primers and can be monitored in real-time with the incorporation of a fluorescent-signalling probe, known as a molecular beacon (Deiman et al. 2002; Walker et al. 2005). Apart from its qualitative function, NASBA® can be turned into a quantitative assay with the addition of an internal control (IC) template (Casper et al. 2005; Casper et al. 2007; Patterson et al. 2005; Ulrich et al. 2010). The IC is a synthetic RNA molecule of known concentration, identical to the assay target "wildtype" RNA sequence, but with a modified molecular beacon binding site. During the reaction, wildtype and IC sequences amplify competitively sharing the same primers and reagents but hybridizing with different molecular beacons.

NASBA® was performed using NucliSENS EasyQ® Basic Kit (bioMérieux UK Limited) and according to manufacturer instructions. The reaction targeted the RuBisCO *rbcL* gene and incorporated one set of forward/reverse primers, along with two molecular beacons: one for the targeted *K. brevis* sequence and one for the IC (Table 2). Primers and molecular beacons were obtained from Eurofins MWG Operon (London, UK). The *K. brevis* molecular beacon was labelled with Alexa Fluor 488 at the 5' end and the quencher BHQ1 at the 3' end, whereas the IC molecular beacon was labelled with CY5 at the 5' end and the quencher BHQ2 at the 3' end.

Sequence Name	Sequence (5' to 3')
K. brevis Forward Primer	**ACGTTATTGGGTCTGTGTA**
K. brevis Reverse Primer	AATTCTAATACGACTCACTATAGGGAGA**AGGTACACACTTTCGTAAACTA**
K. brevis Molecular Beacon	[AF488]-GAGTCGCTTAGTCTCGGGTTATTTTTTCGACTC-[BHQ1]
IC Molecular Beacon	[CY5]-ACGGAGTGGCTGCTTATGGTGACAATCTCCGC-[BHQ2]
K. brevis Target Sequence	GAA**ACGTTATTGGGTCTGTGTA**CACGAATTAACCTTAGTCTCGGGTTATTTTTTGGACA-AGAATGGGC**TAGTTTACGAAAGTGTGTACCT**
IC Sequence	GAA**ACGTTATTGGGTCTGTGTA**CACGAATTAACTGGCTGCTTATGGTGACAATGGACA-AGAATGGGC**TAGTTTACGAAAGTGTGTACCT**

Table 2 Sequences of *K. brevis* and IC primers, beacons, and RNA. Bold text indicates primer binding sites.

Each sample produced two reaction curves; one representing the target or "wild-type" RNA and one for the IC RNA. Transcription of RuBisCO *rbcL* gene was determined through time to positivity (TTP) ratios. TTP is the NASBA equivalent of threshold cycle (Ct) values derived in qPCR, and it is defined as the point in time where the acquired exponential curve rises above a user-set threshold of detection (TOD). Subsequent quantitation was possible by comparing the values against a standard curve (Polstra et al. 2002). Thus a TOD was initially set which in turn gave TTP values for the wild-type and IC-NASBA curves. Quantitation of target *K. brevis* cells was achieved by comparing the ratios between the wild-type and IC TTP values, which described relative RNA amplification kinetics for each sample.

Transcription of RuBisCO *rbcL* gene was determined with the acquisition of quantitation variables; MATLAB™ curve fitting tool was applied to the wildtype and IC curves of each sample, in conjunction with an equation describing the NASBA-driven RNA amplification:

$$Y(t) = \lambda Y_0 - (\lambda - 1)Y_0 \exp\left\{-{}^{1}\!/_{2}\, k_1 a_1 \left[ln\left(1 + e^{a_2(t-a_3)}\right)\right]^2\right\}$$

where Y(t) the fluorescence signal as a function of time, Y_0 the signal at t=0, λY_0 the fluorescence value at its highest point, $\alpha_1\alpha_2$ representing the shape of the curve, α_3 defining the curve location relative to the time axis, and k_1 a reaction rate constant (Weusten et al. 2002). A quantitation variable was acquired through the curve fitting procedure, defined as the $k_1 a_1 a_2^2$ ratio, which is related to the amount of target (WT) RNA in the sample, as described previously in literature (Tsaloglou et al. 2011; Weusten et al. 2002).

Finally the original *K. brevis* culture was employed to determine how normalized *rbcL* transcription per cell changed in each treatment, throughout the course of this study. The aforementioned standard curve was acquired from serial dilutions of the stock culture and by plotting TTP ratios versus cell concentration. This standard curve and its associated equation were used to convert TTP data into normalised *rbcL* transcription. During the experiment the standard curve data was combined with the ratios and cell counts of each treatment, to determine normalized *rbcL* transcription per cell.

2.2.5 Statistical analysis

Statistical analysis was performed using the Sigmaplot 11.0 statistical test package in conjunction with Microsoft Office Excel 2007 data organising tools. Differences in *K. brevis* cell growth were determined with the employment of *Wilcoxon* signed-rank test, whereas transcriptomic variation between treatments was assessed with paired t-tests. All outcomes were based on 5% level of confidence ($P<0.05$). The following hypotheses were tested: 1) There is a significant difference in *K. brevis* cell replication between the three medium conditions, 2) There is a significant difference in TTP ratios and quantitation variable between the three medium conditions.

2.3 Results and Discussion

2.3.1 Growth of *K. brevis*

All cultures were initiated with a starting concentration of 400±30 cells mL^{-1} (Figure 5) and experienced exponential growth conditions throughout the experiment. L1 Aquil* and L1 Solent seawater cells underwent an average of 0.45 div/day each, whereas the NH-15 treatment underwent 0.37 $div.day^{-1}$

There was no significant difference in *K. brevis* cell growth between the two L1 treatments (Z= 0.700, P= 0.547). In contrast there was a significantly lower growth rate (0.37 div/day) between the NH-15 treatment and the two L1 treatments (L1 Aquil* Z= -2.521, P= 0.008; L1 Solent seawater Z= -2.380, P= 0.016).

The L1 enrichments appeared to have identical effects on *K. brevis* growth despite the differences in the nature of water. Aquil* successfully imitated the growth rate achieved in natural seawater which makes it an excellent choice for cultivating phytoplankton species for physiological studies (Morel et al. 1979), since knowledge of the exact nutrient composition facilitates the assessment of environmental factors that may affect growth or transcriptomic response.

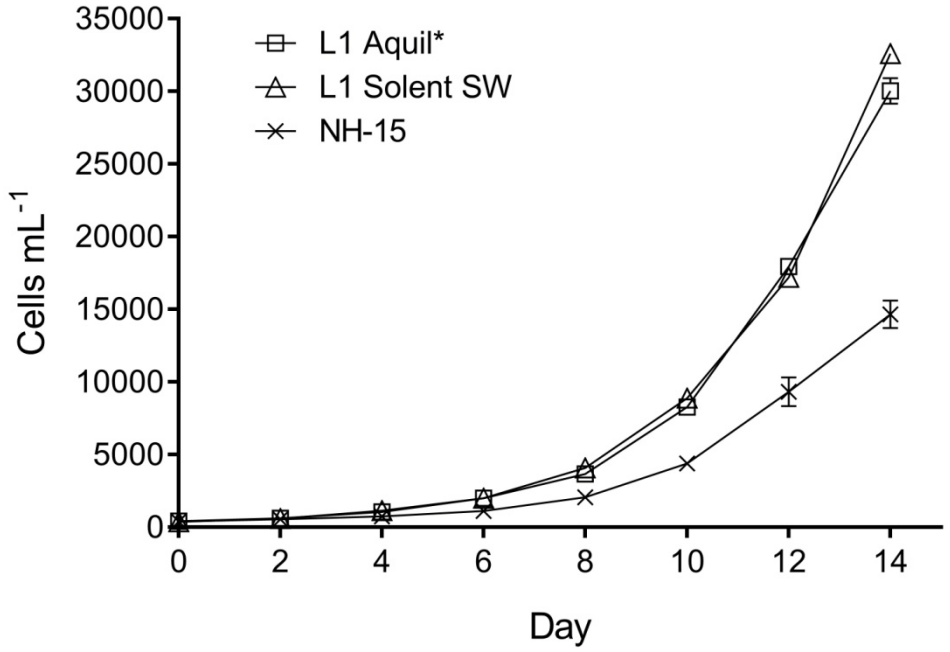

Figure 5 Growth of *K. brevis* under L1 Aquil*, L1 Solent, and NH-15 medium, over a period of two weeks. Data points represent average of triplicate samples, and standard deviation is shown in the form of error bars.

Reduced growth rates in the NH-15 cultures may have taken place for a number of reasons. First of all, the major N source (KNO_3) is one order of magnitude lower than the other two medium treatments ($NaNO_3$) which is known to be a limiting factor in *K. brevis* cultures (Morey et al. 2011). Moreover the additional sulfides and vitamin variation for medium NH-15 may have affected some the physiological aspects of *K. brevis*. Even though sulphides may support long-term growth (Vargo 2009) they may not necessarily improve the initial stages of population growth; when the different media were used for culture maintenance prior to the experiment it was always apparent that *K. brevis* grew slower in the sulphide-containing NH-15 medium, but cells generally appeared healthier (i.e. cells in-tact, more motile) and retained high numbers for longer periods of time. Biotin, B_{12} and thiamine stimulate growth in marine algae, including *K. brevis*, more than any other vitamins (Croft et al. 2006; Vargo 2009). Surprisingly, each of these vitamins are presented in lower concentrations for both L1 treatments, with thiamin differing by two orders of magnitude (0.3 µM for L1 and 32.6 µM for NH-15) and biotin being almost five times more concentrated in NH-15 medium (11 nM) compared to L1 media (2.1 nM). NH-15 medium also contains a higher diversity of vitamins due to the Vitamin 8 enrichment; folic acid, orotic acid, choline chloride, pyridoxine, riboflavin among others. Finally, the differing groups of trace metals may have also influenced growth rates; Zn, Mn, Cr, Cu, Fe, Ni, Ti, Zr, Ba, and V, are thought to be some of the elements stimulating *K. brevis* growth (Vargo 2009). The first six were included in the

L1 enrichments and seven elements (Ti, Zr, Ba, V, Mn, Cr, Fe) where part of the NH-15 trace metal mix.

K. brevis cultures experienced varying growth conditions and physiological states due to differences between the L1 and NH-15 media, and were therefore suitable for our *rbcL* expression study.

2.3.2 Transcription of *rbcL* gene

The standard curve from serial dilutions of 3 x 10^4 cells ml^{-1} (Figure 6) culture, showed a significant correlation between cell abundances and *rbcL* transcript abundance (R^2 of 0.957). A threshold of detection was set, whose value was determined by the total background signal produced by negative controls; the point at which the threshold crossed each NASBA curve was defined as TTP. Average TTP ratio values derived from IC-NASBA for each treatment appeared to follow the trend described by the standard curve, suggesting that total *rbcL* transcription at varying stages of cell growth may be constant and comparable to values of serial dilutions.

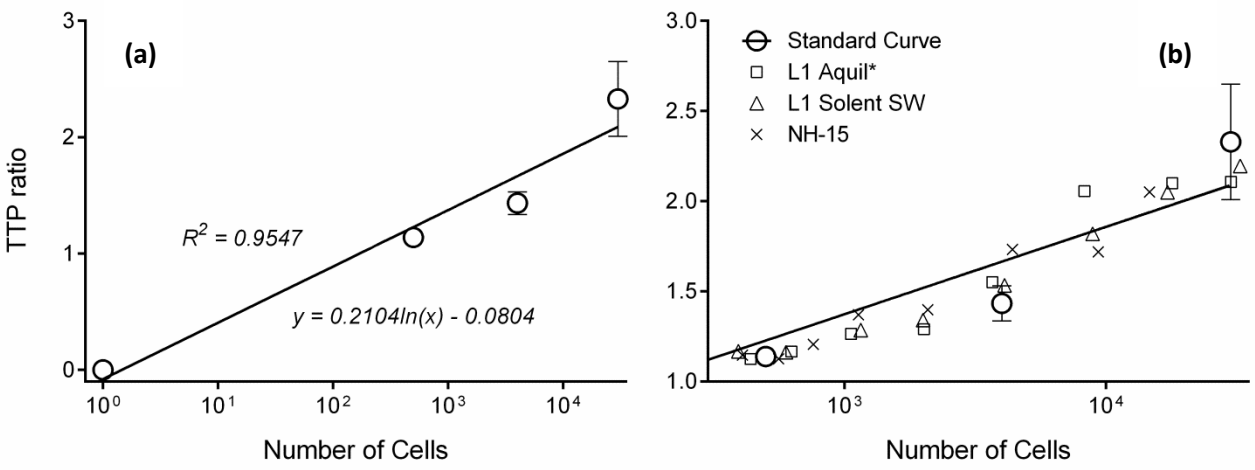

Figure 6 Standard curve of TTP ratios relative to cell number (a) as a result of culture serial dilutions starting from 3 x 10^4 cells ml^{-1}. The equation describing the trendline along with its R^2 value are shown along the trendline. TTP ratios acquired throughout the experiment were plotted along the standard curve (b), representing L1 Aquil*, L1 Solent SW, and NH-15 treatments.

Figure 7 illustrates how the TTP ratio changed in each treatment as cell concentration increased throughout the experiment. On day 0, all culture analysis resulted in TTP ratio values between 1.125 and 1.167 followed by a progressive increase over the next two weeks. On day 14 the average TTP ratio for the L1 Aquil* treatment was equal to 2.107, L1 Solent SW TTP ratio was equal to 2.195, and the NH-15 treatment reached a ratio value of 2.051. There was no significant difference in TTP ratio at any given cell concentration between any of the treatments (L1 Solent

vs. L1 Aquil: $t_{(6)}$= 0.750, P= 0.481; NH-15 vs. L1 Aquil*: $t_{(6)}$= -0.067, P= 0.949; NH-15 vs. L1 Solent SW: $t_{(6)}$= -0.903, P= 0.401).

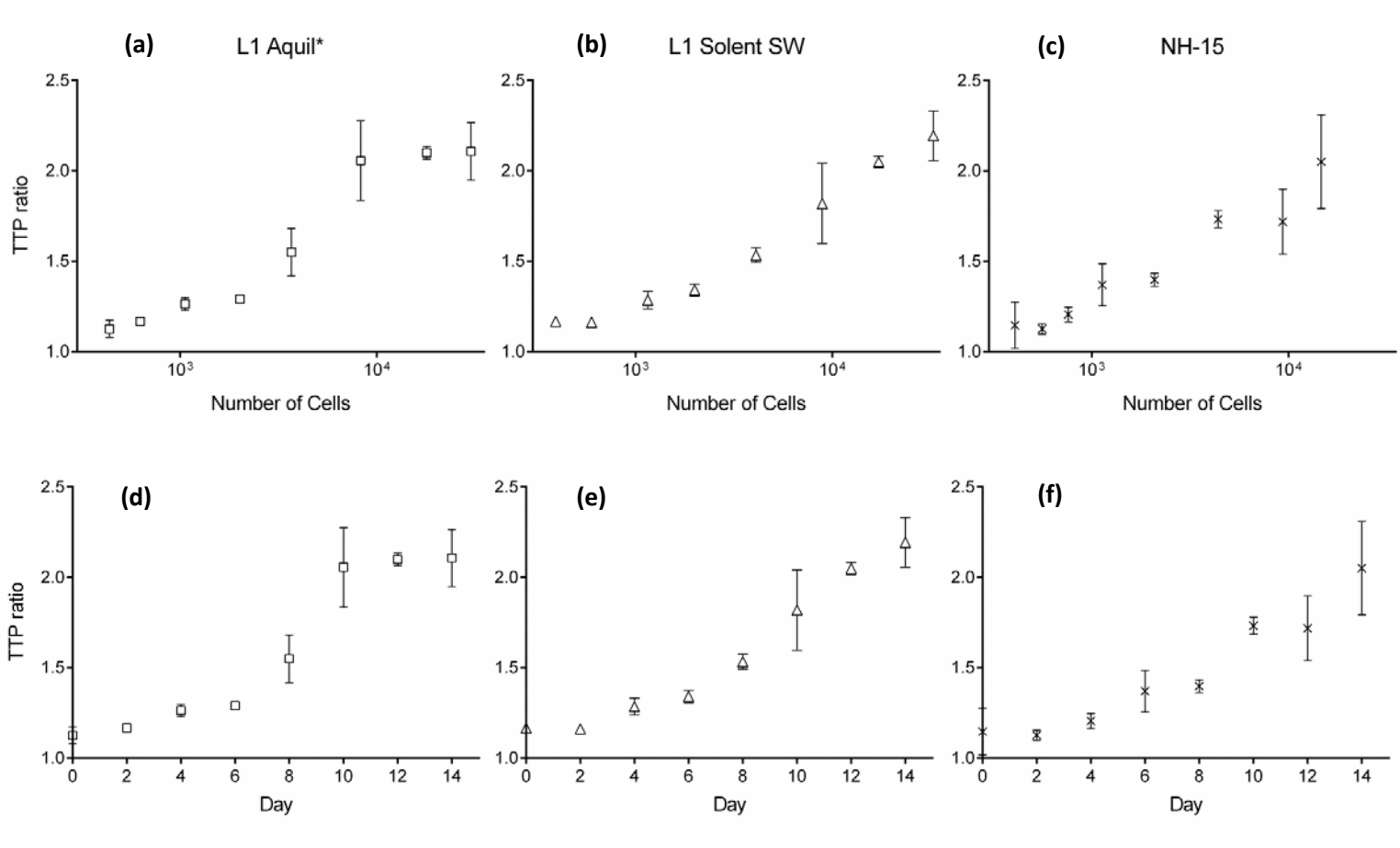

Figure 7 Relationship between TTP ratio and cell concentration (a,b,c) and over the course of the experiment (d,e,f). Treatments L1 Aquil*, L1 Solent SW, and NH-15 are depicted from left to right. Data points represent triplicate samples with associated standard deviation (error bars).

Data was taken from literature (Casper et al. 2004) to compare estimated sample cell concentration through NASBA analysis with sample cell counts (Figure 8). The comparison showed a linear correlation (R^2= 0.8905), which was further supported once our experimental results from all treatments were added to the plot (R^2= 0.8962). Note that only true positives are shown in the figure; some samples gave a positive result during NASBA analysis but their cell count was zero.

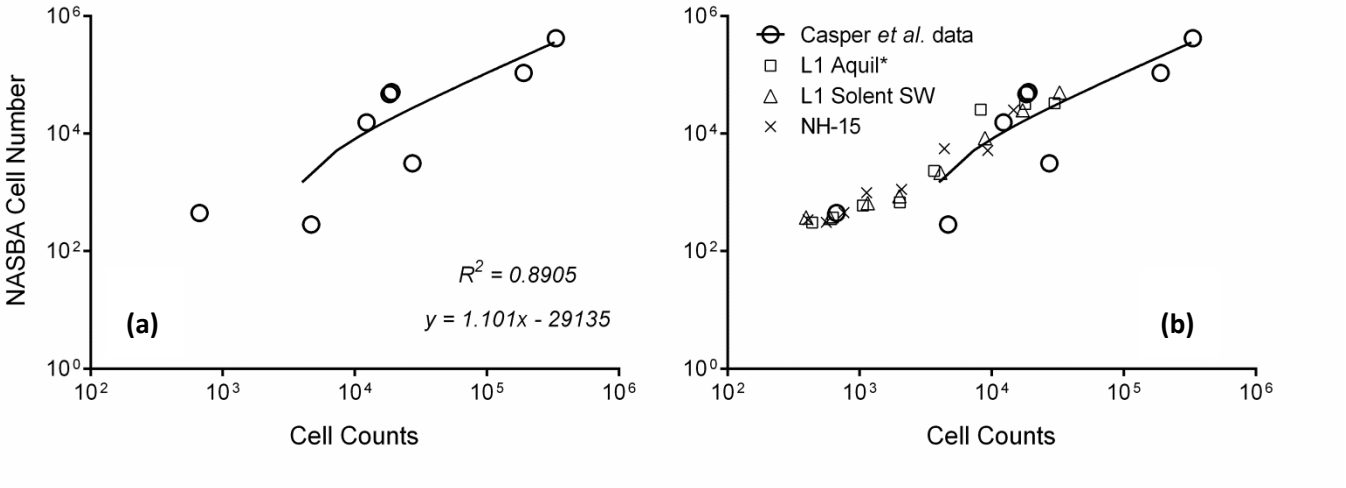

Figure 8 Data acquired by Casper et al. 2004 (a) describing how NASBA-derived *K. brevis* quantification compares to cell counts, with fitted trendline. The equation describing the trendline along with its R2 value are illustrated on the botom right corner of the figure. NASBA-derived *K. brevis* quantification versus cell counts were also depicted for L1 Aquil*, L1 Solent SW, and NH-15 treatments along with the Casper et al. data and associated trendline (b). Treatment data values represent averages of triplicate samples.

Figure 9 illustrates how the quantitation variable changed in each treatment throughout the experiment. On day 0, all cultures experienced $ln(k_1a_1a_2^2\ ratio)$ values between 0.655 and 0.986 followed by a progressive increase over the next two weeks. On day 14 the average ratio for the L1 Aquil* treatment was equal to 3.945, whereas L1 Solent SW and NH-15 cultures reached ratio values of 3.593 and 3.478 respectively

There was no significant difference in $ln(k_1a_1a_2^2\ ratio)$ at any given cell concentration between the two L1 treatments ($t_{(6)}$= -1.992, P= 0.094). Furthermore there was no significant difference in $ln(k_1a_1a_2^2\ ratio)$ when comparing equivalent cell concentrations of the NH-15 medium with either the L1 Aquil* ($t_{(6)}$= -2.247, P= 0.066) or the L1 Solent SW ($t_{(6)}$= -0.853, P= 0.427) treatments.

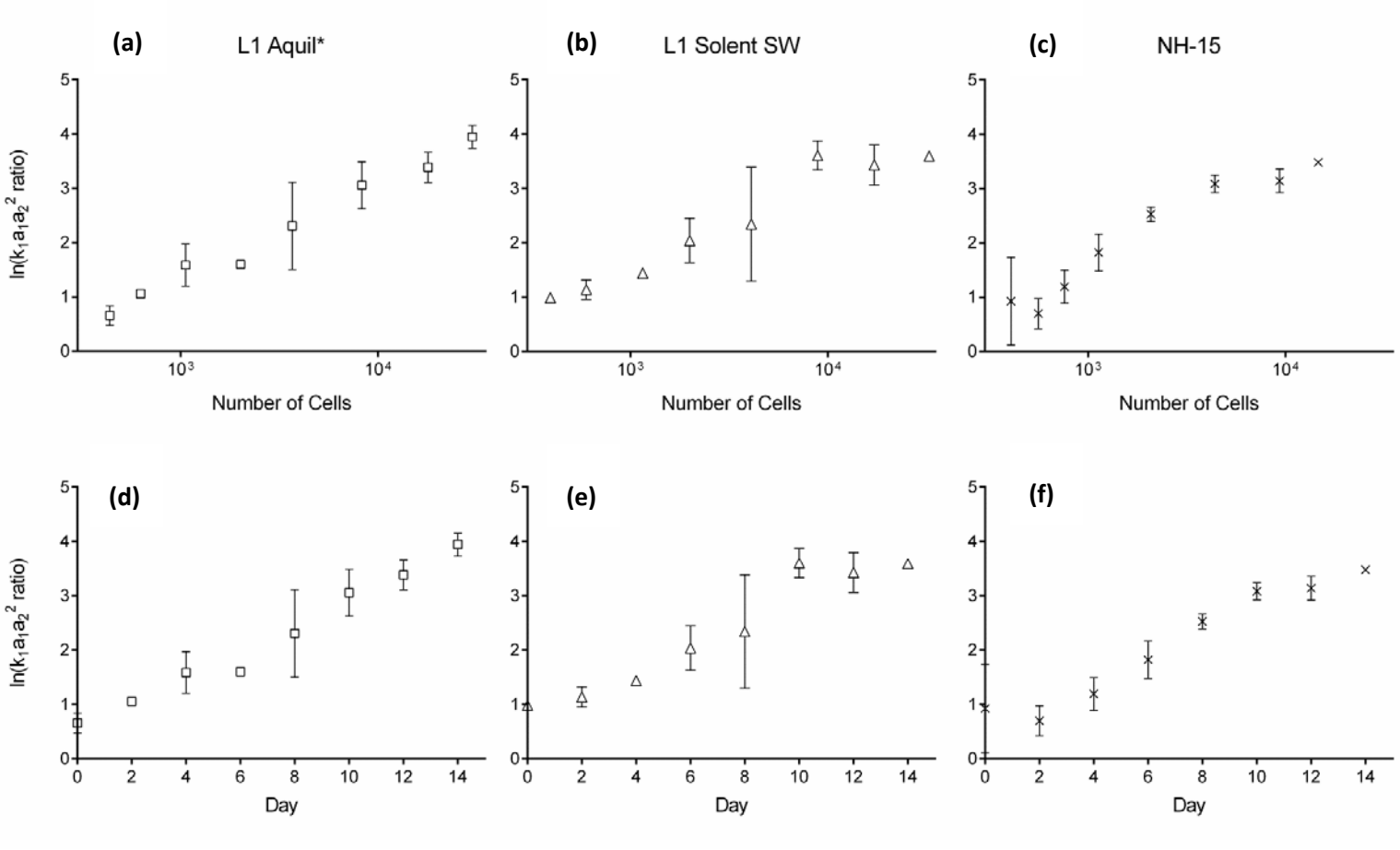

Figure 9 Relationship between $ln(k_1a_1a_2^2\ ratio)$ and cell concentration (a,b,c) and over the course of the experiment (d,e,f). Treatments L1 Aquil*, L1 Solent SW, and NH-15 are depicted from left to right. Data points represent triplicate samples with associated standard deviation (error bars).

The equation describing our standard curve was combined with acquired TTP ratios and recorded cell concentrations; thus we were able to determine how normalized *rbcL* transcription per cell changed over the course of the experiment. Normalized *rbcL* transcription per cell changed in each treatment as cell concentration increased (Figure 10). On day 0, all normalized *rbcL* transcription analysis showed values between 0.717 and 0.982 followed by a progressive increase over the next two weeks. On day 14 relative normalized *rbcL* transcription per cell was equal to 1.342 for the L1 Aquil* treatment, 1.749 for L1 Solent SW and 2.813 for NH-15.

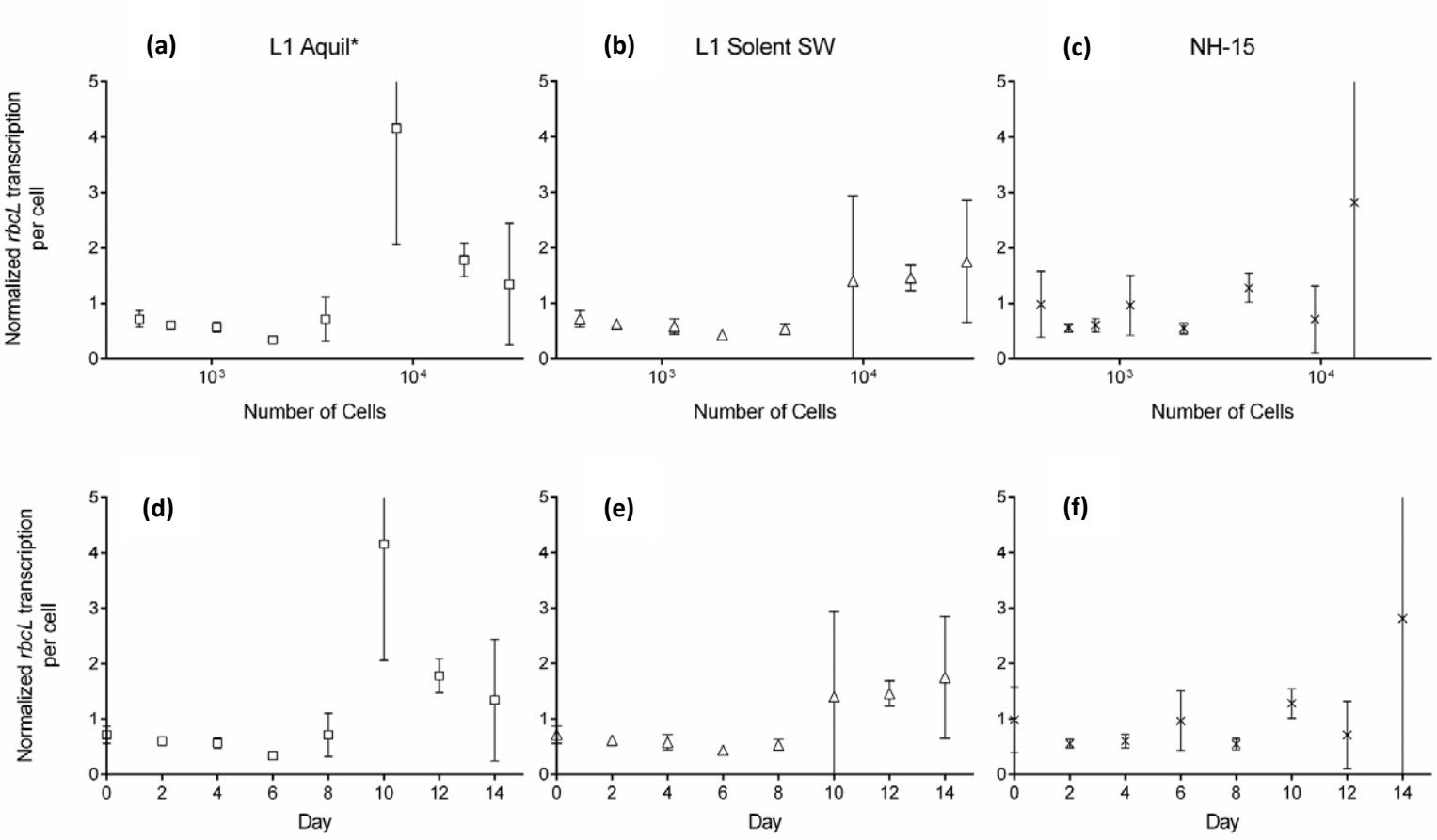

Figure 10 Normalized *rbcL* transcription per cell over increasing cell concentration (a,b,c) and over the course of the experiment (d,e,f). Treatments L1 Aquil*, L1 Solent SW, and NH-15 are depicted from left to right. Data points represent triplicate samples with associated standard deviation (error bars).

When plotting the $ln(k_1 a_1 a_2^2 ratio)$ or TTP ratios against log cell concentration (Figure 7, Figure 9) a similar linear trend was followed between treatments, suggesting that the expression of the RuBisCO *rbcL* gene in *K. brevis* was not affected by media composition or growth rate. Moreover, all experimental TTP data was situated along the trendline defined by our standard curve (Figure 8). As the standard curve values were acquired from serial dilutions of a *K. brevis* culture, and thus were unaffected by growth or other external parameters, it appears that *rbcL* expression may be sufficiently conserved throughout population growth. Average normalized *rbcL* transcription per cell (Figure 10) increased during the later stages of the experiment for the L1 treatments, as cell concentration increased, which may indicate a change in cellular carbon fixing activity over varying growth stages.

Standard deviation between triplicate samples also increased dramatically (day 8 for figure 9; days 10 and 14 for Figure 10) suggesting that RNA extraction at high cell concentrations may become more variable. The results could be misinterpreted as they could either be a product of additional cell interactions, as population increased, or because of increased probability of

pipetting error due to higher cell densities. The experiment took place over a two-week period, so it was not possible to determine if the trend continued at higher cell concentrations, as cultures neared the stationary phase. Nevertheless, results comparing conventional RNA extraction, via pipetting, to sample pre-concentration using a filtering device (see Chapter 5) verify that the conventional method experiences significant variation in amount of extracted RNA at increasing cell concentrations.

Despite clear physiological variation between treatments, *rbcL* transcript abundances correlated with cell abundances, supporting previous conclusions that IC-NASBA targeting *rbcL* could be used as a reliable technique for the quantification of *K. brevis* (Casper et al. 2004) in various physiological states. These results also support previous results describing the high sensitivity of IC-NASBA at lower cell concentrations a crucial aspect of the assay, as *K. brevis* is not always detected via microscopy and its toxicity can have harmful effects even if its population surpasses as little as 5 cells mL^{-1} in culture (Bricelj et al. 2012).

It is interesting to note that some of the Casper *et al.* 2004 environmental samples (below 1000 cells L^{-1}; Figure 8) detected *K. brevis* cells through sample NASBA analysis, though they were undetected by cell counts from the same samples. This might be expected due to the typical limits of detection of cell counts by standard microscopy (LeGresley and McDermott 2010) and the phenotypic plasticity of *K. brevis* in the environment (Haywood et al. 2004). Alternatively, the NASBA assay may be amplifying non-specific transcripts, but this remains untested. The false negatives suggest that cells may not always be preserved for microscopy studies; in the case of toxic or HAB-inducing species, such as *K. brevis*, the employment of molecular methods for HAB monitoring may therefore be encouraged (Costa et al. 2004). Molecular assays such as NASBA or reverse transcription PCR with the addition of melting curve specificity analysis may provide more accurate results when it comes to detecting live cells. During our experiment, cells were successfully detected both through IC-NASBA and microscopy counts for each sample.

It should be noted that, although the *rbcL* gene has been described to be relatively conservative, its transcription has been shown to follow clear patterns of diel variation, with maxima and minima observed at dawn and in the dark respectively (Ashworth et al. 2013; Scott L Pichard et al. 1993; Scott L. Pichard et al. 1996; Zinser et al. 2009). For instance, studies on the marine coccolithophore *Coccolithus pelagicus* and a strain of the marine cyanobacterium *Prochlorococcus* showed that *rbcL* transcription usually peaked around the onset of the light period, and then proceeded to decline in 12 h before the cycle repeated (Wyman et al. 2005; Zinser et al. 2009). Another study on *Prochlorococcus* has even indicated that the observed diel pattern of *rbcL* transcription may be rhythmically entrained (Scott L. Pichard et al. 1996). It would not be unlikely

that dinoflagellates, including *K. brevis*, follow a similar trend; a diel expression rhythm of form II RuBisCO has already been shown for the marine dinoflagellate *Prorocentrum donghaiense* (Shi et al. 2013). Nevertheless, the results presented in this Chapter followed a strict sampling plan, with measurements representing the same point of each light:dark cycle; thus any transcriptional variation as a result of a potential diel trend should be minimal. To further minimise quantification errors in RNA-based techniques, non-protein coding genes (e.g. rRNA and snRNA) may be preferred as alternative targets (Johnson and Martiny 2015). It is safe to conclude that gene expression in phytoplankton is an area that requires further research. To gain a better understanding of phytoplankton physiology, gene expression and their related patterns, highly expressed or repressed gene groups need to be further identified, as well as processes and environmental variables that may affect their response.

IC-NASBA was chosen and preferred amongst other molecular methods of detection for a number of reasons. The sensitivity of RNA towards nucleases combined with its short half-life makes it an ideal candidate when validating physiological activity of organisms in the environment (Costa et al. 2004). NASBA is capable of achieving as much as 10^{14}-fold target amplification within 90 minutes, and is considered robust and efficient as a molecular method (Perlin and Zhao 2009). This allows for low detection limits, which can be reduced even further with the incorporation of filtering systems during seawater sampling. Furthermore NASBA is an isothermal reaction (41^{o}C) with a single melting step at 65^{o}C, making it a preferable method of nucleic acid amplification for biological sensors, or platforms where energy usage is a concern.

2.4 Conclusions

Rapid, accurate, and reliable detection and quantification of toxic microalgae *K. brevis* is needed to monitor potential HAB formation. This study shows that detection and quantification can be successfully achieved under laboratory conditions, by targeting the *rbcL* gene through the employment of NASBA along with IC. Despite the detected differences in growth, deriving from the chemically varying culture conditions, the transcriptomic response of *K. brevis* reference gene was not affected. This method could therefore facilitate *in situ* HAB monitoring and sample analysis, and may either be used as an alternative option or run in parallel with conventional HAB monitoring techniques. The results however do not necessarily reflect cell toxicity, which should also be taken into account when studying toxic species. Polyketide synthesis (PKS) genes, for instance, have been shown to be involved in toxin production of two dinoflagellate species (Kohli et al. 2015) and there have been indications that *K. brevis* PKS expression may also be associated with brevetoxin synthesis (López-Legentil et al. 2010; Monroe et al. 2010). Thus this research may follow two distinct pathways: 1) IC-NASBA could be applied for the detection and quantification of

K. brevis in environmental samples, and compared to our laboratory findings, and 2) *rbcL* expression could be studied in parallel with PKS gene expression, in order to assess how brevetoxin synthesis may vary in *K. brevis* under different growth and physiological conditions.

Chapter 3: Preservation and long-term storage of NASBA assay for the detection and quantification of marine microorganisms

3.1 Introduction

Microfluidic devices often need additional support equipment, such as fridges and freezers to adequately store reagents, limiting their *in situ* application (Garcia et al. 2004). An important requirement for the implementation of portable platforms conducting molecular assays on-field is the long-term preservation of reagents and enzymes. Since many biochemicals cannot be stored adequately in solvents, dry-form preservation is a useful alternative, which would provide sufficient portability and protect reagents from stresses associated with shipping, outdoor transportation, and environmental temperature.

Lyophilisation (freeze-drying) is commonly used for the long-term storage of solid protein pharmaceuticals (W. Wang 2000); a cost-intensive process during which the sample undergoes dehydration under low temperature, typically between -40^{o}C and -50^{o}C, and high vacuum conditions (Kasper and Friess 2011). Lyophilization, however, can also unfold/denature proteins, due to ice-crystal formation, pH and solute concentration changes (W. Wang 2000). Protein stability is therefore protected with the incorporation of various stabilizers in the form of sugars (Kadoya et al. 2010). As explained in Chapter 1, trehalose is a non-reducing disaccharide and thus does not undergo the protein-damaging Maillard reaction (Patist and Zoerb 2005). It retains a glassy state, resulting in high viscosity and low mobility, up to 106^{o}C. During the lyophilisation process, water is substituted with sugar molecules whilst drying, and the proteins are therefore protected from degradation and crystallisation.

Dry reagent storage has also been implemented by desiccating samples, under the presence of the disaccharides sucrose and trehalose (Stevens et al. 2008). Reagents were simply dehydrated at 35^{o}C, without the need for any additional freezing step or incubation, and retained 80-96% of their activity after two months of storage at temperatures between 4°C and 45°C. The interactions between the –OH groups of the two disaccharides and water molecules are closely similar in energy and configuration (Franks and Auffret 2008) and will therefore form hydrogen bonds with proteins in solution, protecting their tertiary structure and overall physical state (Arakawa et al. 2001; Crowe et al. 1998). In addition, sucrose and trehalose also undergo a transition during the preservation process, forming the aforementioned glassy solid which potentially provides additional protection from external stress (Crowe et al. 1998).

The aim of this study is to preserve the reagent and enzyme mastermix components of a NASBA assay, for bench-top and on-chip application. Reagent mastermix preservation was attempted with the employment of a gelifying agent provided by Biotools (Spain), and enzymes were preserved through dehydration with the incorporation of disaccharides. Bench-top tests were

made to evaluate the preservation methods, so that on-chip application could ensue using a microfluidic device in Chapter 4.

3.2 Materials and Methods

3.2.1 Algal cell culture

Karenia mikimotoi strain PLY497A was employed for initial reagent gelification experiments. The species was obtained from the Marine Biological Association, and was originally isolated from the English Channel as a non-axenic culture. *K. mikimotoi* was maintained in static cultures at 19±1°C in Aquil* L1 medium, and with a 12 hour photoperiod using cool fluorescent light (85-95 µmol photons m^{-2} s^{-1}; measured with a LI-189 light meter LI-COR®, Lincoln, USA). The Aquil* L1 medium contained 882.5 µM $NaNO_3$, 36.2 µM NaH_2PO_4.H2O, 909 nM $MnCl_2.4H_20$, 80 nM $ZnSO_4.7H_2O$, 50 nM $CoCl_2.6H_2O$, 10 nM $CuSO_4.5H_2O$, 82.2 nM $Na_2MoO_4.2H_2O$, 10 nM H_2SeO_3, 10 nM $NiSO_4.7H_2O$, 10 nM NH_4VO_3, 10 nM K_2CrO_4, 11.7 µM $FeCl_3.6H_2O$, 11.7 µM $Na_2EDTA.2H_2O$, 2.1 nM biotin, 0.37 nM B_{12} cyanocobalamin, 296.5 nM thiamin HCl, 420 mM NaCl, 9.4 mM KCl, 55 mM $MgCl_2.6H_2O$, 10.5 mM $CaCl_2.2H_2O$, 28.8 mM Na_2SO_4, 2.38 mM $NaHCO_3$, 840 µM KBr, 63.8 µM $SrCl_2.6H_2O$, 71.4 mM NaF, 200 nM KI, 485 µM H_3BO_3; the pH was 8.5±0.1.

Karenia brevis strain CCMP2228 was employed for long-term reagent preservation and all enzyme preservation experiments. The species was obtained from the Provasoli-Guillard National Center for the Culture of Marine Phytoplankton, and was originally isolated from the Gulf of Mexico, Sarasota Bay as a non-axenic culture. *K. brevis* was maintained in static cultures at 19±1°C in natural seawater (Solent, UK) containing L1 medium enrichment, and with a 12 hour photoperiod using cool fluorescent light (85-95 µmol photons m^{-2} s^{-1}; measured with a LI-189 light meter LI-COR®, Lincoln, USA). The L1 medium contained 882.5 µM $NaNO_3$, 36.2 µM NaH_2PO_4.H2O, 909 nM $MnCl_2.4H_20$, 80 nM $ZnSO_4.7H_2O$, 50 nM $CoCl_2.6H_2O$, 10 nM $CuSO_4.5H_2O$, 82.2 nM $Na_2MoO_4.2H_2O$, 10 nM H_2SeO_3, 10 nM $NiSO_4.7H_2O$, 10 nM NH_4VO_3, 10 nM K_2CrO_4, 11.7 µM $FeCl_3.6H_2O$, 11.7 µM $Na_2EDTA.2H_2O$, 2.1 nM biotin, 0.37 nM B_{12} cyanocobalamin, 296.5 nM thiamin HCl; the pH was 8.5±0.1.

3.2.2 RNA isolation

This section describes the methods used for the extraction of cellular contents from the algal cell cultures and subsequent RNA extraction and purification. For *K. mikimotoi* a commercial extraction kit (NucliSENS miniMAG®, bioMérieux, UK, Limited) was used and the protocol supplied by the manufacturer was followed. For *K. brevis* the same process was used but with the custom

buffers described in Chapter 1. All chemicals were of highest purity and of molecular biology grade (Sigma-Aldrich, UK).

All samples were taken directly from the *K. mikimotoi* and *K. brevis* cultures by pipetting volumes of 1 mL. *K. mikimotoi* samples were then placed into a tube containing 2 mL of commercial lysis buffer, giving a final volume of 3 mL; the lysis buffer was provided by the manufacturer. *K. brevis* samples were placed into a tube containing 1 mL of custom lysis buffer, giving a final volume of 2 mL; the custom lysis buffer contained 100 mM Tris-HCl (pH 7.5), 4 M GuSCN, 500 mM LiCl, 10 mM EDTA and 1 % (v/v) Triton X-100. Samples were then incubated for ten minutes; 50 µL of magnetic bead stock (bioMérieux, UK, Limited) was then added; followed by a further ten-minute incubation, to complete cell lysis. Mixing between each step was induced via vortexing.

All samples were then washed according to the following procedures. Samples were centrifuged (1500 x g for two minutes) and pipetting was used to remove and discard the supernatant solution. For washing of *K. mikimotoi*, the manufacturers kit instructions were followed. For *K. brevis*, 500 µL of a custom washing buffer was added to the remaining beads; the custom washing buffer contained 10 mM Tris-HCl (pH 7.5), 150 mM LiCl and 1 mM EDTA. Samples were then transferred to a NucliSENS® miniMAG® and subjected to magnetic attraction and mixing for thirty seconds. A subsequent 500 µL of the custom washing buffer was used to wash the beads a second time.

Finally, samples were eluted with the addition of 25 µL of commercial elution buffer (custom elution buffer in the case of *K. brevis*; 10 mM Tris-HCl, pH 7.5), followed by shaking on an Eppendorf thermomixer at 60°C, 1200 rpm, for five minutes. Samples were then placed on a magnetic rack and the supernatant containing the RNA was removed. All extracted RNA samples were stored at -20°C in preparation for NASBA® analysis.

3.2.3 Nucleic Acid Sequence Based Amplification (NASBA)

All NASBA reactions were carried out using reagents and enzymes supplied in the NucliSENS® EasyQ Basic Kit v2 (bioMérieux UK Limited), and custom oligonucleotide primers and molecular beacon probes (Table 3). NASBA was carried out using a bench-top micro-plate reader (EasyQ analyser, bioMerieux, Netherlands), according to the manufacturers recommendation, with modifications for the use of preserved reagents and enzymes as described in the following sections. NASBA was used to amplify an 87 nucleotide sequence within the RuBisCO (*rbcL*) gene transcript encoded on *K. brevis*, or alternatively a 93 nucleotide sequence within the RuBisCO (*rbcL*) gene transcript encoded on *K. mikimotoi* (Ulrich et al. 2010). RNA amplification was measured in real time, based on the fluorescence output from a molecular beacon probe

modified to contain Cy5 at its 5' terminus and ECLIPSE at its 3' terminus for *K. mikimotoi* or BHQ2 for *K. brevis*. Primers and molecular beacons were obtained from Eurofins MWG Operon (London, UK). NASBA amplification followed a 2-step procedure in which the RNA template was mixed with oligonucleotide primers, molecular beacon probes, and a reaction buffer (reagent mastermix), and heated to 65 ^{o}C for 2 minutes for optimal primer annealing. The reaction mixture was then cooled to 41 ^{o}C prior to addition of enzyme mastermix. Amplification proceeded at 41°C for 60 to 120 minutes.

K. mikimotoi	Sequence (5' to 3')
Forward Primer	**AACCTAAAATGATTAAAGGA**
Reverse Primer	AATTCTAATACGACTCACTATAGGGAGGAGA**CCCATTCTTGCGAAAAATAA**
Molecular Beacon	[CY5]- CGATCGAACAACTAAACATGATTTTGCGATCG -[ECLIPSE]
Target Sequence	**AACCTAAAATGATTAAAGGA**TTTTATAAGACACTTCTGGATTTAACAACTAA-ACATGATTTTGCTTACGGTCT**TTATTTTTCGCAAGAATGGG**
K. brevis	Sequence (5' to 3')
Forward Primer	**ACGTTATTGGGTCTGTGTA**
Reverse Primer	AATTCTAATACGACTCACTATAGGGAGA **AGGTACACACTTTCGTAAACTA**
Molecular Beacon	[CY5]-GAGTCGCTTAGTCTCGGGTTATTTTTTCGACTC-[BHQ2]
Target Sequence	**ACGTTATTGGGTCTGTGTA**CACGAATTAACCTTAGTCTCGGGTTATTTTTTGG-ACAAGAATGGGC**TAGTTTACGAAAGTGTGTACCT**

Table 3 List of the sequences of *K. mikimotoi* primers, beacons, and RNA (top); and the sequences of *K. brevis* primers, beacons, and RNA. Bold underlined text indicates primer binding sites.

3.2.4 Reagent mastermix preservation

The preserved NASBA reagent mastermix was prepared using the reagents supplied in the NucliSENS® EasyQ Basic Kit v2 (bioMérieux UK Limited), a set of oligonucleotide primers and molecular beacon probes (Table 4) and a patented reagent stabilisation (Gelification) component (BioTools B&M Labs S.A., Madrid, Spain). Each Gelified reagent mixture contained 800 nM forward primer, 800 nM reverse primer, 200 nM wild-type molecular beacon, 200 nM IC molecular beacon, 200 nM KCl, 160 mM gelifying agent, in a final volume of 100 µL with the addition of the kit-supplied lyophilised reagent sphere. The mixture was added in sterile, nuclease free polycarbonate tubes (10 µL aliquots) and dehydrated at 35°C and 30 mbar for 35 minutes. The preserved reagents remained in a gelified state at 4°C for the remainder of the experiment. Prior to each NASBA reaction, gelified reagent mixtures were rehydrated with the addition of 6 µL nuclease-free water (Ambion) and mixed well via vortexing.

Reagent	Stock Volume used for Mastermix	Master mix Concentration
Reagent diluent	65 µL	-
Forward primer	2.00 µL	800 nM
Reverse primer	2.00 µL	800 nM
Molecular beacon	2.00 µL	200 nM
KCl	12.80 µL	200 nM
Gelifying Agent	12.20 µL	160 mM
	=96 µL	-

Table 4 NASBA reagent mastermix prepared for gelification. This is an adjusted protocol for use with the NucliSENS® EasyQ Basic Kit v2 and with the inclusion of the gelifying agent. The mixture contains all the reagent components needed for NASBA; the kits lyophilised reagent sphere is added to the final solution and preserved via dehydration.

3.2.5 Enzyme mastermix preservation

The preserved NASBA enzyme mastermix was prepared using enzymes supplied in the NucliSENS® EasyQ Basic Kit v2 (bioMérieux UK Limited), and a sugar solution containing 50% (w/v) each of sucrose and trehalose in sterile, nuclease free water (Table 5). Each enzyme-sugar mixture contained 10% (w/v) of each disaccharide in a total volume of 50 µL with the addition of the kit-supplied lyophilised enzyme sphere. The mixture was added in sterile, nuclease free polycarbonate tubes (5 µL aliquots) and dehydrated at room temperature (25°C) and 30 mbar overnight (approximately 16 hours). The resulting preserved enzymes remained in this dried state, at room temperature, for the remainder of the experiment. Prior to each NASBA reaction, the dry enzyme mixture was rehydrated with the addition of 4.5 µL nuclease-free water (Ambion) and mixed gently via pipetting.

Reagent	Stock volume used for master mix	Master mix Concentration
Enzyme diluent	35 µL	-
Disaccharide mixture	10 µL	10% (w/v)
	=45 µL	-

Table 5 NASBA enzyme mastermix prepared for preservation with disaccharides. This is an adjusted protocol for use with the NucliSENS® EasyQ Basic Kit v2 and with the inclusion of sucrose and trehalose. The mixture contains all the enzyme components needed for NASBA; the kits lyophilised enzyme sphere is added to the final solution and preserved via dehydration.

3.3 Results and Discussion

3.3.1 Reagent and enzyme mastermix preservation

Hydrated NASBA master-mixtures were usually prepared using the commercially available EasyQ Basic Kit. These preparations are unstable at room temperature, must be stored at -80°C and deteriorate quickly without refrigeration. Dry preservation of these mixtures can significantly extend their lifetime, and is a requirement for the development of deployable or portable lab-on-a-chip NASBA apparatus. Accordingly, a method was developed for preparing stabilised reagent and enzyme mixtures, which could be stored for long periods (weeks to months) while kept at room temperatures or cool conditions.

Benchtop NASBA was performed targeting the RuBisCo *rbcL* gene of *K. mikimotoi*, and preservation was initially evaluated by combining the gelified reagents with freshly prepared NASBA enzymes. Gelified reagents were rehydrated immediately before use and compared to reactions carried out using freshly prepared reagents from the EasyQ Basic Kit. Pre-preserved reactions were successful despite the addition of gelifying agent to the reagent mastermix at a final concentration of 160 mM (Figure 11). When compared to a positive control (no additions to either NASBA mastermix) it was evident that the reagent mastermix containing gelifying agent delayed RNA amplification by approximately ten to fifteen minutes. Furthermore the gelifying agent appeared to affect maximum fluorescence with the positive control reaching almost double relative fluorescence values. Nonetheless, initial results appeared promising for the continuation of long-term preservation experiments despite the projected negative effects. One of the aims within this thesis is to successfully quantify our target microorganism, which is achieved with the incorporation of an internal control of known concentration (as demonstrated in Chapter 2); amplification of both wild-type and IC RNA would be equally affected by the presence of gelifying agent and thus, the changes in reaction kinetics illustrated in Figure 11 should not inhibit quantification properties of IC-NASBA.

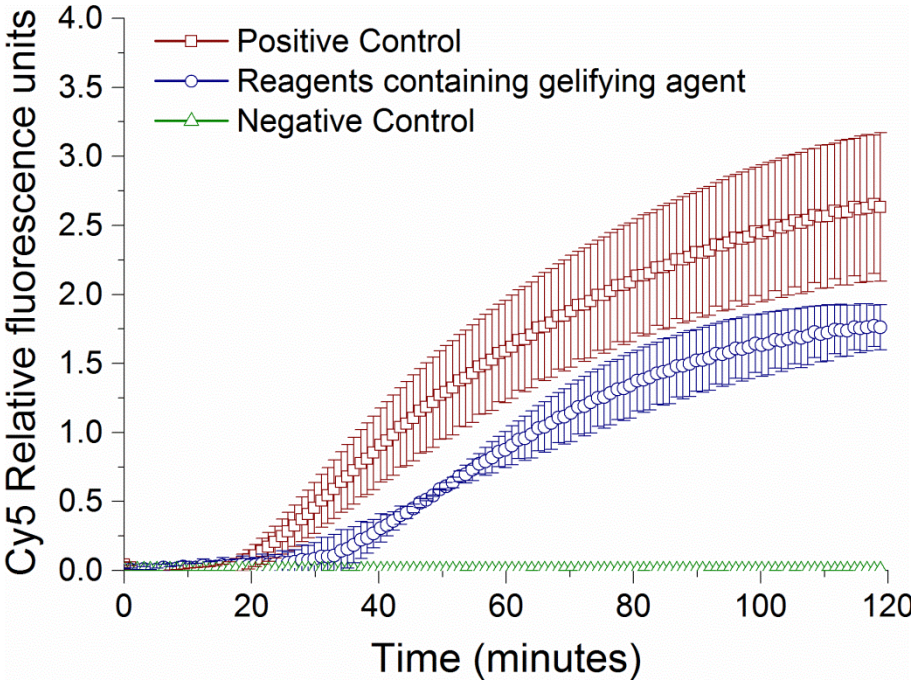

Figure 11 Real-time bench-top NASBA on *K. mikimotoi* RNA. One treatment uses a reagent master-mixture containing 160 mM gelifying agent (blue circles) and is plotted against a positive control (red squares) and a negative control (green triangles). Error bars represent standard deviation between triplicate samples.

Bench-top NASBA was performed targeting the RuBisCo *rbcL* gene of *K. brevis*, and preservation was initially evaluated by combining the dehydrated, sugar-containing enzymes with freshly prepared NASBA reagents. Preserved enzymes were rehydrated immediately before use and compared to reactions carried out using freshly prepared enzymes from the EasyQ Basic Kit. Pre-preserved reactions were successful despite the addition of sucrose and trehalose to the enzyme mastermix at a final concentration of 10% (w/v) (Figure 12). When compared to a positive control (no sugar additions to NASBA reaction) it was evident that the disaccharide-containing enzyme mastermix delayed RNA amplification by approximately three to five minutes. The error bars, representing standard deviation between triplicate samples, indicate that there was no significant difference in maximum fluorescence between positive control and experimental samples. The physico-chemical properties of trehalose, and to a lesser extent sucrose, are widely regarded to facilitate the preservation of protein structure (Franks and Auffret 2008; Stevens et al. 2008). Specifically, trehalose may replace the hydration layer of a protein to stabilise its tertiary structure during dehydration (Arakawa et al. 2001; Franks and Auffret 2008). When the enzyme-trehalose complexes are re-hydrated the trehalose is substituted and the hydration layer is re-formed.

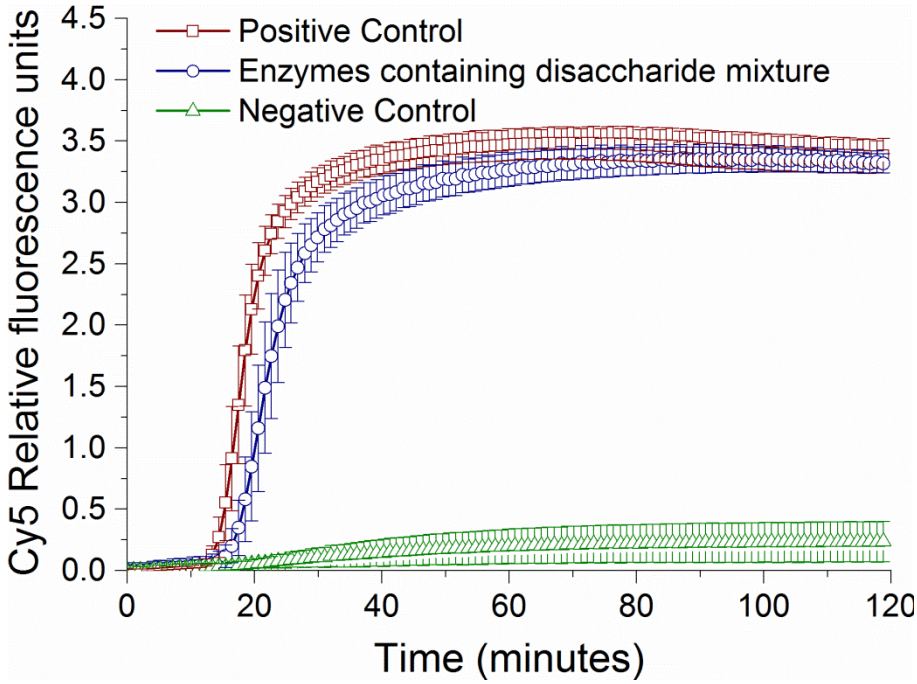

Figure 12 Real-time bench-top NASBA on *K. brevis* RNA. One treatment uses an enzyme master-mixture containing 10% (w/v) sucrose and trehalose (blue circles) and is plotted against a positive control (red squares) and a negative control (green triangles). Error bars represent standard deviation between triplicate samples.

Benchtop NASBA was performed targeting the RuBisCo *rbcL* gene of *K. brevis*, and using preserved enzyme and reagent master-mixtures, after short and long-term storage. Enzymes were dehydrated under the presence of disaccharides (10% w/v final concentration) and stored at room temperature for 24 hours and up to 5 months. Reagents were dehydrated under the presence of gelifying agent (160 mM final concentration) and stored under cool conditions (4°C) for 6-11 months.

The results demonstrate successful preservation of the NASBA enzyme mastermix for up to six weeks, and the NASBA reagent mastermix for up to six months. The stored mixtures supported RNA amplification, even after the enzymes had been kept at ambient temperatures for up to six weeks (Figure 13). Signs of RNA amplification started around the 15-minute mark for almost all reactions, and at 18 minutes for the reaction containing 1-week-old enzymes and 6-month-old reagents. However any observed differences between the NASBA curves are likely associated with the quality of the RNA samples, which were extracted prior to each run. Reactions attempted after 6 weeks of enzyme storage and 6 months of reagent storage gave a negative result. Thus the lifespan of the preserved enzyme mastermix was somewhere between 6 weeks and 5 months. The gelified NASBA reagent mastermix has been shown to last for a period of up to 8 months (Tsaloglou et al. 2013); therefore reagents must have expired sometime between 8 and 11 months.

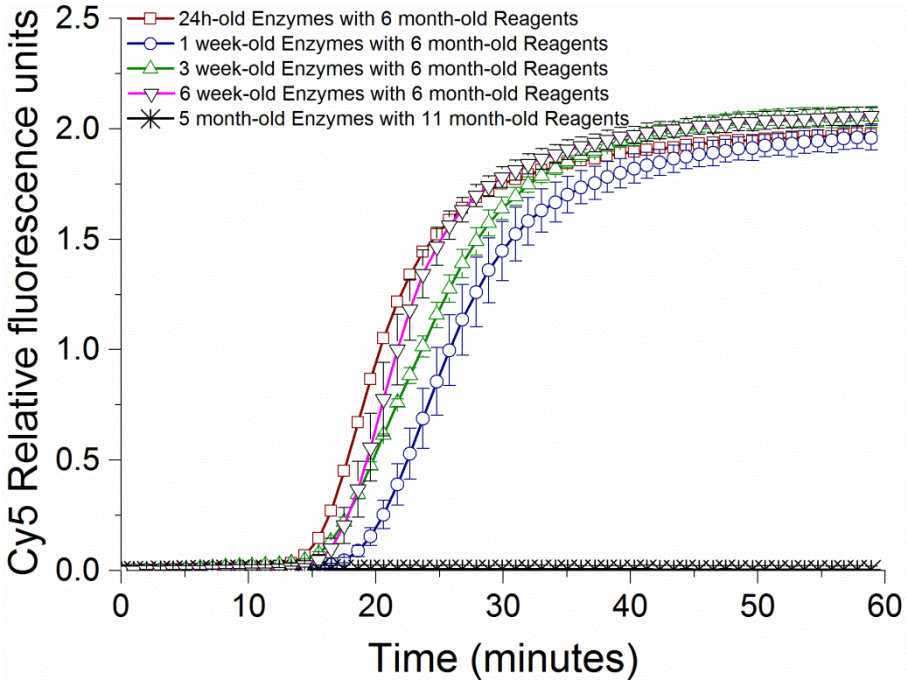

Figure 13 Real-time bench-top NASBA on *K. brevis* RNA, testing the long-term preservation of the sugar-containing, dehydrated enzyme master-mixture, and the gelified reagent master-mixture. The enzyme master-mixture was stored at room temperature for 24 hours and up to 5 months, and the reagent master mixture for 6 months and up to 11 months. Error bars represent standard deviation between triplicates.

3.4 Conclusions

Successful NASBA preservation is reported in this Chapter, by tackling three objectives: (1) the use of preserved reagents for the detection of *K. mikimotoi*, (2) the use of preserved enzymes for the detection of *K. brevis*, and (3) the use of complete, preserved NASBA reaction mixtures for the detection of *K. brevis* after long-term storage.

Bench-top data, verifies that NASBA enzymes and reagents can be preserved for a minimum of 6 weeks, suggesting that the described assay can become a useful tool for *in situ* environmental analysis. What remains to be seen, however, is the effect of the combined presence of gelifying agent and disaccharides on the quantification properties of IC-NASBA. Therefore the next step in this study should address the above hypothesis by combining the presented preservation methods with IC-NASBA for the detection and quantification of *K. brevis* on-chip, using a microfluidic system.

Chapter 4: Detection and quantification of the toxic microalgae *Karenia brevis* with a fully preserved, multiplexed Lab-on-a-Chip NASBA assay

4.1 Introduction

Nucleic acid sequence analysis is a state of the art analytical tool for identification (Holinger et al. 2014; Mollasalehi and Yazdanparast 2013; Valiadi et al. 2014), quantification (Casper et al. 2005; Ulrich et al. 2010) and, by proxy, physiological analysis (Kohli et al. 2015; Monroe et al. 2010) of harmful microorganisms in environmental samples. Conventional methods of nucleic acid analysis require delivery of "bottle" samples to centralised laboratories, bulky apparatus and skilled operators (Karlson et al. 2010). Autonomous systems that make measurements *in situ* and in near real-time would not only remove "bottling artefacts" from sample collection and transit but also increase the rapidity of data collection enabling faster intervention, better risk analysis and management.

Recently, a method for detecting and quantifying the harmful microalga, *Karenia brevis*, has been developed using Nucleic Acid Sequence Based Amplification (NASBA) of the *rbcL* (RuBisCo) gene transcript (Casper et al. 2004; Tsaloglou et al. 2011; Tsaloglou et al. 2013). The *rbcL* gene product catalyses the first step in CO_2 fixation and its expression is considered to be a reliable measure of viable phytoplankton cells (Ishida and Green 2002; Takishita et al. 2000), and has been further demonstrated in Chapter 2. *K. brevis,* and other marine algae, produce potent neurotoxins (Lekan and Tomas 2010), which pose a threat to marine life and human health (Backer et al. 2015; Bean et al. 2011; Bricelj et al. 2012; Fleming et al. 2011). The threat is most pronounced when algal populations rapidly expand leading to the formation of harmful algal blooms (HABs) (Bricelj et al. 2012; Fleming et al. 2011). Methods to predict HABs, by measuring a flux in cell concentration, would enable accurate intervention and risk mitigation. HABs are currently, primarily monitored using multi-spectral satellite imagery (Carvalho et al. 2010; Siswanto et al. 2013), but this has a typically high limit of detection (LOD). Other methods including cytometry (Gan et al. 2010) and microscopy (LeGresley and McDermott 2010) are more sensitive, but have limited taxonomical resolution. NASBA features a practical LOD of 10 cells per litre of processed water (see Chapter 5), and unequivocal taxonomic analysis (Brenier-Pinchart et al. 2014; Mollasalehi and Yazdanparast 2013). Furthermore, the *rbcL* mRNA is only sysnthesised by metabolically active cells (Gray et al. 2003) ensuring specific amplification of material from viable *K. brevis* in a mixed species background (Casper et al. 2007).

Previously, *rbcL* NASBA has been demonstrated using a minaturised Lab-on-a-Chip platform (Casper et al. 2007) (see section 1.3), or lab-card with a portable, battery operated LabCardReader (Tsaloglou et al. 2013) featuring fluidic controls, thermal regulation and real-time fluorescence detection (some of this work was conducted during this PhD and is connected with Chapters 3 & 4). If used in tandem with a portable sample extraction apparatus the concentration of *K.*

brevis cells in seawater could be determined in the field. This Chapter reports on a lab-on-chip NASBA assay including the preparation of complete, preserved reaction mixtures on-chip, and the use of IC-NASBA for on-chip quantitation of *K. brevis*. The microfluidic protocol enables the specific amplification of *K. brevis* mRNA sequence, in tandem with a synthetic internal control RNA construct for quantification in the range of 50 to 5,000 viable *K. brevis* cells in under 95 minutes.

4.2 Materials and Methods

4.2.1 Algal cell culture

Karenia brevis strain CCMP2228 was obtained from the Provasoli-Guillard National Center for the Culture of Marine Phytoplankton, and was originally isolated from the Gulf of Mexico, Sarasota Bay as a non-axenic culture. *K. brevis* was maintained in static cultures at 19±1°C in natural seawater (Solent, UK) containing L1 medium enrichment, and with a 12 hour photoperiod using cool fluorescent light (85-95 µmol photons m^{-2} s^{-1}; measured with a LI-189 light meter LI-COR®, Lincoln, USA). The L1 medium contained 882.5 µM $NaNO_3$, 36.2 µM NaH_2PO_4.H2O, 909 nM $MnCl_2.4H_20$, 80 nM $ZnSO_4.7H_2O$, 50 nM $CoCl_2.6H_2O$, 10 nM $CuSO_4.5H_2O$, 82.2 nM $Na_2MoO_4.2H_2O$, 10 nM H_2SeO_3, 10 nM $NiSO_4.7H_2O$, 10 nM NH_4VO_3, 10 nM K_2CrO_4, 11.7 µM $FeCl_3.6H_2O$, 11.7 µM $Na_2EDTA.2H_2O$, 2.1 nM biotin, 0.37 nM B_{12} cyanocobalamin, 296.5 nM thiamin HCl; the pH was 8.5±0.1.

4.2.2 RNA Isolation

Total RNA was isolated from 1 mL samples of a 50 mL culture containing exponentially dividing *K. brevis* cells. Each sample was mixed with 1 mL of a custom lysis buffer containing 100 mM Tris-HCl (pH 7.5), 4 M GuSCN, 500 mM LiCl, 10 mM EDTA and 1 % (v/v) Triton X-100. Cell lysis proceeded at room temperature for 10 minutes, followed by the addition of a 50 µL colloidal suspension of magnetic beads (bioMérieux UK Limited). After 10 minutes each sample was centrifuged at 1500 x g for two minutes and the supernatant was discarded. For the preparation of RNA samples containing an Internal Control (IC), a known quantity of IC RNA construct was added to the lysis buffer prior to the addition of the magnetic beads (details of IC construction are given below). After centrifugation the beads were washed twice in 500 µL of a custom wash buffer containing 10 mM Tris-HCl (pH 7.5), 150 mM LiCl and 1 mM EDTA using a NucliSENS® miniMAG® (bioMérieux UK Limited). RNA was eluted from the beads after resuspension in 10 mM Tris-HCl (pH 7.5) and heated to 60°C for five minutes with agitation at 1,200 rpm (Eppendorf Thermomixer). The beads

were removed by centrifugation, and the supernatant containing the eluted RNA was stored at -20°C.

4.2.3 Nucleic Acid Sequence Based Amplification (NASBA)

NASBA was carried out using reagents and enzymes supplied in the NucliSENS® EasyQ Basic Kit v2 (bioMérieux UK Limited), and custom oligonucleotide primers and molecular beacon probes (Table 6). Bench-top NASBA, using a fluorescence micro-plate reader (EasyQ™ analyser, bioMérieux, Netherlands) was carried out according to the manufacturer's recommendation. Alternatively, NASBA reactions took place on single-chamber chips for analysis on a prototype platform, and on disposable lab-cards using a portable LabCardReader with modifications for the use of preserved reagents and enzymes (see Chapter 3). The oligonucleotide primers 87 nucleotide sequence within the RuBisCO (*rbcL*) gene transcript encoded on the *K. brevis* genome and measured in real time, based on the fluorescence output from a molecular beacon probe covalently modified to contain AF488 at its 5' terminus and BHQ1 at its 3' terminus. Primers and molecular beacons were obtained from Eurofins MWG Operon (London, UK). NASBA amplification followed a two-step procedure in which the RNA template was mixed with oligonucleotide primers and molecular beacon probes, and a reaction buffer, and heated to 65°C for two minutes (five minutes on chip) for optimal primer annealing, and then, the reaction mixture was cooled to 41°C prior to addition of a heat-intolerant enzyme mixture. Amplification proceeded at 41°C for 90 minutes.

K. brevis	Sequence (5' to 3')
Forward Primer	**ACGTTATTGGGTCTGTGTA**
Reverse Primer	AATTCTAATACGACTCACTATAGGGAGA **AGGTACACACTTTCGTAAACTA**
Molecular Beacon	[AF488]-GAGTCGCTTAGTCTCGGGTTATTTTTTCGACTC-[BHQ1]
Target Sequence	GAA**ACGTTATTGGGTCTGTGTA**CACGAATTAACCTTAGTCTCGGGTTATTTTTTGGACAAGAATGGGC-**TAGTTTACGAAAGTGTGTACCT**
Internal Control	Sequence (5' to 3')
Molecular Beacon	[CY5]-ACGGAGTGGCTGCTTATGGTGACAATCTCCGC-[BHQ2]
Sequence	GAA**ACGTTATTGGGTCTGTGTA**CACGAATTAACTGGCTGCTTATGGTGACAATGGACAAGAATGGGC-**TAGTTTACGAAAGTGTGTACCT**

Table 6 List of the sequences of *K. brevis* primers, beacons, and RNA and Internal Control (IC). Bold underlined text indicates primer and beacon binding sites.

4.2.4 Internal Control (IC)

An Internal Control (IC) construct was prepared as previously described (Casper et al. 2005; Patterson et al. 2005; Tsaloglou et al. 2013), and contained the same primer annealing sites as the

rbcL target sequence, but a unique internal sequence and molecular beacon binding site (Table 6). The IC molecular beacon was covalently modified to contain Cy5 at its 5' terminus and BHQ2 at its 3' terminus. For quantitative NASBA the RNA samples were spiked with IC RNA copies (IC copy number chosen depending on the optimization stage), which were amplified in tandem.

The IC construct was prepared with the following protocol (Casper et al. 2005; Patterson et al. 2005; Tsaloglou et al. 2013): a DNA template was synthesised (Eurofins MWG Operon, UK) to contain primer annealing sites at the extreme 5' and 3' termini, which were identical to the annealing sites of the target sequence, an internal molecular beacon binding site and a 3' T3 RNA polymerase promoter. Then, T3 RNA polymerase was used to prepare IC RNA constructs (37°C for two hours), which were purified (RNeasy kit, Qiagen, Netherlands), quantified (Ribogreen RNA quantification kit, Invitrogen, UK), and stored at -20°C.

4.2.5 Quantification of RNA amount with NASBA analysis method

NASBA analysis of *K. brevis* samples produced two fluorescence monitored reaction curves for each sample; one representing wild-type amplification and one representing IC amplification.

Quantification of wild-type RNA, which serves as an indication of cell concentration, was initially attempted through time-to-positivity (TTP) ratios (Polstra et al. 2002). A threshold of detection (TOD) was set, and the point in time where each bi-exponential NASBA curve rose above the TOD, was defined as a TTP value. The ratio of wild-type TTP and IC TTP was subsequently used as a quantitative indicator for the concentration in each sample.

A second, curve fitting method was also used for data analysis, by employing MATLAB™ in conjunction with the following equation:

$$Y(t) = \lambda Y_0 - (\lambda - 1)Y_0 \exp\left\{-{}^{1}\!/_{2}\, k_1 a_1 \left[ln\left(1 + e^{a_2(t-a_3)}\right)\right]^2\right\}$$

This equation describes NASBA-driven RNA amplification, where $Y(t)$ the fluorescence signal as a function of time, Y_0 the signal at t=0, λY_0 the fluorescence value at its highest point, $\alpha_1\alpha_2$ representing the shape of the curve, α_3 defining the curve location relative to the time axis, and k_1 a reaction rate constant (Weusten et al. 2002). Each curve fit results in a set of parameters whose values represent the appropriate NASBA curve. Every IC-NASBA reaction produces two curves (one for the WT-RNA and one for the IC-RNA) and two sets of parameters. The quantitation variable is then determined by calculating the $k_1 a_1 a_2^2$ ratio from the parameters for the WT and IC curves. This method produces a quantitative metric for the concentration of WT RNA in the original sample.

In summary, for this work, the MATLAB™ curve-fitting tool was used to produce a quantitation variable, defined as the $k_1 a_1 a_2^2$ ratio, which is linearly related to the logarithm of the amount of wild-type RNA in a sample (Tsaloglou et al. 2011) and is an indicator of target cell concentration.

4.2.6 Component-testing prototype

Prior to any experiments involving the microfluidic system, three major material components of the on-chip NASBA reaction were tested (detector, micro-heater, and chips). A prototype platform was used, consisting of a micro-heater with embedded temperature sensors (Ikerlan, Spain) and a dual wavelength fluorescence detector (FluoSens integrated, QIAGEN Lake Constance GmbH). The micro-heater maintained the temperature needed for the NASBA reaction (41°C), and the detector monitored the reaction at 530 nm and 680 nm. Both were connected to a desktop PC which from which temperature monitoring and control was achieved with a user interface. Fluorescence data was saved in text format and transferred for further analysis. NASBA master-mixtures were prepared on-bench, loaded on a single-chamber polymer chip (see "chip manufacturing and preparation") via pipetting, and manually inserted into the micro-heater.

4.2.7 Lab-on-a-chip microfluidic system

The portable microfluidic system used in this study, named "LabCardReader" (Figure 14), was developed as part of the European LABONFOIL project (LABONFOIL 2013). It consists of a main control unit which directs all on-chip microfluidic processes, a lab-card holder for the insertion of compatible chips (lab-cards), and the accompanied user interface software installed on a tablet PC. The system was designed to be flexible and customisable for a variety of molecular reactions and processes, such as NASBA and PCR, targeting both DNA and RNA molecules (Sun et al. 2013; Tsaloglou et al. 2013).

Figure 14 Image depicting the LabCardReader, a lab-on-a-chip system developed as part of the European LABONFOIL project. The device is plugged to a power source and connected to a tablet PC running the associated software.

The lab-card holder provided a simple insertion and removal mechanism for LabCardReader-compatible chips, referred to as “lab-cards”. Lab-cards were pushed into the holder and clamped into place with by tightening a pair of protruding screws by hand (Figure 15). Microfluidics were controlled by three peristaltic micro-pumps and the activation of seven pin-like micro-valves. Two micro-heaters with embedded temperature sensors (Ikerlan, Spain) were used for temperature control and real-time temperature monitoring, and a dual wavelength fluorescence detector (FluoSens integrated, QIAGEN Lake Constance GmbH) monitored ongoing molecular reactions real-time at 530 nm and 680 nm. Each pump, valve, or heater could be controlled independently and incorporated into an automatic protocol using the user interface from the tablet PC.

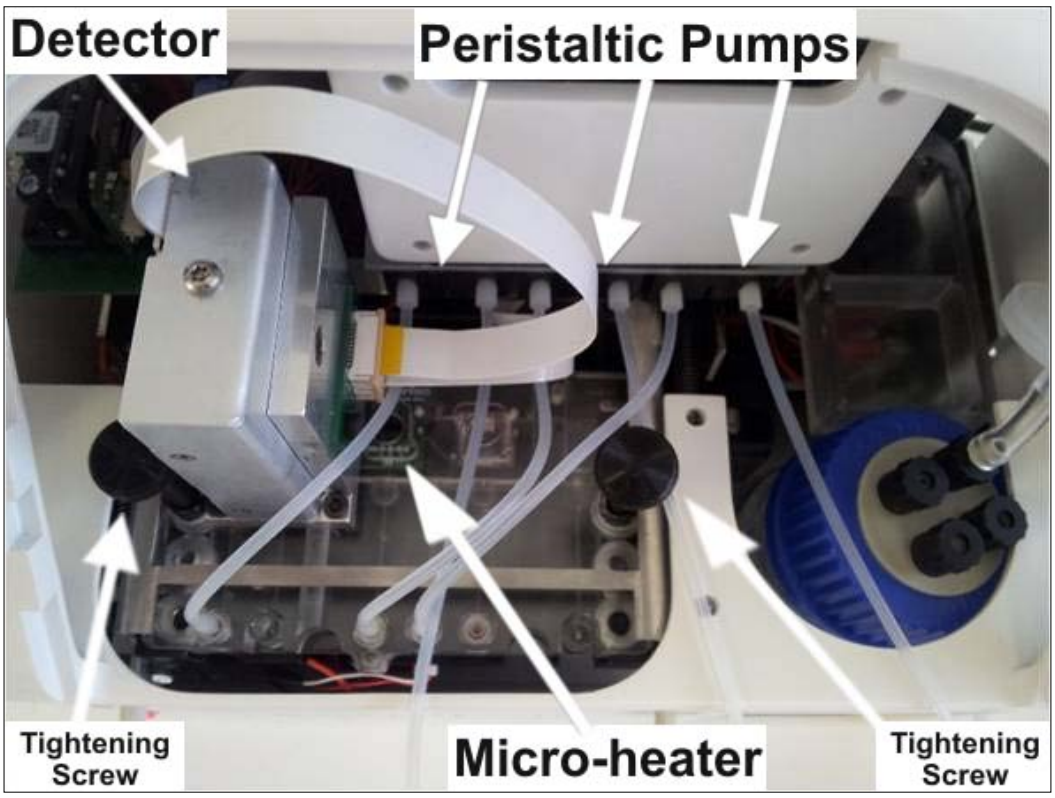

Figure 15 Close up of the LabCardReader. The fluorescence detector is fixed on the lab-card holder, on top of the microfluidic chips chamber, where the final reaction occurs. Three peristaltic pumps control sample movement on the lab-card and are connected to the lab-card holder with a series of tubes. Two micro-heaters are embedded in the lab-card holder, controlling temperature of chambers in the lab-card; only one micro-heater can be seen on this image, as the second one is situated directly under the fluorescence detector. The lab-cards are pushed into the holder from a side opening and clamped into place with the tightening of two screws, on either side of the holder, by hand.

A prototype setup was also used for experiments with single chamber chips to test the compatibility of some core LabCardReader components. The prototype consisted of a single micro-heater with embedded temperature sensors (Ikerlan, Spain) and a mounted dual wavelength fluorescence detector (FluoSens integrated, QIAGEN Lake Constance GmbH). Temperature was controlled and monitored in real-time, using a custom user interface from a desktop personal computer. The micro-heater was opened and closed manually for single chamber chip placement. The detector was then placed on top of the micro-heater/chip complex, to measure fluorescence of ongoing molecular reactions at 530 nm and 680 nm.

4.2.8 Lab-card and chip manufacturing and preparation

Cyclic-olefin copolymer (COC) single chamber chips and lab-cards were manufactured, with the latter incorporating two chambers and a series of microfluidic channels (Figure 16). The chips were fabricated by injection moulding (microLIQUID, Spain) with a feature depth of 450 µm and a

channel width of 250 µm. A strip of polypropylene film, coated with a PCR-compatible pressure-sensitive adhesive (PROgene, Ultident, Canada) was used to seal all chips by lamination before storage or use.

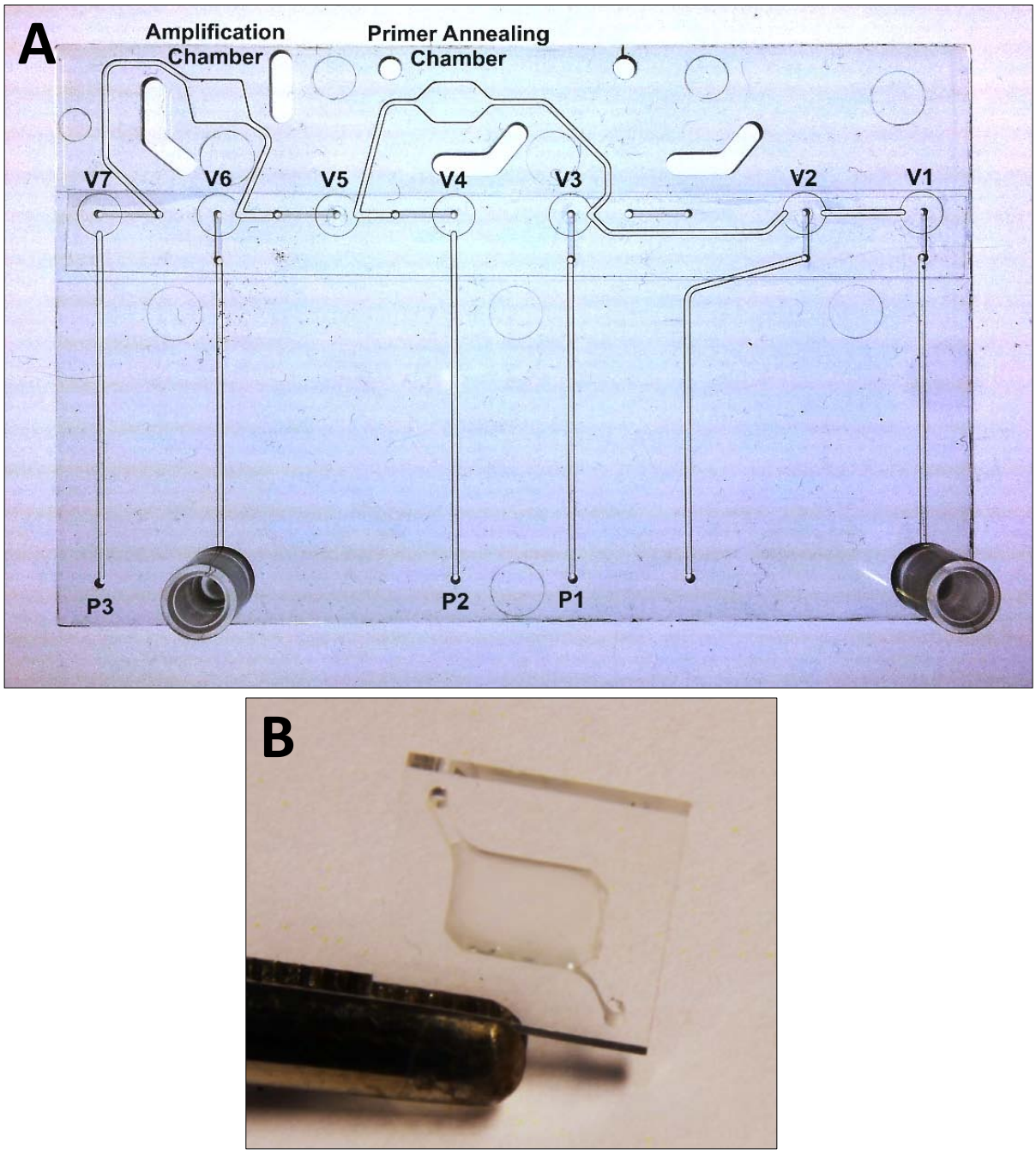

Figure 16 Depicted is the image of a COC lab-card containing two chambers and a series of microfluidic channels (A). One chamber was used for primer annealing, and the second chamber was used for the final amplification reaction. Circular structures (V1-V7) are grooves in which valve disks were placed for microfluidic control. The right luer inlet reservoir was used for RNA sample insertion, and the left luer inlet was unused during our protocols. Three channel outlets were automatically connected to peristaltic pumps (P1-P3), once the lab-card was inserted and clamped into the lab-card holder of the LabCardReader. Also depicted is the image of a COC single-chamber chip (B). The chamber contains gelified NASBA reagents and is connected to an inlet/outlet on either corner end, for sample and enzyme insertion.

Single-chamber chips consisted of two openings at opposite corners, which were used to add and remove samples. Lab-cards incorporated two luer inlet reservoirs and four outlet points, destined for connection with the peristaltic pumps of the LabCardReader. Each of the last three outlets were connected to a separate pump (P1-P3) and the first outlet was left disconnected. The lab-cards included “on-chip” valves actuated via off-chip linear actuators integrated in the lab-card-reader. These “on-chip” valves were formed from seven circular structures (V1-V7) integrated between chambers and lab-card inlets/outlets in which valve disks were placed; the disks kept the adhesive on the sealing PCR-compatible polypropylene film from sticking to the COC of the injection moulded part of the lab-card whenever the pin-like micro-valves actuators were activated by the LabCardReader to control microfluidics. Valve disks were made from cyclic-olefin polymer (COP) and MD700 material, using a 2 mm puncher (Harris Uni-Core™).

Each COC reaction platform was treated prior to use or further preparation. Single chamber chips and lab-cards were initially submerged in RNaseZap® and sonicated for five minutes. They were then submerged in RNase-free water and sonicated for five minutes. The last step was repeated a further two times, and the RNase-free water was renewed before each repeat. All reaction platforms were finally dried for two hours at 60°C and 30 mbar, using a vacuum oven.

At the end of the treatment process, single-chamber chips were sealed for immediate use, whereas lab-cards underwent a further four-step process preparation process (Figure 17). COP valve disks were placed at the center of V1 and V3, and MD700 disks were placed at the center of V6 and V7; no disks were placed in the remaining circular structures (V2, V4, V5). A droplet of NASBA enzyme mastermix containing disaccharides (3.375 µL) was placed within the amplification chamber and dehydrated overnight at room temperature, under 30 mbar pressure, using a vacuum oven. A droplet of NASBA reagent mastermix containing gelifying agent (6.75 µL) was placed within the primer annealing chamber and dehydrated for 35 minutes, at 35°C, under 30 mbar pressure, using a vacuum oven. Lab-cards were finally sealed with adhesive film, using an EVG bonder (or if not available manually, with a roller) and stored at 4°C until transported.

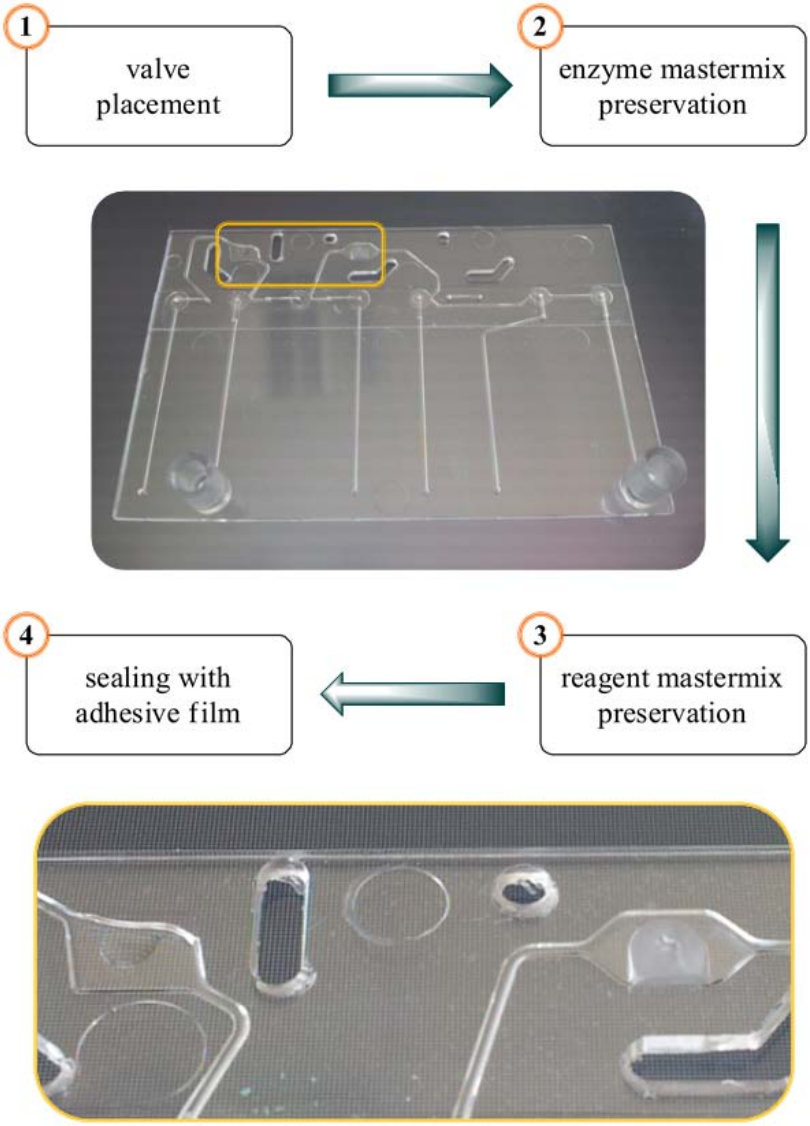

Figure 17 LabCard preparation as a four-step process (top) and close up of preserved enzyme and reagent NASBA master mixtures (bottom): enzymes were preserved in the amplification chamber (left) whereas reagents were preserved in the annealing chamber (right).

4.2.9 LabCardReader NASBA protocol

All initial LabCardReader experiments were performed with manual controls using the software graphical user interface. This involved manual opening and closing of valves, and adjustment of pumping direction and pumping strength. Microfluidic movement was assessed visually thanks to the transparency of the lab-card and lab-card-holder material. During the process, the microfluidic detector was removed from the top of lab-card holder and reattached as soon as the amplification chamber was filled with the final NASBA reaction mixture. The timing, valve and pump operation was recorded, and the information was then used for the development and optimisation of a fully automated NASBA protocol on the LabCardReader.

Placement and viability of preserved NASBA master-mixtures were tested on lab-cards. Each chamber could contain a total volume of approximately 10 µL; the final NASBA reaction was in excess of this volume and was 13.5 µL, to make sure that the amplification chamber was always filled and to avoid bubble formation. Thus, 6.75 µL of NASBA reagent mastermix were prepared and preserved in the primer annealing chamber, 3.375 µL of NASBA enzyme mastermix were prepared and preserved in the amplification chamber, and 3.375 µL of RNA sample was loaded through the right luer inlet reservoir (Figures 16 & 17).

In the following, the fully automated LabCardReader NASBA protocol is described. After successful insertion of the lab-card in the lab-card holder, a message was automatically prompted to the user with the instructions to be followed. The NASBA process performed on the lab-card was initiated by pipetting 3.375 µL of RNA sample with 8.2 µL of RNase-free water to the right inlet luer; during the preservation process, the enzyme and reagent master-mixtures lost approximately 80% of their total volume and thus the additional water was used for rehydration purposes and to reach the target final volume (13.5 µL). A message was shown to the user to confirm sample addition so that the protocol may continue. The diluted RNA sample was transferred into the annealing chamber by closing valves V2, V3, V4, and V6, and activating pump suction on outlet P3. The gelified reagent mastermix was rehydrated upon contact with the solution in the annealing chamber, and primers were annealed with the first micro-heater raising the temperature at 65°C for five minutes. The temperature was then decreased to 41°C for five minutes, to prepare the reagent/sample mixture for transfer to the amplification chamber. Valves V2, V3, V4, and V6 remained closed and a pump performed suction on outlet P3 once again. Reagents and sample rehydrated the preserved enzyme mastermix in the amplification chamber, and the chamber maintained a temperature of 41°C using a second micro-heater for the remainder of the NASBA reaction. The detector monitored the reaction in the amplification chamber by measuring fluorescence every 30 seconds for 90 minutes. Microfluidic transfer, temperature control, and detection described in the above protocol were set up in the user interface of the tablet PC and were fully automated. NASBA curves resulting from each reactions were depicted real-time in the user interface, and raw data files were extracted for further analysis using other software packages, such as Microsoft Excel®, MATLAB® etc.

4.3 Results and Discussion

4.3.1 Single-chamber chip experiments

An internal control RNA construct was designed to contain the same primer annealing sites as the target *K. brevis rbcL* sequence, but a unique internal sequence featuring an annealing site for a molecular beacon. Thus, in a single reaction, both target wild-type RNA and IC RNA are amplified in tandem, competing for the same primer pool, leading to the liberation of fluorescence from two molecular beacons. Each beacon features different fluorescence emission maxima, representing either wild-type RNA or IC RNA, which can be measured using the two-channel fluorescence detector of the LabCardReader. A prototype was constructed (Figure 18) to test the following: (1) detection efficiency of the LabCardReaders optical apparatus, (2) reaction stability using the LabCardReaders micro-heater, and (3) IC-NASBA compatibility with COC material (used for lab-card manufacturing), in the form of single-chamber chips.

IC-NASBA reaction mixtures were prepared containing wild-type RNA from 2,000 *K. brevis* cells and 1,000 IC RNA copies. The amount of IC RNA copies was chosen based on previously conducted optimisation experiments; on-chip reactions appeared to require a higher number of IC copies (1,000-3,000 copies) than bench-top equivalents (400-900 copies) for meaningful wild-type and IC amplification comparisons. Primer annealing was conducted on bench and samples were subsequently pipetted into single-chamber COC chips. Each prepared chip was immediately inserted into the micro-heater and RNA amplification was monitored for 60 minutes, at 41°C. Figure 18 illustrates on-chip IC-NASBA for three different runs of the same sample. Amplification curves for the same RNA sample, but run on different chips, were highly variable, reflecting the differences in chip-to-chip kinetics. Chamber temperature was maintained at 41°C±1, and any potential changes to this number were due to the occasional “freezing” of the prototypes user interface software. The detector successfully monitored the reaction and detected fluorescence changes over the course of one hour at 530 nm and 680 nm. On-chip IC-NASBA reactions were overall successful using the prototype despite illustrated differences in amplification kinetics between runs; the variability was applied to both wild-type RNA and IC RNA and thus, quantification analysis in the final system is expected to be more consistent.

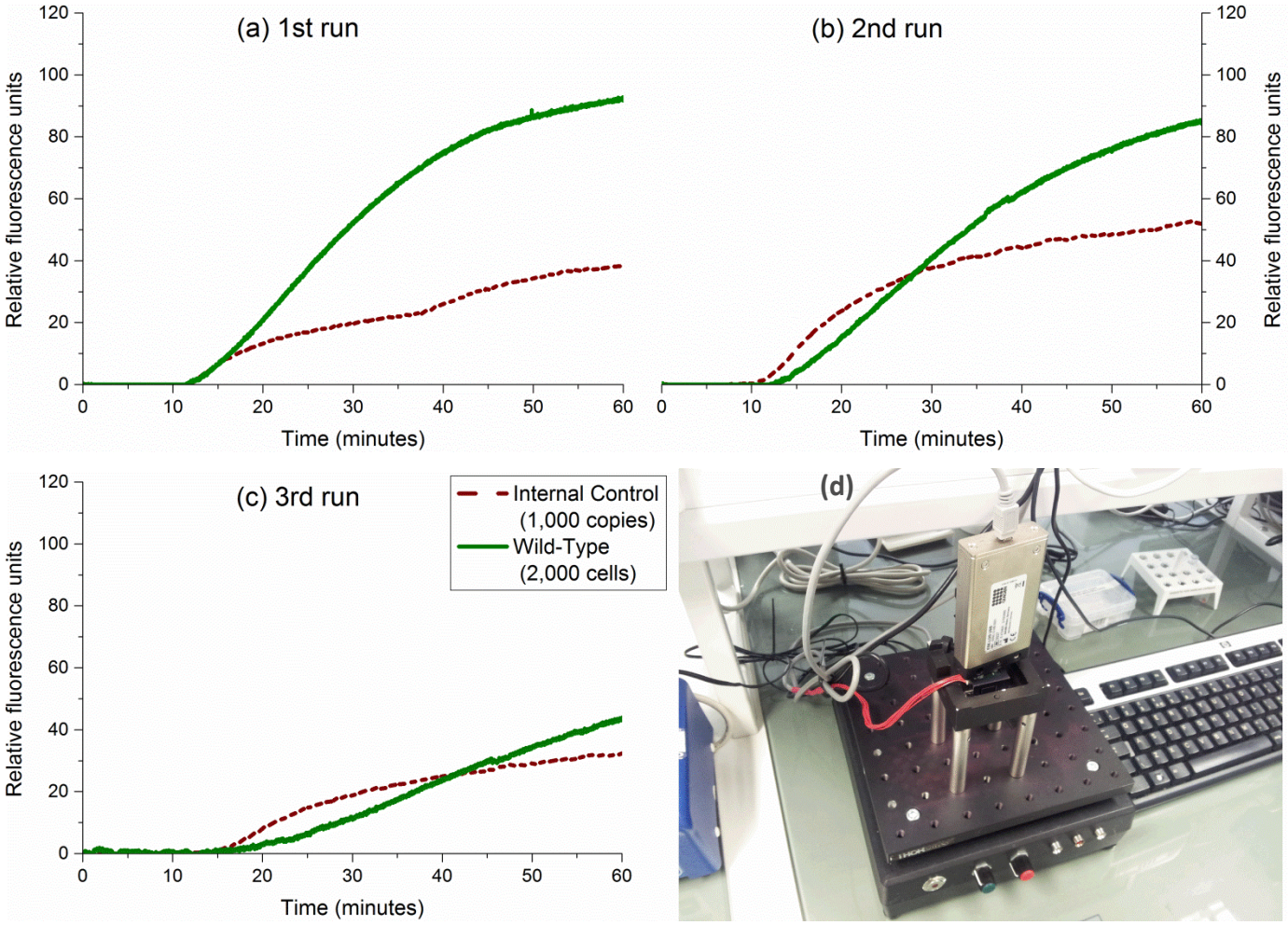

Figure 18 IC-NASBA on a single-chamber chip, using a prototype setup preceding the LabCardReader and its associated experiments. Depicted are three separate on-chip NASBA runs (a, b, c) of a sample containing 2,000 *K. brevis* cells and 1,000 IC copies; an image of the prototype consisting of a micro-heater and a fluorescence detector (d). Chips were loaded with the final NASBA reaction mixture and manually inserted in the micro-heater. The prototype was connected to a desktop PC and managed via a custom user interface.

4.3.2 Assessment of IC-NASBA on the lab-card

Following initial prototype experiments, IC-NASBA was run on a lab-card using the complete LabCardReader system. Samples containing RNA from 9,000 *K. brevis* cells and 800 IC copies were run on the lab-on-chip system and compared to bench-top equivalents. All NASBA reaction mixtures were prepared on bench. During LabCardReader runs, primer annealing was conducted in the lab-card annealing chamber (65°C for five minutes), and RNA amplification was monitored real-time in the lab-card amplification chamber (41°C).

A direct comparison between lab-card and bench-top IC-NASBA runs, using fresh reagents and enzymes, is shown in Figure 19. The LabCardReader amplified sample RNA successfully and two distinct curves were monitored over the course of an hour. When compared to the bench-top

equivalent, lab-card IC RNA showed a significant delay and decrease in the rate of amplification, reflected by increased time to positivity (TTP) and a larger difference between wild-type and IC maximum fluorescence. A small increase in TTP was also noticed for wild-type RNA amplification on the lab-card. This is likely due to changes in amplification kinetics within the lab-card chamber, and was noticed throughout optimisation experiments using the previously described prototype and the LabCardReader. Changes in amplification kinetics may be attributed to the lab-card design, which uses large and wide chambers and do not necessarily emulate the smaller and narrower tubes used for bench-top reactions.

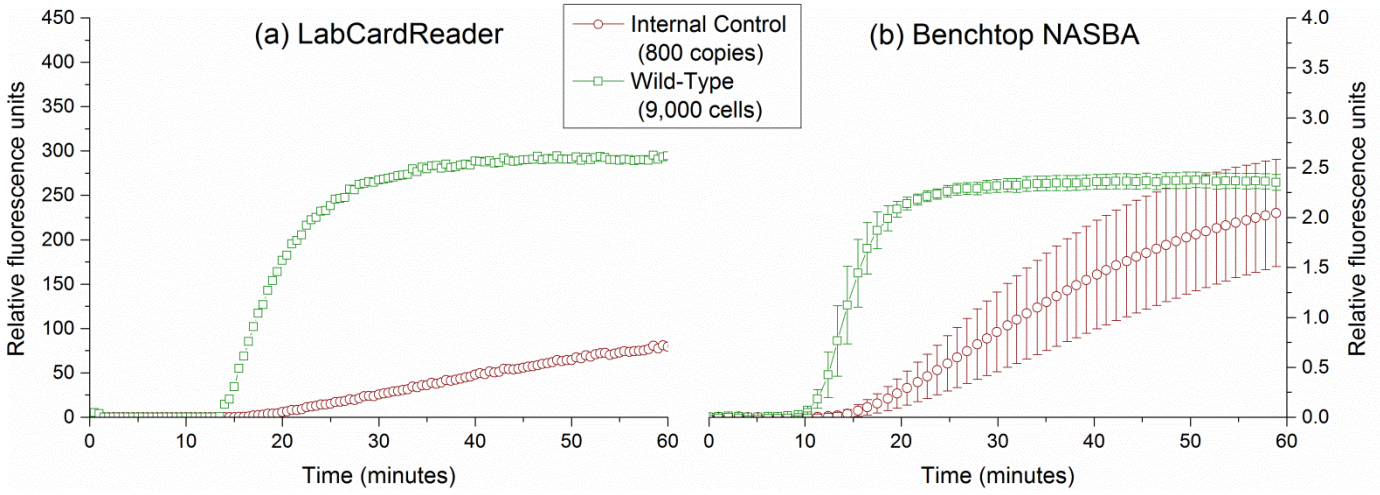

Figure 19 Comparison of IC-NASBA between the LabCardReader (a) and benchtop runs (b) using fresh NASBA reaction mixtures. The *y-axis* represents relative fluorescence units, as measured by the LabCardReader, and the *x-axis* represents time in minutes. WT-RNA amplification is shown as green squares and IC-RNA is shown as red circles. NASBA was run for 9,000 cell equivalents of *K. brevis* with 800 IC copies. Error bars represent standard deviation between triplicate samples.

The delay and reduced rate of RNA amplification was more prominent when IC-NASBA was run on lab-cards using gelified reagents and dehydrated, sugar-containing enzymes (Figure 20). In order to detect IC RNA amplification, NASBA was run for 90 minutes on the LabCardReader. This was expected, due to the increase in reaction mixture viscosity induced by the gelifying agent and disaccharides. In addition, some time would be needed for the preserved enzymes to rehydrate within the amplification chamber, and since the lab-card design did not incorporate any form of active mixing, the time for complete rehydration would have been suboptimal. At this stage it was clear that a direct comparison between fully preserved on-chip IC-NASBA assay and a bench-top control could not be made, and a larger number of IC RNA copies was required to conduct *K. brevis* quantification experiments using the LabCardReader. Furthermore, since there was a marked reduction in rate of RNA amplification for the fully preserved lab-cards, NASBA runs would have to increase in duration. In summary, quantification experiments would require

K. brevis RNA samples to be extracted with at least 3,000 IC RNA copies, and LabCardReader runs would be extended to 90 minutes of amplification time (see below).

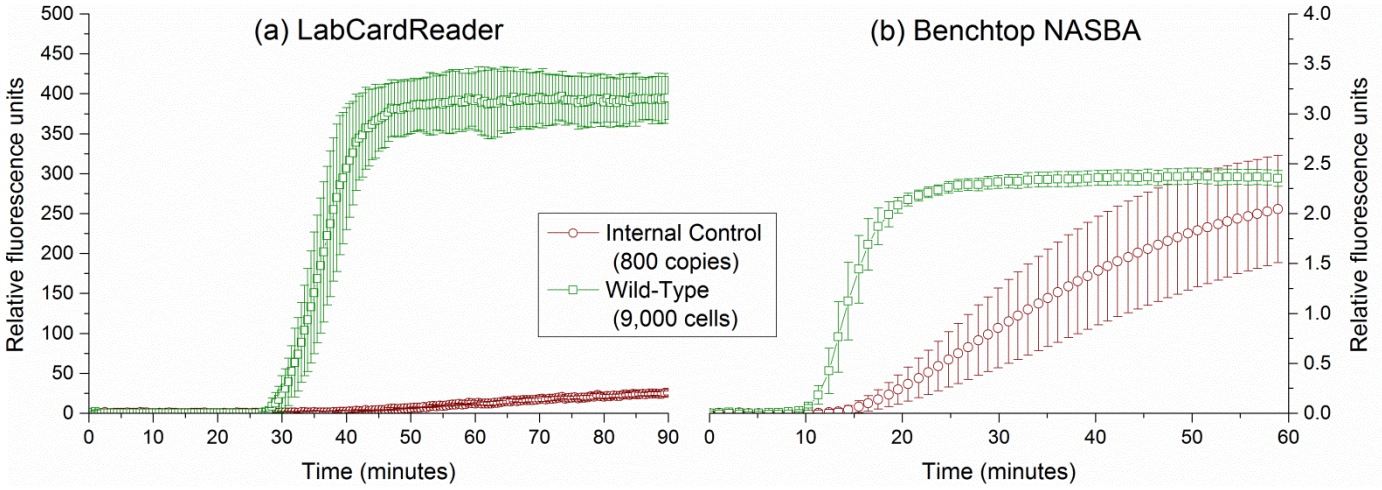

Figure 20 Comparison of fully preserved IC-NASBA on the LabCardReader (a) and benchtop IC-NASBA with fresh reagents and enzymes (b). The *y-axis* represents relative fluorescence units, as measured by the LabCardReader, and the *x-axis* represents time in minutes. WT-RNA amplification is shown as green squares and IC-RNA is shown as red circles. NASBA was run for 9,000 cell equivalents of *K. brevis* with 800 IC copies. Error bars represent standard deviation between duplicate (a) and triplicate (b) samples.

4.3.3 On-chip quantification of *K.bevis*

On-chip IC-NASBA was performed on a lab-on-chip device (LabCardReader) using fully preserved enzymes and reagents, to detect and quantify toxic microalgae *K. brevis*. All NASBA components were preserved on-chip (lab-cards), which were then sealed and transported at varying temperatures and over the course of a month before use: 1) manufactured in Mondragon, Spain, 2) posted to Southampton, U.K., 3) transported by bus to London Heathrow airport, 4) flown to Copenhagen, Denmark, and 5) run on LabCardReader.

The LabCardReader successfully detected and quantified *K. brevis* RNA, extracted from 5,000, 500, and 50 cells, using IC-NASBA with 3,000 IC RNA copies. Results were acquired within 90 minutes from the start of the reaction, after an additional on-chip primer annealing step (2 minutes). Wild-type curves experienced an increase in fluorescence at approximately seven minutes before IC curves at 5,000 cells (Figure 21). Simultaneous fluorescence increase was shown at 500 cells, and finally the initial wild-type and IC curve relationship was reversed at 50 cells. However, each NASBA curve was depicted with large standard deviation (error bars) suggesting significant variation between samples. This is to be expected as the LabCardReader could only process one

lab-card at a time, and a variety of factors may have affected RNA amplification kinetics. Nonetheless, since wild-type RNA and IC RNA showed similar degrees of variation, it was suspected that *K. brevis* quantification with low standard deviation would still be applicable.

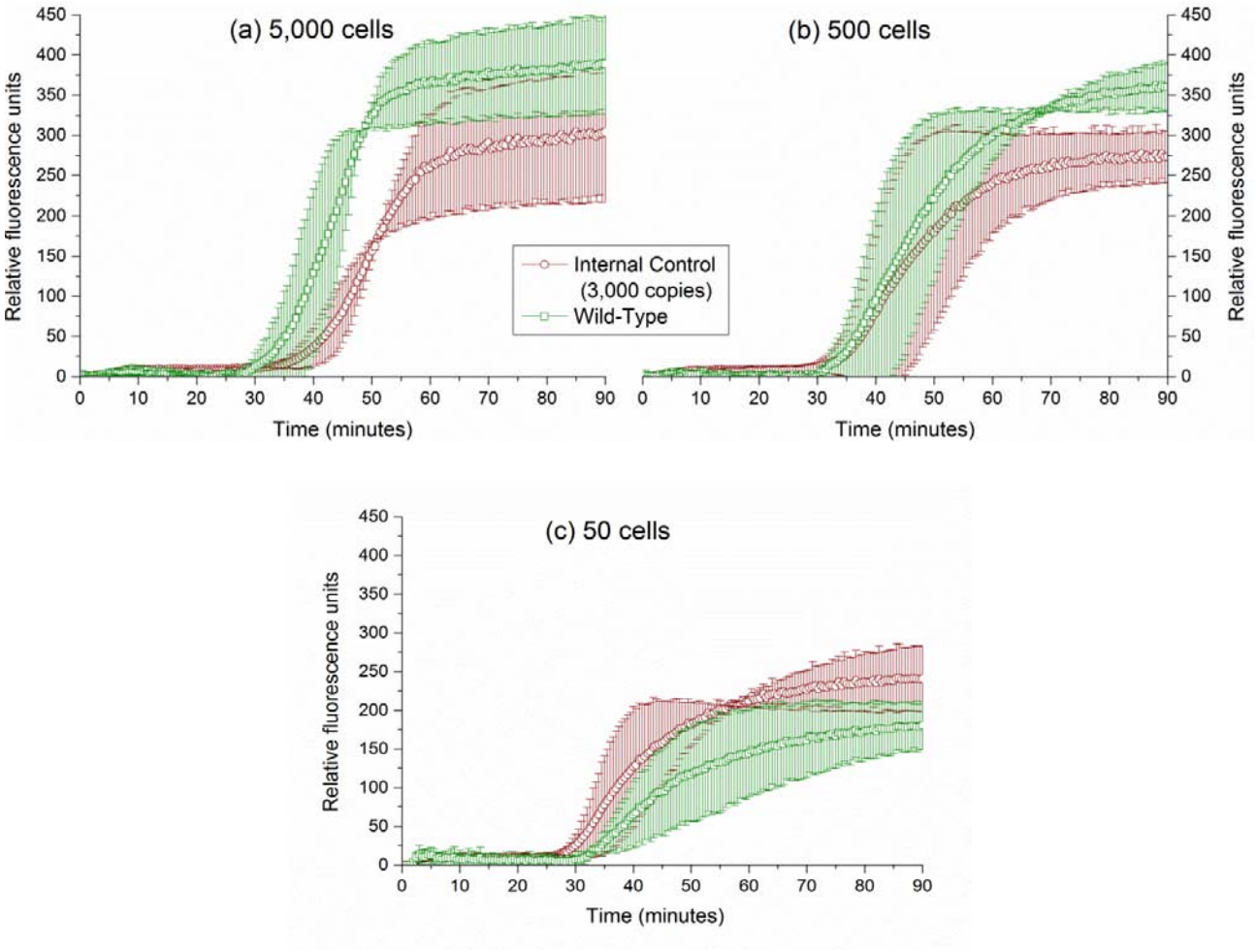

Figure 21 Real-time on-chip IC-NASBA on *K. brevis* RNA with fully preserved enzyme and reagent master-mixtures. The *y-axis* represents relative fluorescence units, as measured by the LabCardReader, and the *x-axis* represents time in minutes. WT-RNA amplification is shown as green squares and IC-RNA is shown as red circles. NASBA was run for 5,000 (a), 500 (b), and 50 (c) cell equivalents of *K. brevis* with 3,000 IC copies. The enzyme master-mixture was originally dehydrated on-chip with the presence of sugars, and the reagent master-mixture was gelified on-chip subsequently. Rehydration of both master-mixtures was achieved by introducing the RNA sample. Error bars represent standard deviation between duplicate samples.

In order to demonstrate the quantification properties of the LabCardReader system using lab-cards with fully preserved reagents and enzymes, our NASBA curves were further examined using TTP and quantitation variable analysis (Figure 22). The results illustrate a clear trend between TTP ratio or the value of $\ln(k_1 a_1 a_2^2$ ratio) and logarithmic cell number. A linear trendline was fitted to both sets of data, with an R-squared value of 99.6% for the TTP analysis and 96.8% for the quantitation variable analysis.

The fit to the trend is marginally better for the TTP ratio than the quantitation variable for quantification analysis, suggesting potentially higher accuracy for the TTP analysis. However, the trendline fitted to $\ln(k_1a_1a_2^2$ ratio) had a much larger slope value (0.637) than the TTP equivalent (0.160); this indicates that the quantitation variable method be preferable for samples run on the LabCardReader, as it distinguishes cell numbers more prominently. Furthermore, TTP standard deviation (error bars) increased with increasing cell number, reaching a value of ±0.067 (1.163 ratio average) at 5,000 cells. In contrast, the standard deviation of $\ln(k_1a_1a_2^2$ ratio) appeared to be overall significantly smaller, and reached its highest value at 50 cells, equal to ±0.120 (-0.573 ratio average). Therefore, the quantitation variable may provide increased precision for cell quantification using our fully preserved on-chip IC-NASBA method.

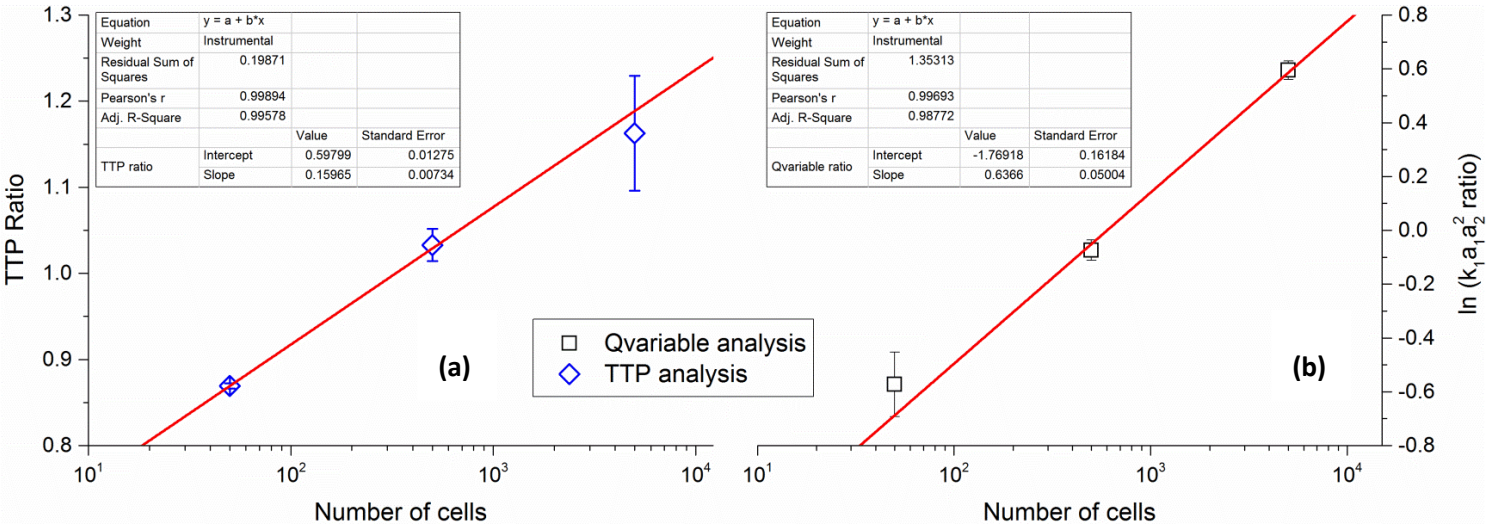

Figure 22 Quantification analysis of on-chip IC-NASBA results, using TTP analysis method (a, blue diamonds) and Quantitation variable analysis method (b, black squares). TTP ratios and $\ln(k_1a_1a_2^3$ ratios) were plotted over increasing cell concentration (log scale). Error bars represent standard deviation between duplicate samples. Also shown are the lines of best fit and their respective values above each line.

The LabCardReader user interface, installed on a tablet PC, worked well throughout the course of the study. However, experiments often failed due to pump inconsistencies, channel blockage induced by valve disks, bubble formation in the amplification chamber, and adhesive film preventing temperature sensors to connect properly.

Microfluidic movement along the lab-card was achieved with the activation of three peristaltic pumps, performing “pushing” or “suction” of air using respective channel outlets (see Figure 15; Figure 16). Pumping strength was adjusted using the integrated user interface, but the same input number would not translate into the same pumping strength across pumps. Furthermore, samples often appeared stationary, despite pumps being activated, only to suddenly “shoot” from one lab-card end to the other. The final optimised NASBA protocol only required one pump for

microfluidic movement. Over time, the most consistent pump was identified, and was then connected to the P3 outlet.

To decrease the chances of lab-card failure, due to valve disks unintentionally blocking microfluidic channels, the number of valve disks placed per lab-card was reduced from seven to four. Towards the end of the project, a lab-card setup was tried containing no valve disks. The setup led to permanent closing of each activated valve, as the adhesive film would stick directly on the lab-card; this appeared to work well with the single-flow NASBA protocol optimised on lab-cards, but valves disks (and therefore valve reopening) would still be needed if a situation required sample redirection using microfluidic controls. In addition, COC valve disks worked considerably better than the more "sticky" MD700 valve disks, and were less prone to blocking lab-card channels. However, COC valve disks were often difficult to place on their assigned lab-card positions due to movement induced by static electricity. Thus, two valve disks of each material were used in the final design to facilitate overall lab-card manufacturing, while improving lab-card operation.

Sealing of chips (lab-cards and single-chamber chips) with PCR-compatible pressure-sensitive adhesive film (PROgene, Ultident, Canada) proved very useful and eased overall lab-card preparation. Once lab-cards were sealed, excess adhesive film had to be cut around each lab-card to allow for proper insertion in the lab-card holder. Furthermore, adhesive film was cut out from holes situated around the primer-annealing and amplification chambers (see Figure 16). The holes allowed embedded micro-heater sensors to pass through and connect; if sensor connection was not successful, micro-heaters were unable to record and manage chamber temperature, and LabCardReader runs would not initiate. Thus, adhesive film surrounding the lab-card holes had to be cut out carefully, and the embedded micro-heater sensors were regularly cleaned and inspected.

Finally, air-bubbles were occasionally observed in the amplification chamber, obstructing fluorescence measurements by the LabCardReader detector. Placement of enzyme droplets (to be preserved) around the corners or in the center of the amplification chamber was attempted in effort to minimise bubble formation. Even so, there was no obvious improvement and random bubble formation persisted throughout a small number of LabCardReader runs.

Overall our long-term enzyme and reagent preservation method has been successful for the on-chip quantification of *K. brevis*. Full RNA amplification was completed within 92 minutes after sample introduction, despite potential preservation-induced changes in amplification kinetics, or stresses applied on the lab-cards due to transport, and temperature fluctuations. Both data analysis methods gave quantifiable results, with TTP trading off precision for marginally higher

accuracy compared to the quantitation variable. When coupled with our benchtop data, which verify that enzymes and reagents can be preserved for a minimum of 6 weeks, it is clear that lab-on-chip systems can become a useful tool for *in-situ* environmental analysis; an area which receives increasingly more attention (F. Liu et al. 2014; Tsaloglou et al. 2013; Tsopela et al. 2016; Umar et al. 2015). The fully preserved lab-cards provide simple, rapid, precise and accurate detection and quantification of microbial RNA, making the LabCardReader system a viable option for in-field monitoring of HABs, and otherwise toxic or harmful marine and freshwater microorganisms.

4.4 Conclusions

In this study, IC-NASBA was performed to detect and quantify toxic microalgae *K. brevis* using a LabCardReader, and lab-cards containing fully preserved enzymes and reagents, prepared using the dehydration and gelification protocols described in Chapter 3.

IC-NASBA has been successful for the quantification of *K. brevis* using the lab-card lab-on-a-chip system. When coupled with our benchtop data from Chapter 3, which verifies that enzymes and reagents can be preserved for a minimum of 6 weeks, it is clear that this system can become a useful tool for *in-situ* environmental analysis; an area which receives increasingly more attention (F. Liu et al. 2014; Tsaloglou et al. 2013; Tsopela et al. 2016; Umar et al. 2015). However, the system is still not fully automated and deployable for field-work, as fully automated RNA extraction is still missing from the LabCardReader functionality; a process that requires trained individuals and may bring the user in indirect contact with harmful lysis buffers. Furthermore, in order to increase the methods sensitivity and potentially reduce the LabCardReader NASBA reaction time, sample collection and concentration should be optimised (see Chapter 5). Nevertheless, the fully preserved lab-cards provide simple, rapid, precise and accurate detection and quantification of microbial RNA, making the LabCardReader system a viable option for in-field monitoring of HABs, and otherwise toxic or harmful marine and freshwater microorganisms.

Chapter 5: A novel portable filtration system for the concentration of marine microalgae for subsequent quantification with IC-NASBA

Note: During the writing of this PhD, the contents of this section were submitted to Harmful Algae to be considered for publication as a Journal Article, using the same title as this Chapter. At the time of submission of the Thesis, the article was still under review.

5.1 Introduction

Harmful algal blooms (HABs) including “red tides”, are typically the result of rapid proliferation and high biomass accumulation of harmful microalgal species in the water column or at the sea surface. They are common in coastal marine ecosystems and are often regarded as a global threat to marine resources and human health (Backer et al. 2015; Hoagland et al. 2002; Lewitus et al. 2012; Reich et al. 2015).

HABs are often held accountable for increased mortality of higher vertebrates, and long term exposure may cause significant changes in marine community structure (Flaherty and Landsberg 2011; Hallett et al. 2015). Thousands of fish and other species are killed annually by *Karenia brevis* red tides alone, and persistent blooms may cause widespread die-offs of benthic communities and short-term declines in local fish populations (Landsberg et al. 2009). Even though there may be multiple causes of red tides, nutrients such as nitrates and phosphorus have an important role in sustaining microalgal blooms (Vargo et al. 2008). As a result, it is not surprising that areas of significant human induced pollution may lead to increased frequency of red tide outbreaks (L. Liu et al. 2013). HAB toxicity can be especially pronounced once phosphorous limitation occurs, as this has been suggested to be an important factor regulating cellular toxicity (Hardison et al. 2013). In order to adequately manage waste contamination and resulting HABs, particularly in regions of rapid economic and industrial growth, environmental monitoring is required.

Toxin-producing species are particularly significant; the dinoflagellate *Gambierdiscus*, for instance, is estimated to be responsible for approximately 50,000 human poisoning events per year and some human deaths are annually attributed to the ingestion of microalgae-induced paralytic shellfish poisoning (Medlin 2013). Brevetoxin-producing *K. brevis* has also been linked with 24 confirmed cases of neurotoxic shellfish poisoning between 2005 and 2007 through consumption of contaminated shellfish (Reich et al. 2015).

In order to respond to, and adequately manage HABs, monitoring of toxic microalgae is required. This practice helps prevent direct or indirect damage to human health, as well as potentially significant financial losses within the fisheries and aquaculture industry and also serves as a means of identifying waste spills and contamination of the environment. Current methods for monitoring microalgal species using morphological assessment by microscopy or analogous techniques can be time-consuming, limiting the number of samples which can be analysed and the size of those samples. In addition, the acquired information may be limited regarding species-specific definition and toxin production. By contrast, molecular techniques, if automated, may accelerate the rate of sample analysis, while providing the benefits of increased accuracy and simultaneous examination of multiple parameters (Medlin 2013).

This section presents a novel filtration/concentration system, designed for the collection and concentration of seawater samples, which are characterised particularly by very low cell concentrations and therefore the requirement to process very large volumes. The system is intended primarily for *in-situ* (in the field) sample processing of the sort required by environmental monitoring. Test samples processed by the system are subsequently analysed using a molecular method for the detection and quantification of marine microorganisms. In order to assess the viability of our method, we examine system operation, detection capabilities for two marine micro-organisms, and quantification of a HAB-inducing species.

5.2 Background

5.2.1 Sample Collection and Molecular Tools for Environmental Analysis

Molecular tools have been employed for the study of microbial diversity and ecology in natural environments since the mid-1980s (DeLong et al. 1989). Marine biology is an interdisciplinary study of life in the world's oceans, estuaries, and inland seas (Thakur et al. 2008) and it has witnessed significant growth in the application of molecular techniques. As a result, new fields of investigation have opened (Keeling et al. 2014), the distribution and composition of microbial populations has been re-defined (Valiadi et al. 2014), and in some cases, previous studies have been re-evaluated (Burton 1996). Marine molecular biology is constantly evolving to solve problems regarding the exploration of marine organisms for human health and welfare purposes (Thakur et al. 2008). Genomics, transcriptomics, proteomics, and metabolomics have already provided information on phylogenetic relationships among HAB taxa, pathways of toxin production, HAB diversity patterns, as well as genetic responses to grazers or inter- and intra-species-specific competition (Anderson et al. 2012a; Kohli et al. 2015).

One of the recent trends in this area, which has the potential to have a huge impact on environmental science in the future, is the use of technology to perform *in-situ* analysis. Handheld analyzers for the detection of marine micro-organisms in environmental samples have been investigated (Casper et al. 2007), as well as the application of biological sensors in the field of oceanography (Zehr et al. 2008). Microfluidic systems, both within and outside the field of oceanography, have been designed for numerous purposes such as molecule separation (Brody and Yager 1997), genotyping (Rich et al. 2011) and for the performance of various biochemical and molecular assays (Lin et al. 2009). Also referred to as Lab-on-a-Chip (LOC), such systems have also been employed to monitor cell growth (Jeong et al. 2014; J.-H. Lee et al. 2008), detect water-borne pathogens (Zhao et al. 2012), and observe a range of cellular functions (Dimov et al. 2011) and behaviours associated with environmental toxicity (Huang et al. 2015; Zheng et al. 2014). LOC

technologies provide the user with the benefits of miniaturisation, integration and automation. They offer several advantages over conventional techniques: portability, speed of analysis, the ability to multiplex (Lutz et al. 2010), and platform and device compatibility with multiple molecular techniques (Sun et al. 2013; Tsaloglou et al. 2013). When coupled with appropriate molecular tools, LOC devices may provide a greater understanding of the ecology and the evolution of HAB at species level and bloom dynamics.

HABs can be initiated by cells present at very low concentrations and some microorganisms, such as the toxic marine dinoflagellate *Karenia brevis*, are capable of having adverse effects on human health starting from concentrations as little as 5 cells mL^{-1} (Bricelj et al. 2012). This is at odds with the volume of fluid typically analysed by LOC devices (typically a few microlitres). Reliable *in situ* detection of low cell concentrations with potential LOC-based detectors may therefore require robust collection methods, and pre-concentration of sample material.

Environmental sampling of phytoplankton may be achieved with a variety of sampling devices, typically mounted on ships and boats, but automated samplers can also be equipped on buoys, and autonomous under-water vehicles (Karlson et al. 2010). Collected microorganisms are often fixed and preserved with the use of chemicals such as Lugols iodine, aldehydes (Edler and Elbrächter 2010), saline ethanol etc. or via freezing (Cembella and Rafuse 2010). Sample concentration may then be achieved via filtering, sedimentation or centrifugation.

The aim of this study is to validate a novel filtration system which concentrates cells from several litres of sample into a single filter, while coupled with species-specific cell detection and quantification via NASBA analysis. This sampling method is designed to be simple, quick, and robust, without the need for additional chemical fixation of cells, or sample concentration steps.

5.3 Materials and Methods

5.3.1 Filter Concentrator System

The filter concentrator system was designed to improve *in situ* monitoring and acquired knowledge of the dynamics of phytoplankton populations, with requirements as follows. It should be capable of collecting large sample volumes, and condensing those samples to a volume manageable for molecular analysis, with a resulting concentration factor of several thousand. The user should be able to operate the system without the need for additional or otherwise specialized equipment, and without a source of electricity or other fuel source. The overall method should be able to accurately detect and quantify target species over a wide range of cell concentrations. *K. brevis*, for instance, is reportedly monitored by the Florida Fish and Wildlife

Conservation Commission (FWRI 2015) at concentrations between 10^3 cells L^{-1} (bloom not present) and 10^6 cells L^{-1} (bloom with high cell density).

The filter concentrator system is shown in Figure 23 and consists of a portable filter/concentrator/pump formed from an adapted agricultural chemical spray backpack (Hozelock 12L Pressure Sprayer Plus: 4712) with a 12-litre sample capacity. The system passes the sample through a three stage filtering process: a plastic coarse (2mm pore size) initial filter to trap large objects; a large area (73.5 cm^2) second stage intermediate (40 μm pore size) internal multi-use filter used to prevent large unwanted particles such as sand collecting in the sample filter; and a standard, commercially available, fine (0.2 μm) CellTrap™ CT40 (MEMTEQ Ventures Ltd, UK) collection filter. The multiuse filter was custom designed and manufactured from corrosion-resistant 316 stainless steel woven 40-μm wire-cloth, soldered onto a 2-mm filter mesh (G. Bopp & Co. Ltd.), to retain a robust barrel shape (Fig. 23). The filter was capped at one end with a stainless steel plate.

The input of the sprayer was modified to hold the first two filters, with the collected sample (large volume – up to 10 litres) poured into the container through both filters and into the main body of the vessel. The output of the sprayer (at the end of the pump) was also modified to allow direct connection to the third filter - the CellTrap™ sample filter. This filter is designed for small-scale environmental sampling and targets sample volumes between 10 mL and 25 L. The integrated hand pump is used to pump the pre filtered (40 μm) sample through the CellTrap filter, which is intended to trap particles greater than the pore size (0.2 μm). As a result, cells and other particles in the 0.2 μm - 40 μm range are collected prior to extraction and processing. The CT40 filter has an approximate internal volume of 1 mL, giving a maximum concentration factor of 10,000.

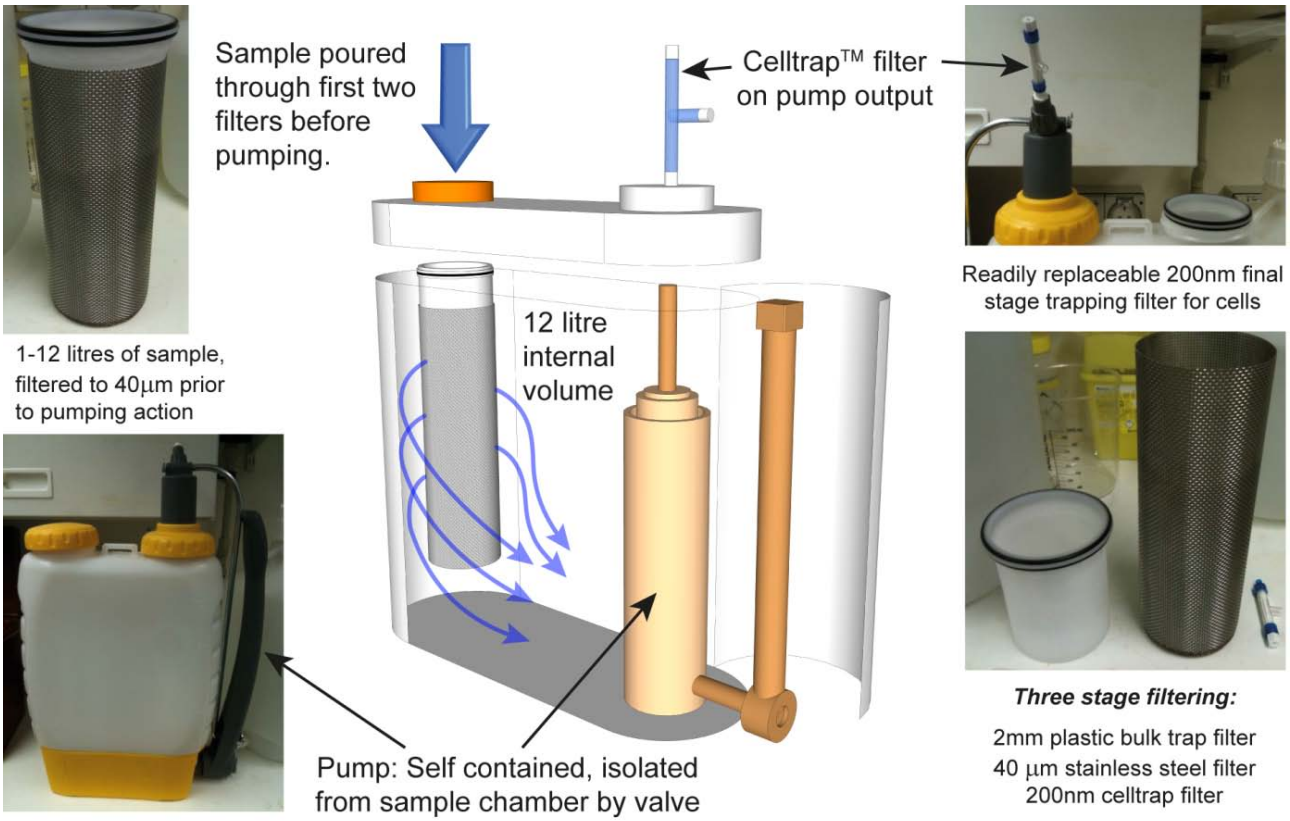

Figure 23 Schematic diagram of the internal structure of the filter/concentrator pump system, constructed from a Hozelock™ chemical spray backpack and consisting of a plastic fluid vessel which contains the filters and a hand operated pressure pump on opposite sides. Samples are processed through three stages of filtering, concurrent with a high degree of sample concentration. The first stage is a 2 mm pore size plastic pre-filter to catch large floating objects. The second stage is a 40 µm pore size 316 stainless steel woven wire-cloth main filter with a height of 26 cm and diameter of 9 cm, with a filtering surface area of 73.5×10^3 mm^2. These two stages perform the initial filtering of the sample as it is poured into the vessel prior to pumping, and retains particles larger in size than 40 µm, with the large surface area ensuring minimal clogging. The hand pump is then used to push the filtered sample through the third stage filter, the Celltrap™ CT40 0.2 µm filter, attached to the output of the pump. The complete system is configured to retain material between 0.2 and 40 µm, passing up to 10 litres of sample through the final stage filter, simultaneously reducing the sample volume to 1 mL.

5.3.2 Filter test Procedure

For each test run of a sample the filter system was filled with five litres of artificial seawater spiked with target cells at varying concentrations. The 5 L samples were loaded by pouring into the vessel through the coarse filter as described above. 4 L of this sample was divided into four sub-samples by pumping 1 L successively through four different CellTrap™ collection filters. To account for initial variability caused by pressurising the hand pump and air being trapped and

released in parts of the system, the first collection filter was discarded. The subsequent three were retained for analysis, giving three independent measurements for each sample.

To monitor pump performance, the flow rates were determined for every sub-sample during the operation of the filter concentrator. The filtrate was collected in a measuring cylinder and the time for every 100 mL increase in volume was recorded up to the maximum volume of 1 L. The flow rate was then calculated for a granularity of 100 mL by dividing this volume by the difference in the recorded times.

Tests were run with two different species (described in the next section) for the purposes of determining limit of detection for the system and the accuracy of the concentration measurements.

For these measurements, the filter samples were processed by extracting the cellular contents from the filter (including RNA) with 1 mL of chemical lysis buffer (method described below). The resulting lysate was then processed with a benchtop NASBA protocol (see below).

5.3.3 Culture Information

Tetraselmis suecica strain MBA305 was employed as a model organism in order to determine the limit of detection of the system. The species was obtained from the Marine Biologica Association of the UK, and was originally collected from the Mediterranean, La Spezia as a non-axenic culture. The *T. suecica* strain was maintained in Erdschreiber medium, without shaking at 19±1 °C on a 12:12 hour light:dark cycle, under cool fluorescent light (85-95 µmol photons m^{-2} s^{-1}; measured with a LI-189 light meter LI-COR®, Lincoln, USA). Tests run with *T. suecica* were at concentrations of 2×10^5 cells L^{-1}, 2×10^2 cells L^{-1}, and 20 cells L^{-1}, with the culture diluted to the required number of cells per litre by adding seawater.

Karenia brevis strain CCMP2228 was employed as a model organism in tests of the full analytical system (the filtration system coupled to IC-NASBA) to assess its ability to quantify HAB microalgae. The species was obtained from the Provasoli-Guillard National Center for Culture of Marine Phytoplankton, and was originally isolated from the Gulf of Mexico, Sarasota Bay as a non-axenic culture. The *K. brevis* strain was maintained in L1 Aquil* medium, without shaking at 19±1 °C on a 12:12 hour light:dark cycle, under cool fluorescent light. *K. brevis* tests were at concentrations of 10^6 cells L^{-1}, 10^5 cells L^{-1}, 10^4 cells L^{-1}, 10^3 cells L^{-1}, and 10 cells L^{-1}, with the culture diluted to the required number of cells per litre by adding seawater. NASBA was run with an internal control, as described below, to give quantitative measurements (Tsaloglou et al. 2013).

Positive control samples (without filter concentration) were run with a benchtop NASBA protocol, to evaluate the quantification efficiency of the system. The control samples were taken directly from the *K. brevis* culture and concentrated to a final volume of 1 mL via centrifugation. RNA extraction and benchtop NASBA took place in parallel with the Filtered samples.

5.3.4 Internal Control (IC) RNA synthesis

This section describes the production of the Internal Control (IC) RNA. The IC RNA employed for *K. brevis* experiments followed the same sequence as the wild-type RNA molecule of its *rbcL* gene, with a length of 87 bp. The beacon binding site however was replaced with an enterovirus sequence, which could be recognised by a second molecular beacon within the NASBA assay.

Synthesis of the IC RNA followed previously described protocols (Casper et al. 2005; Patterson et al. 2005; Tsaloglou et al. 2013). A DNA template (Eurofins MWG Operon, UK) was therefore designed containing a T3 RNA polymerase promoter at the 5' end of the sequence. The DNA template was employed for the transcription of IC RNA over the course of 2 hours at 37°C, which was then purified (RNeasy kit, Qiagen, Netherlands) and quantified (Ribogreen RNA quantification kit, Invitrogen, UK) before storage at -20°C (Tsaloglou et al. 2013).

In order to validate and assess the effectiveness of the IC, serial dilutions of a *K. brevis* sample were prepared. NASBA with internal control (IC-NASBA), as described in the following section, was then performed for test concentrations of $8x10^3$, 10^3, $5x10^2$, and 250 cells, along with a negative sample containing no cells.

5.3.5 RNA extraction and NASBA assays

This section describes the methods used for the extraction of cellular contents from the CellTrap™ collection filter and subsequent RNA extraction and purification. For *T. suecica* a commercial extraction kit (NucliSENS miniMAG®, bioMérieux, UK) was used and the protocol supplied by the manufacturer was followed. For *K. brevis* the same process was used but with the custom buffers described in Table 7. All chemicals were of highest purity and of molecular biology grade (Sigma-Aldrich, UK).

The first stage of extraction for filtered samples used a 1 mL syringe to elute the contents of the CellTrap™ filter. The syringe was preloaded with 0.2 mL of lysis buffer, which was then pushed into the filter and then extracted. Positive control samples were taken directly from the *K. brevis* culture and concentrated to a final volume of 1 mL.

Table 1.	**Custom RNA extraction Buffers**	
Custom Buffer A	**Custom Buffer B**	**Custom Buffer C**
0.1M Tris pH 7.5	0.01M Tris pH 7.5	0.01M Tris pH 7.5
0.01M EDTA	1mM EDTA	
0.5M LiCl	0.15M LiCl	
4M GuSCN		
1% Triton X-100		

Table 7 Composition of the custom RNA extraction buffers used in this work. Buffers A, B, and C were used for lysis, washing, and elution steps, respectively.

All samples were then placed into a tube containing an additional 1 mL of lysis buffer, giving a final volume of 1.2 mL for filtered samples and 2 mL for positive control samples. The lysis buffer for *T. suecica* was provided by the manufacturer and for *K. brevis*, Custom Buffer A was used. For all *K. brevis* samples, 2.5 µL of internal control (IC), containing 400 copies of IC RNA was then added.

Samples were then incubated for ten minutes; 50 µL of magnetic bead stock (bioMérieux UK Limited) was then added; followed by a further ten-minute incubation, to complete cell lysis. Mixing between each step was induced via vortexing.

All samples were then washed according to the following procedures. Samples were centrifuged and pipetting was used to remove and discard the supernatant solution. For washing of *T. suecica*, the manufacturers kit instructions were followed. For K*. brevis*, 500 µL of Custom Buffer B was added to the remaining beads. Samples were then transferred to a NucliSENS® miniMAG® and subject to magnetic attraction and mixing for thirty seconds. A subsequent 500 µL of Buffer B was then used to wash the beads a second time.

Finally, samples were eluted with the addition of 25 µL of elution buffer (Buffer C in the case of *K. brevis*), followed by shaking on an Eppendorf thermomixer at 60°C, 1200 rpm, for five minutes. Samples were then placed on a magnetic rack and the supernatant containing the RNA was removed. All extracted RNA samples were stored at -20°C in preparation for NASBA® analysis.

The NucliSENS EasyQ® Basic Kit (bioMérieux UK Limited) was employed for all NASBA® assays, and according to manufacturer instructions. In the case of *T. suecica*, the reaction targeted the RuBisCO rbcL gene and incorporated one set of forward/reverse primers, along with a molecular beacon (Table 2). Another set of primers was used to target the RuBisCO rbcL gene of *K. brevis*. Two molecular beacons were integrated in the assay; one targeting *K. brevis* "wild-type" sequence

and one targeting the IC (Table 2)(Tsaloglou et al. 2013). All primers and molecular beacons were obtained from Eurofins MWG Operon (London, UK).

T. suecica molecular beacon was labelled with CY5 at the 5' end and the quencher ECLIPSE at the 3' end. *K. brevis* wild-type molecular beacon was labelled with Alexa Fluor 488 at the 5' end and the quencher BHQ1 at the 3' end, whereas the IC molecular beacon was labelled with CY5 at the 5' end and the quencher BHQ2 at the 3' end.

T. suecica	Sequence (5' to 3')
Forward Primer	**ACTGGCTTCAAAGCTGGTGT**
Reverse Primer	AATTCTAATACGACTCACTATAGGGAGAAG**TCCGTCCATACAGTTGTCCA**
Molecular Beacon	[CY5]- GAGTCG**AGATTACCAAGTAAAAGATACTGAC**CGACTC -[ECLIPSE]
Target Sequence	**ACTGGCTTCAAAGCTGGTGT** AAAAGACTACCGTTTAACTTACTACACTCC- **AGATTACCAAGTAAAAGATACTGACATTCT** TGCAGCATTCCGTTGTAACCCTCAACCAGGTGTTCCACCTG- AAGAGTGTGGTGCAGCTGTAGCCGCTGAGTCATCAACTGGTACTT **GGACAACTGTATGGACGGA**
K. brevis	Sequence (5' to 3')
Forward Primer	**ACGTTATTGGGTCTGTGTA**
Reverse Primer	AATTCTAATACGACTCACTATAGGGAGA **AGGTACACACTTTCGTAAACTA**
Molecular Beacon	[AF488]-GAGTCGCTTAGTCTCGGGTTATTTTTTCGACTC-[BHQ1]
Target Sequence	GAA**ACGTTATTGGGTCTGTGTA**CACGAATTAACCTTAGTCTCGGGTTATTTTTTGGACAAGAATGGGC- **TAGTTTACGAAAGTGTGTACCT**
Internal Control	Sequence (5' to 3')
Molecular Beacon	[CY5]-ACGGAGTGGCTGCTTATGGTGACAATCTCCGC-[BHQ2]
Sequence	GAA**ACGTTATTGGGTCTGTGTA**CACGAATTAACTGGCTGCTTATGGTGACAATGGACAAGAATGGGC- **TAGTTTACGAAAGTGTGTACCT**

Table 8 List of the sequences of *T. suecica* primers, beacons, and RNA; the sequences of *K. brevis* Internal Control (IC) primers, beacons, and RNA. Bold underlined text indicates primer binding sites.

5.3.6 Quantification of RNA amount with NASBA analysis method

NASBA® analysis of *K. brevis* samples produced two fluorescence monitored reaction curves for each sample; one representing wild-type amplification and one representing IC amplification.

Quantification of wild-type RNA, which serves as an indication of cell concentration, was initially attempted through time-to-positivity (TTP) ratios (Polstra et al. 2002). A threshold of detection (TOD) was set, and the point in time where each bi-exponential NASBA® curve rose above the TOD, was defined as a TTP value. The ratio of wild-type TTP and IC TTP was subsequently used as a quantitative indicator for the concentration in each sample.

A second, curve fitting method was also used for data analysis, by employing MATLAB™ in conjunction with the following equation:

$$Y(t) = \lambda Y_0 - (\lambda - 1)Y_0 \exp\left\{-{}^{1}\!/_{2}\, k_1 a_1 \left[ln\left(1 + e^{a_2(t-a_3)}\right)\right]^2\right\}$$

This equation describes NASBA-driven RNA amplification, where $Y(t)$ the fluorescence signal as a function of time, Y0 the signal at t = 0, λY_0 the fluorescence value at its highest point, $\alpha_1\alpha_2$ representing the shape of the curve, α_3 defining the curve location relative to the time axis, and k_1 a reaction rate constant (Weusten et al. 2002). Each curve fit results in a set of parameters whose values represent the appropriate NASBA curve. Every IC-NASBA reaction produces two curves (one for the WT-RNA and one for the IC-RNA) and two sets of parameters. The quantitation variable is then determined by calculating the $k_1 a_1 a_2^2$ ratio from the parameters for the WT and IC curves. This method produces a quantitative metric for the concentration of WT RNA in the original sample.

In summary, for this work, the MATLAB™ curve-fitting tool was used to produce a quantitation variable, defined as the $k_1 a_1 a_2^2$ ratio, which is linearly related to the logarithm of the amount of wild-type RNA in a sample (Tsaloglou et al. 2011) and is an indicator of target cell concentration.

5.4 Results and Discussion

5.4.1 Filtering System Operation

Data describing the flow through the filtering system are illustrated in Figure 24. The results are shown as cumulative volume against cumulative time demonstrating the main linear period of operation followed by the slower period approaching one litre as the operator reduced pressure (Figure 24a). The same data is also plotted as average volumetric flow rate, determined for each 100 mL sub-sample, against cumulative volume (Figure 24b).

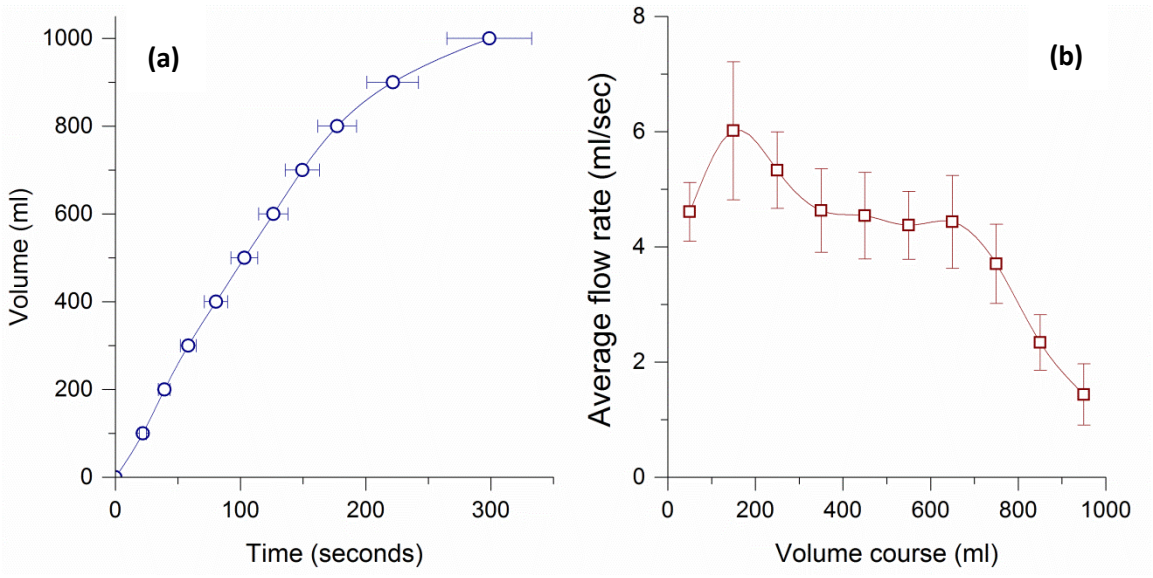

Figure 24 Volumetric flow rate through the filter system. Data are averages of nineteen runs at varying cell concentrations with the error bars representing standard deviation (a) graph of cumulative volume passed through the filtering system against cumulative time taken and (b) graph of volumetric flow rate against cumulative volume. The pump runs consistently at a rate of approximately 4.6 mL/sec, with a small rise and fall at the start of pumping as the hand pump is pressurised, followed by a consistent flow rate until the end of the required volume where the flow rate tapers off as the hand pump pressure is allowed to fall off.

The results provide evidence of constant flow rate at approximately 5 mL/s for the first two thirds of the operating period, with an increase near the beginning; this is due to variable charging of the volume of fluid contained within the barrel of the hand pump. Moreover, as the hand pump is user-controlled and inherently variable, significant flow rate variation was observed between runs (28% at 200 mL processed volume) whereas anticipation of the point at which 1 L of sample is processed led to the significant reduction (up to 300%) of flow rate after 200 seconds and 700 mL. This end point is related only to the discharge of pressure: in tests where 5 litres was processed, the flow rate remained constant until 300 mL before end of pumping.

The filtering system retained an approximately constant flow rate throughout the testing period. The hand-powered pump was capable of processing 1 L of sample in five minutes, while achieving sample concentration of 1000:1 within the CellTrap™ filter. The system, therefore, performed a rapid and consistent sample collection, suitable for our *in situ* environmental testing.

5.4.2 Limit of detection: *Tetraselmis suecica*

NASBA was performed on filtered *T. suecica* samples at different concentrations and produced three distinct curves (Figure 25). Amplification for the $2x10^5$ cells L^{-1} concentration samples was

observed from thirteen minutes, reaching 29.08 relative fluorescence units (RFUs) at the peak of the reaction. The 200 cells L^{-1} concentration samples showed amplification from nineteen minutes and peaked at 27.65 RFUs. Samples from the 20 cells L^{-1} concentration amplified after twenty-minutes, and reached a maximum fluorescence of 22.80 RFUs. Standard deviation between samples increased as cell concentration decreased, and highest standard deviation values were observed for the 20 cells L^{-1} samples (6.52). The error bars show the standard deviation of each data point.

T. suecica was successfully detected at all concentrations, ranging from $2x10^5$ cells L^{-1} to 20 cells L^{-1}. The shape of the NASBA curves, show a discernible trend with varying concentration: that of a steeper rising curve coupled with a shorter time to positivity (TTP) as cell numbers increased. These initial results demonstrate that the filter concentrator system can be considered for quantitative measurements, down to a concentration of 20 cells L^{-1}.

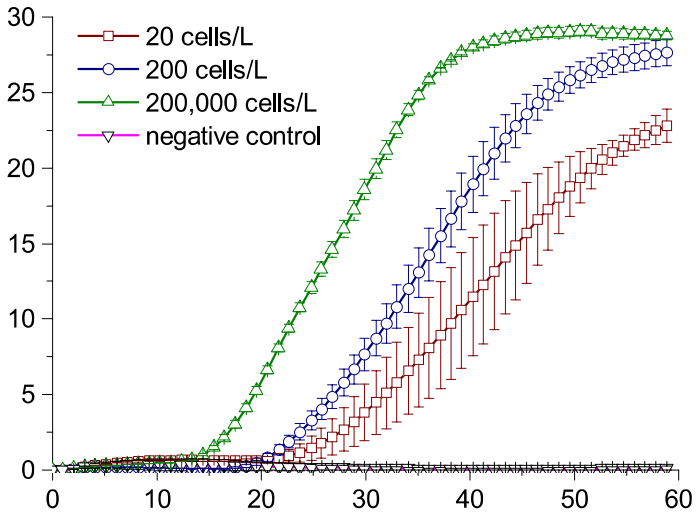

Figure 25 NASBA results for *T. suecica*. The *y-axis* represents relative fluorescence units, as measured by the EasyQ benchtop incubator, and the *x*-axis represents time in minutes. WT-RNA amplification of 20 cells equivalents is shown as red squares, 200 cells are shown as blue circles, 2×10^5 cells are shown as green triangles, and the negative control (zero cells) is shown as purple reverse triangle. Error bars denote one standard deviation of triplicate samples.

5.4.3 Quantitative measurement: *Karenia brevis*

5.4.3.1 Initial measurements and verification of method

IC-NASBA was run on serial dilutions of a *K. brevis* sample and a standard curve was produced as shown in Figure 26. This illustrates the relationship between the value of ln(Qvariable ratio) and

log10(number of cells). Note that data points represent single replicates, and not triplicate samples.

The results showed a clear trend, closely following (R^2=0.997) a linear function. This demonstrated the effectiveness of the Internal Control and the curve-fitting method of quantitation, allowing for the subsequent detection and quantification of *K. brevis*.

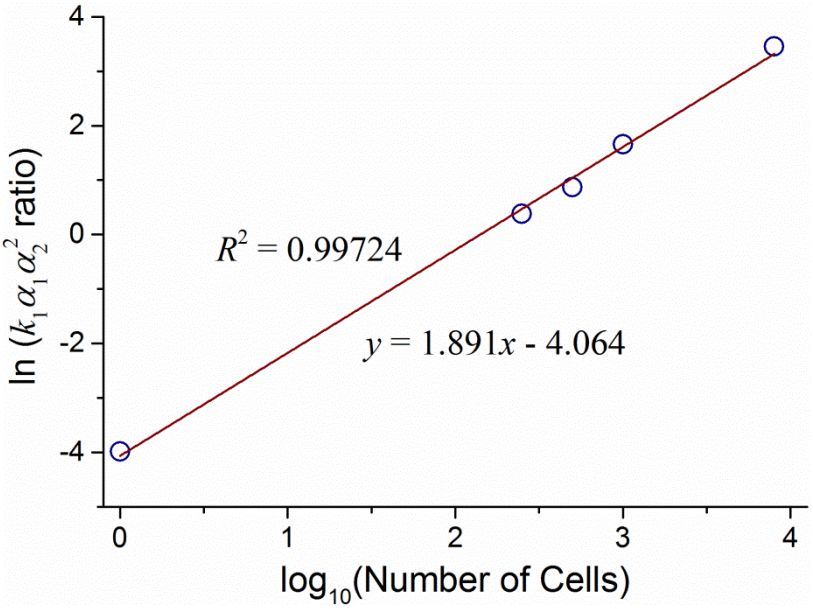

Figure 26 Standard Curve showing how the quantitation variable changes with cell number (round circles). Also shown is a fitted trendline to the data, with the fitting equation and the R^2 value shown. The graph is plotted with log10 of the number of cells so that the fitted equation has a simple representation.

5.4.3.2 **Filter results**

NASBA on filtered *K. brevis* samples was performed successfully and the relationship between IC and wild-type curves changed as cell concentration decreased. Appendix C contains the complete set of data on the results of NASBA, as well as the matching parameters derived from the curve fitting.

Wild-type curves experienced an increase in fluorescence at approximately nine minutes before IC curves at 10^6 cells L^{-1}. This temporal gap decreased as cell concentration decreased, until at 10^4 cells L^{-1} amplification occurred at the same time. At even lower concentrations, the wild-type and IC curve relationship was reversed, and the wild-type fluorescence signal increase occurred later. The overall wild-type signal was at its lowest for the 10 cells L^{-1} samples and never surpassed 0.42 RFUs. The Control samples followed a similar trend.

Looking more closely at the results, using the example of the IC-NASBA results for the 10^5 cells sample (Figure 27) it is apparent that the difference in gradient of the rising section of the curve between the WT-RNA and the IC-RNA for the amplification signals, is greater for the control samples than for the filtered samples. In addition, the filtered replicates show IC amplification approximately seven minutes after WT amplification, and IC maximum fluorescence is reached 15-20 minutes after the WT equivalent. By comparison, the corresponding times for the control samples are less than five minutes, and 10-15 minutes.

These results indicate that there is a relationship between wild-type and IC curves which is dependent on *K. brevis* concentration in both filtered samples and corresponding Control samples.

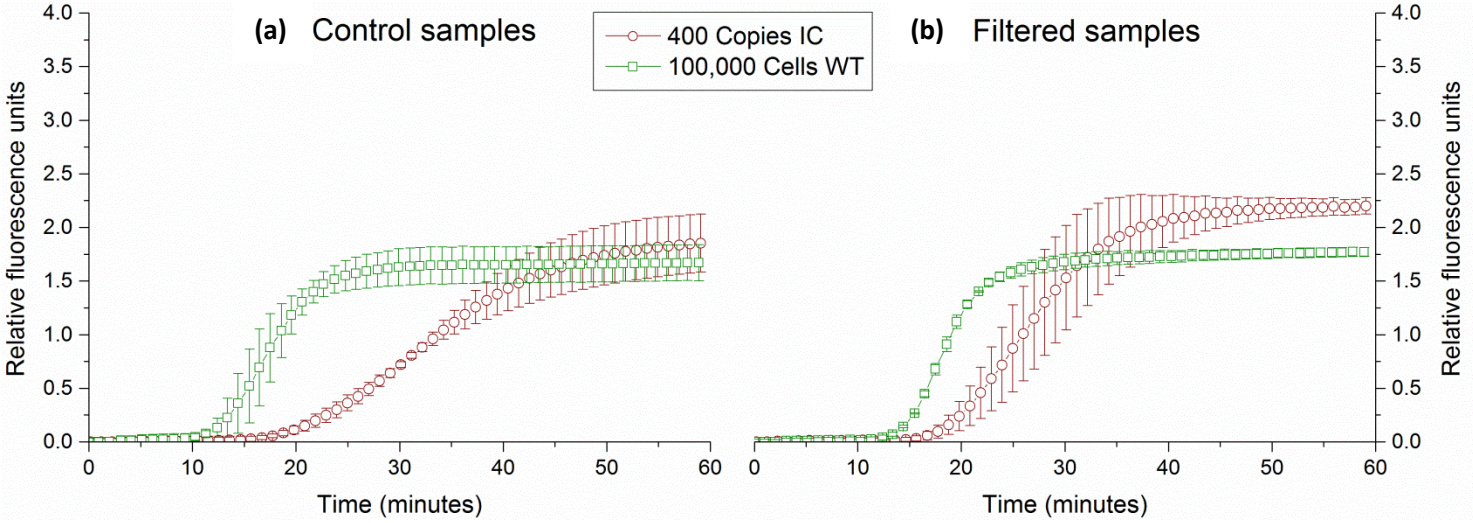

Figure 27 IC-NASBA results for 10^5 cell equivalents of *K. brevis* with 400 IC copies. The y-axis represents relative fluorescence units, as measured by the EasyQ benchtop incubator, and the x-axis represents time in minutes. WT-RNA amplification is shown as red squares and IC-RNA amplification is shown as green circles. Control samples are illustrated on the left whereas filtered samples are shown on the right. Error bars denote one standard deviation of triplicate samples.

5.4.3.3 Analysis and quantification of *Karenia brevis*

In order to demonstrate the quantification properties of our chosen method and system, the NASBA results were analysed using the TTP ratios and quantitation variable. Following the example sample (Figure 27), the calculated values indicate that at 10^5 cells, the control method extracted a higher amount of *K. brevis* RNA, with an average quantitation variable value of 2.04. By comparison, the filtered equivalent was 1.05. The graphs contained in Figure 28 show the complete set of values calculated from the whole data set (given in Appendix C) with TTP ratios

and quantitation variable plotted against increasing cell concentration for filtered samples and control samples (Figure 28).

The results indicate that samples processed by the filter concentrator system produced a more consistent linear trend with logarithmic cell number than the bench top controls. For both sets of samples the trendlines fitted to the TTP ratio data were had very similar intercept and slope values but with an R-squared value of 99.8% for the filtered samples and 83.4% for the control samples. The fitting for the quantitation variable data showed more variability and less agreement between the fit parameters, with an R-square value of 98.3% for the filtered samples and 87.4% for the control samples.

The fit to the trend is marginally better using the TTP ratio data rather than the quantitation variable for quantification, and significantly better for the filtered samples compared to the controls samples. Overall, this suggests that RNA quantification using the filter system would be more accurate. However, the results from the filter system show slightly increased variability (decreased precision) vs the control. This is more pronounced at low concentrations and for results using the quantification variable. This variability arises from the fact that the samples have a large volume with very low cell numbers, compounded by needing to recover small cell numbers at the elution stage. This can be mitigated by increasing the number of replicates and/or increasing the volume sampled for low cell concentrations to increase the number of cells.

The results from the two analysis methods lead to several conclusions. The filter concentrator demonstrated the measurement of cell concentration, with the TTP analysis providing a better quantification of this than the quantitation variable method. The Control samples in these experiments did not provide the same accuracy. The two different methods also provide different calculations of variability with the TTP ratio values having smaller standard deviations at lower concentrations than the quantitation variable method, with the conclusion that the first method provides a more accurate determination of the concentration of small cell numbers in these experiments. Based on the successful repeated measurement of samples at a concentration of 10 cells L^{-1}, the limit of detection can be estimated as approximately three times the smallest measured concentration or 30 cells L^{-1}, well below the detection limit required for early detection of bloom formation.

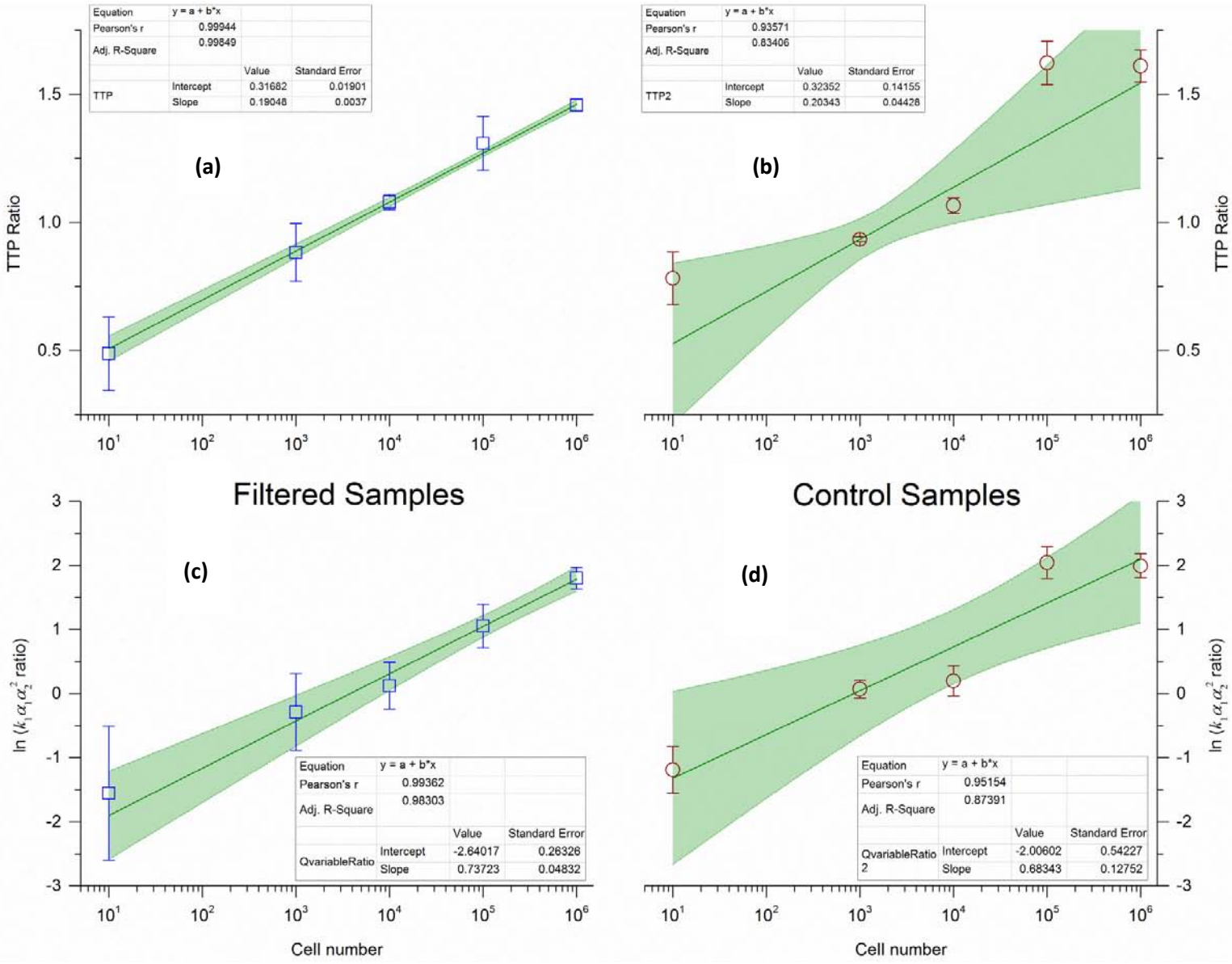

Figure 28 Quantitation analysis on IC-NASBA results, using TTP analysis method (a,b) and Quantitation variable analysis method (c,d), for the filtered samples (a,c) and the control samples (b,d). TTP ratios and $\ln(k_1a_1a_2^2$ ratios) were plotted over increasing cell concentration (log scale). Control samples are represented by red circles and filtered samples are represented by blue squares. Error bars denote one standard deviation of triplicate samples. Also shown are the lines of best fit and the shaded area represents the 95% confidence bands.

The filter processes litres of sample prior to analysis, which reduces the inaccuracy associated with sampling small numbers. Control samples, by comparison, involved the handling of significantly smaller volumes (a few mL at a time) thus increasing the chances and degree of sampling error. More importantly, the error experienced in our control samples would have been enough to misjudge target cell concentration by one or two orders of magnitude.

This data supports the need for large-volume sample concentrators within the field of phytoplankton and HAB studies, for more accurate and precise monitoring and estimation of bloom formation.

For the operation of the filter contractor system, at higher cell concentrations factors such as increased compaction, large differential pressures, or high levels of RNA, all could affect the quality of cell extraction and lysis. An effective mitigation strategy would then be to filter smaller volumes when cell concentrations reach 10^5 cells L^{-1}. To improve consistency in calculated values for cell concentrations below 10^2 cells L^{-1}, the solution would simply be to filter larger volumes of sample.

5.5 Conclusions

This Chapter presents a novel filter-concentrator system, designed for the collection and concentration of seawater samples, characterised particularly by very low cell concentrations and the requirements of processing large volumes for *in situ* sample processing. The filtering system was capable of maintaining an approximately constant flow, with a rapid and consistent sample collection at 1 L in five minutes. *T. suecica* was successfully detected at all filtered concentrations, ranging from $2x10^5$ cells L^{-1} to 20 cells L^{-1}. Initial IC-NASBA results showed correlation with *K. brevis* concentration in filtered samples. Further analysis showed that samples derived from the filter system more accurately followed a linear trend versus logarithmic cell number than the bench top controls. When compared to standard benchtop analysis, our filtering system improved accuracy of *K. brevis* quantification via IC-NASBA (higher R^2 value), but a small decrease in precision was observed (higher standard deviation values). Our sampling method successfully quantified *K.* brevis across all concentration ranges used by the Florida Fish and Wildlife Conservation Commission for bloom monitoring. This included concentrations of 10 cells L^{-1} which is two orders of magnitude below the minimum of what is recognised as a bloom (1000 cells L^{-1})(FWRI 2015) and could permit detection and measurement of populations in a pre-bloom state.

This filter-concentrator system provides simple, rapid, and consistent sample collection and concentration, and could become a useful tool for in-field monitoring of HABs, water-borne parasites, and pathogens associated with faecal matter. Additional research will be required to further optimise extraction methods. Coupling of the system with other molecular analysis methods would demonstrate flexibility regarding its application. Finally, using it in conjunction with Lab-on-a-Chip devices, to analyze environmental samples, could prove to be a viable and powerful tool for on-field monitoring of HABs and human pollution.

Chapter 6: Discussion and further work

6.1 Conclusion

The purpose of this work has been to develop and optimise a fully automated molecular assay on a novel lab-on-a-chip system, which performs RNA-based amplification, for the detection and quantification of marine microorganisms in future *in situ* environmental applications. Even though a fully automated on-chip nucleic acid extraction process has not been implemented, the issues tackled in the thesis provide important developments in the field of lab-on-chip technology, as well as *in-situ* sample collection and processing for HAB monitoring. This thesis reports on (1) the optimisation of an IC-NASBA assay for the detection and quantification of microorganisms while examining the validity of the technique under varying physiological states and growth conditions; (2) the long-term preservation and storage of NASBA reaction components; (3) the development of a fully automated, fully preserved, lab-on-a-chip-based IC-NASBA protocol for real-time detection and quantification of microorganisms; (4) the development of a simple, rapid, and reliable sample collection and concentration method, aimed for *in situ* application and compatibility with nucleic acid analysis techniques.

Detection, and amplification of RNA was preferred over DNA as it is more indicative of physiologically active organisms within a sample, and IC-NASBA was chosen as an appropriate molecular tool for detection and quantification because it requires low temperature operation (41°C) with a single primer annealing step at 65°C. Thus, there is no need for additional reverse transcription steps (contrary to PCR and other DNA-based methods) and the lack of thermal cycling greatly eases the challenge when converting to LOC (power consumption, temperature-induced bubble formation, etc.). *K. brevis* was chosen as a central model microorganisms for experiments throughout the course of this PhD due to assay availability (Casper et al. 2004; Casper et al. 2007; Tsaloglou et al. 2013), extensive monitoring of its associated HABs and toxicity-induced damage (Bricelj et al. 2012; Flaherty and Landsberg 2011; Fleming et al. 2011; Reich et al. 2015), and because it has been an overall well-characterised harmful marine microorganism, both in terms of previously conducted physiological studies and molecular work (Casper et al. 2007; Hardison et al. 2013; Hardison et al. 2014; López-Legentil et al. 2010; Morey et al. 2011; Tsaloglou et al. 2011).

6.1.1 IC-NASBA as a monitoring tool

In Chapter 2, an IC-NASBA assay targeting the RNA sequence of the RuBisCO *rbcL* gene of *K. brevis* was optimised, and its quantification properties and validity were tested. The work represents the initial stages of this PhD and is considered particularly important, since the NASBA assay became a fundamental element of the overall work. This was the first study to address potential changes in

K. brevis rbcL expression after long-term exposure to varying growth conditions, which could influence the precision and accuracy of similar IC-NASBA detection and quantification methods; a very likely scenario to occur in environmental populations.

A question not addressed in literature, but studied in this PhD, concerned changes in *rbcL* expression as a result of varying growth conditions and associated physiological states. Transcription of certain genes can be significantly affected by environmental triggers such as nutrient availability (Hardison et al. 2013; Morey et al. 2011) and CO_2 concentration (Hardison et al. 2014). The *rbcL* gene of *K. brevis*, which has been previously used for cell detection and quantification with IC-NASBA, may have also undergone changes in rate of expression when cells experienced similar triggers. If this was the case, quantification of *K. brevis* would be impossible; for example, a population of 500 cells L^{-1} with double the expression rate, would have shown an estimated concentration of 1,000 cells L^{-1} after IC-NASBA analysis, and vice versa. The resulting error would determine the on-time detection of what current monitoring standards consider a *K. brevis* low-bloom (FWRI 2015). Previous studies performed short term stress tests in regards to *rbcL* transcription for *K. brevis* (Casper et al. 2004) and *K. mikimotoi* (Ulrich et al. 2010). The tests exposed cells to periods ranging from 4 to 72 hours, and out of the tested conditions (low nutrient, low salinity, high-light and low-light), only the high light treatment appeared to increase *rbcL* transcription, resulting to cell death within the first 24 hours. However, these short-term stresses do not necessarily reflect changes in transcription after long-term exposure and acclimation of phytoplankton populations in different environmental conditions with varying chemistry. The experiments presented in Chapter 2 aimed to produce varying growth conditions and physiological states, connected to differences in medium chemical composition. The resulting data suggested that the expression of gene *rbcL* is relatively stable, and thus added credibility to the IC-NASBA method for quantification.

A key aspect of the optimisation dealt with the synthesis of the internal control and its incorporation in the nucleic acid extraction protocol. Once the concentration of the synthesised IC stock was determined, a known amount of IC RNA copies was added specifically to the lysis buffer along with the sample to be extracted. This differs from previous studies using IC-NASBA, which report addition of the IC template to each reaction instead (Casper et al. 2005; Patterson et al. 2005; Ulrich et al. 2010). A portion of target product is naturally lost during nucleic acid extraction, leading to potentially significant sample to sample variability. In addition, a set of custom extraction buffers were used for *K. brevis* experiments, further increasing extracted

sample variability from batch to batch[8]. Incorporating the IC RNA in the initial lysis step, meant that the percentage of wild-type and IC RNA lost during extraction would be the same, and the wild-type to IC ratio would therefore remain unaltered. This small, yet significant variation within the IC-NASBA method (i.e. adding the IC template to each sample during the lysis step instead of the NASBA reaction mixture) should provide the user with more accurate quantification results and a better representation of sample cell concentration.

However it is important to note that, over the course of the PhD, each stock of synthesised IC showed variations in amplification efficiency; for example one experiment may have used 2.5 μL of IC stock containing 800 IC RNA copies to successfully quantify 1,000 cells, but during another experiment 2.5 μL of the same stock may have wrongly given a significantly higher or lower cell estimation for a 1,000 cell sample. This may have been due to degradation of IC RNA stocks over time, batch-to-batch variations in NASBA reaction mixtures, or batch-to-batch differences in custom extraction buffers. Therefore, before any quantification experiment, a standard curve was produced with cell serial dilutions to acquire a more accurate view of the dynamics between wild-type RNA and used IC RNA. Furthermore, each individual experiment used its own separate batch of custom extraction buffers and NASBA kit, to eliminate sample-to-sample variation as a result of batch-to-batch differences.

Two methods were used for the quantification analysis of NASBA results: time to positivity (TTP) ratios, and the quantitation variable. TTP is defined as the point in time over which a set threshold of detection crosses a NASBA curve, and its value will increase as sample original RNA concentration decreases; accordingly, samples containing higher RNA concentrations will result in lower TTP values. The quantitation variable is defined as the ratio of a set of parameters ($k_1a_1a_2^2$), derived from fitting of a previously described equation[9] (Weusten et al. 2002) to individual NASBA curves. Out of the two methods, TTP analysis is typically used but the quantitation variable analysis takes into account more parameters describing a NASBA curve. The quantitation variable analysis would, in theory, give more accurate quantitative results in situations where fluorescence measurements occur with high sample-to-sample variability, as seen throughout the single-

[8] The custom extraction buffers were under development by a previous PhD student (Dr Mahadji Bahi) and a Masters student (Ysobel Baker) to improve extraction on phytoplankton cells, and were further developed and optimised as part of the thesis, targeting *K.brevis*. Commercial buffers are typically designed and optimised to extract nucleic acids from blood or plant cells, whose cell walls tend to break down easier than those of most phytoplankton species. Furthermore, the manufacturing of a custom set of extraction buffers allows users to adjust their known composition as they see fit, and reduces expenses.

[9] The equation was developed by Weusten et al. (2002) to quantify viral loads using NASBA-based RNA amplification. The quantitation algorithm takes into account a series of information and characteristics describing a typical NASBA curve, as a function of amplification time and relevant kinetic parameters.

chamber chip and lab-card experiments (see Chapter 4). Furthermore, quantitation variable values formed trendlines with steeper slopes, suggesting that the method may be more effective at distinguishing a range of different cell concentrations; albeit there could be a trade-off in precision when compared to TTP ratio analysis (see Chapter 5). Finally, using two different approaches to quantify cells with IC-NASBA provided additional verification of results, and allowed for a better understanding of the wild-type and IC dynamic.

6.1.2 IC-NASBA integration on the LabCardReader

Chapter 3 and Chapter 4 aimed to achieve full integration of IC-NASBA on-chip, using a fully automated LOC system and preserved reaction mixtures. More specifically, Chapter 3 dealt with the development of two separate preservation protocols (one for each NASBA mastermix) and Chapter 4 realised IC-NASBA functionality on lab-cards, to be analysed by the LabCardReader.

Preservation of the NASBA reagent and enzyme master-mixtures was a process that started early on in this PhD and overlapped with all other work undertaken and presented in this Thesis. Reagents and enzymes were provided in the form of lyophilised spheres and were rehydrated with the use of prepared buffer mixtures. The resulting master-mixtures have to be used within the same day before loss of functionality occurs, but NASBA was tested and successfully conducted up to 24 hours after preparation. Thus, for *in-situ* sensor deployment and sample analysis, long-term storage of the NASBA reaction has to be implemented.

Lyophilisation is one of the most widely used methods of preservation of nucleic acids, enzymes, and proteins (Andersen et al. 2008; Kadoya et al. 2010; Kasper and Friess 2011; W. Wang 2000), and would have theoretically been an excellent choice for the preservation of reaction components on-chip (Lutz et al. 2010). However the presence of KCl and other potential diluent components, not listed on the NucliSENS EasyQ® Basic Kit, would have hindered the freeze-drying process. Consequently, gelification and dehydration under the presence of sugars were chosen as alternative preservation methods, which did not require any form of freezing. The gelifying agent, supplied by Biotools (a collaborator on the LABONFOIL project), was initially used to attempt preservation of both NASBA reagents and enzymes. Gelification optimisation involved estimating sample water loss during earlier testing stages, as well as optimal time needed for droplet dehydration using an EVG 501 bonding chamber (EVGroup, Austria) (see Appendix A). Part of the later stages of the optimisation focused on NASBA reagent mastermix preservation on-chip (targeting *K. brevis*), and was published as part of a collaborative paper (Tsaloglou et al. 2013).

Enzymes appeared to lose functionality when gelified, and thus an alternative preservation method was investigated. Dehydration of reagents under the presence of sugars has been

successfully attempted before for a microfluidic immunoassay (Stevens et al. 2008); the addition of sucrose and trehalose to the NASBA enzyme mastermix, followed by dehydration, appeared to give similarly positive results and the preservation method was quickly tested for long-term storage capabilities, and compatibility with the gelified NASBA reagent mastermix. Long-term storage of the fully preserved NASBA assay was finally achieved, with Chapter 3 results indicating successful preservation for a minimum of six weeks; Chapter 4 results further confirmed the ability for long-term storage on-chip, as well as the durability of the preserved assay through the extensive transport of lab-cards under varying temperature conditions.

On-chip IC-NASBA implementation for analysis on the LabCardReader was demonstrated in Chapter 4. All initial work involved developing a treatment protocol on single-chamber chips for the subsequent optimisation of on-chip NASBA. At first, the protocol included multiple chip washing steps, including the use of RNaseZAP®, molecular grade ethanol, bovine serum albumin (BSA), and RNase-free water. The washing steps aimed to render chips (or lab-cards at later stages) RNase-free, to prevent wild-type RNA and IC-RNA degradation, while keeping chamber and microfluidic channel surfaces compatible with NASBA. This protocol was used for early on-chip experiments, some of which are included in a previously published paper (see Appendix B) (Tsaloglou et al. 2013). However, the vast majority of treated chips failed; this may have been either due to RNases remaining on the chip surfaces (which was considered unlikely), or due to insufficient rinsing with RNase-free water which potentially led to RNaseZAP®, ethanol, and BSA residues interfering with NASBA reactions. Nevertheless, treatment with RNaseZAP®, followed by multiple rinsing/washing steps with RNase-free water and subsequent drying in a vacuum oven, resulted to successful RNA amplification both on single-chamber chips and on lab-cards.

Overall, the LabCardReader demonstrated to have potential for good technical and scientific impact on environmental applications. The short time to achieve real-time results, using a fully automated protocol with a primer-annealing step and preserved reaction mixtures, is an unprecedented achievement for microorganism detection with IC-NASBA. The lab-on-a-chip technology developed and presented in this thesis combines portability, ease of use, assay flexibility (Sun et al. 2013; Tsaloglou et al. 2013), and the possibility for *in situ* environmental application as a result of long-term reagent and enzyme storage on lab-cards. Its main weakness, in comparison to other currently deployable systems (Doucette et al. 2009; Fukuba et al. 2011b), lies with the lack of automated RNA extraction with IC RNA integration. In addition, despite the LabCardReader's ability to acquire quick results, only one IC-NASBA reaction can be run per lab-card at any given time. Thus, when compared to the state of the art, the presented LOC device provides better portability and great potential for long-term *in situ* application to monitor HABs

and other pathogenic marine species; but to become competitive, full integration of sample preparation inside lab-cards is needed along with multiplex targets capabilities.

6.1.3 Sample collection and preparation

Work involving the portable filtration system for *in situ* sample collection is presented in Chapter 5. The development of a portable filtration system presented a great opportunity to apply the optimised IC-NASBA method for quantification on a significantly wider range of cell concentrations (from 10 cells L^{-1} to 10^6 cells L^{-1}) and to develop a simple sample collection/concentration method for *in situ* microorganism population studies and applications.

Two microorganisms were used for initial testing, varying significantly in size: *T. suecica* (approximately 6-13 μm length, 4-10 μm width) and *K. brevis* (approximately 28-36 μm length, 28-36 μm width). *T. suecica* and *K. brevis* were both successfully captured, extracted from the final concentration filter, and detected using NASBA, demonstrating the effectiveness of the setup. Furthermore, *K. brevis* samples were successfully quantified, using IC-NASBA, and results suggested that the filtering system provided improved accuracy compared to non-filtered samples.

Quantification analysis was conducted using TTP and quantitation variable methods. The wide *K. brevis* concentration range provided a better understanding of the differences between the two methods. TTP analysis appeared to offer overall more accurate and precise quantification, despite the smaller slope of the trendline describing TTP ratio values. Thus, results suggested that the TTP method is more than adequate for processing benchtop IC-NASBA results, and may be preferred over the more complicated quantitation variable method. However, the latter may be a better choice when sample replicates are amplified in different runs (like lab-cards run on the LabCardReader), since the quantitation variable considers a variety of NASBA curve parameters. More information on quantification analysis, using the quantitation variable method through curve fitting, can be found in Appendix C.

6.2 Further work

This section focuses on suggestions to further extend and improve research on the topic of the overall PhD. These suggestions are listed in the following:

6.2.1 IC-NASBA as a monitoring tool

- Chapter 2 investigated potential changes in *rbcL* gene expression in *K. brevis*, due to medium composition, which may inadvertently affect quantification with IC-NASBA. More factors should be investigated that may trigger different transcriptomic responses, such as light conditions, CO_2 concentration, etc.
- More optimisations are needed to reduce the time and facilitate the conduction of NASBA. The use of heat-resistant enzymes, or equivalent, may allow for preparation of a single NASBA mastermix (instead of separate enzyme and reagent master-mixtures); this would simplify future NASBA protocols and remove the separate primer-annealing step.
- Multiplex NASBA assays could be developed to study changes in transcription of genes associated with toxin production. Polyketide synthesis (PKS) genes have been shown to be involved in toxin production (Kohli et al. 2015; López-Legentil et al. 2010; Monroe et al. 2010) and their expression could be compared with *rbcL* expression to monitor toxicity levels of HABs.
- Alternative custom extraction techniques should be developed to limit direct user contact with harmful chemicals, like Guanidine and potent lysis detergents. A combination of thermal and mechanical lysis, under the presence chemicals to protect against RNase-induced RNA degradation may be a safer alternative.

6.2.2 IC-NASBA integration on a LOC platform

- Automated nucleic acid extraction is a significant function currently missing from the LabCardReader. Thus, future work on this system or future LOC platforms should investigate different on-chip extraction methods and implement a fully automated extraction protocol. This would involve a lab-card protocol redesign and could require use of additional extraction chambers on-chip, the operation of a magnet for magnetic bead control during extraction, and additional space/containers serving as extraction buffer storage and waste deposits.
- Additional enzyme and reagent preservation methods could be studied to improve long-term storage of NASBA assays. The future of ocean monitoring relies on long-term deployment of sensors, and efficient storage of molecular reaction components is therefore imperative. Ideally, optimisation of a lyophilisation protocol would provide long-term stability, and improve reaction kinetic efficiency when compared to the preservation methods presented in this thesis.
- The LabCardReader IC-NASBA protocol presented in this study (Chapter 4) is a significant simplification of the original concept. However, lab-card failure still occurred on a regular

basis due to peristaltic pump inconsistency, or valve disks being stuck and blocking microfluidic channels. Syringe pumps may be a preferred alternative, as they offer increased flexibility and high-level analytical performance during long-term microfluidic system deployment (Beaton et al. 2012; Nightingale et al. 2015). Furthermore the use of alternative materials for valve disk preparation may prevent channel blockage more effectively.

- Automated quantification analysis of NASBA results on the LabCardReader graphical user interface would allow for real *in situ* detection and quantification of marine microorganisms. The software accompanying the LabCardReader should complete TTP and quantitation variable analysis for every sample, at the end of each IC-NASBA protocol.

6.2.3 Sample collection and preparation

- *In-situ* environmental application of the portable filtration system (presented in Chapter 5) has to be tested. Clogging of the filter is a commonly expected problem when processing environmental samples, as they can be rich in particles and debris of various sizes. The incorporation of different-sized meshes in the systems sample input opening (see Figure 23) should be able to filter out larger particles before further sample concentration in the final filter, but their functionality has to be practically tested.
- Sample extraction/elution from the filter should be optimised and simplified. The system is easy to use and does not require a specialised skill set, but removal of the final concentrated sample from the filter, for IC-NASBA analysis, can be sometimes tricky, and exposes the user to harmful lysis buffers. It also is reliant on air to segment the flow and limit the lysis and elution volumes. This method would not work in submerged applications and alternatives must be developed for this application.
- Real *in-situ* monitoring of marine microorganisms could be attempted by coupling the portable filtration system with a LOC device. The LabCardReader currently lacks fully automated nucleic acid extraction, but future implementation would make such a study feasible.

Appendices

Appendix A

Presented in this section are supplementary images and figures associated with the preservation of NASBA reagents and enzymes via gelification (see Chapter 3). Note that gelification technology was initially used for the preservation of both enzyme and reagent master-mixtures. However, enzyme mastermix gelification led to the inactivation of NASBA enzymes, and thus enzyme mastermix preservation with disaccharides ensued.

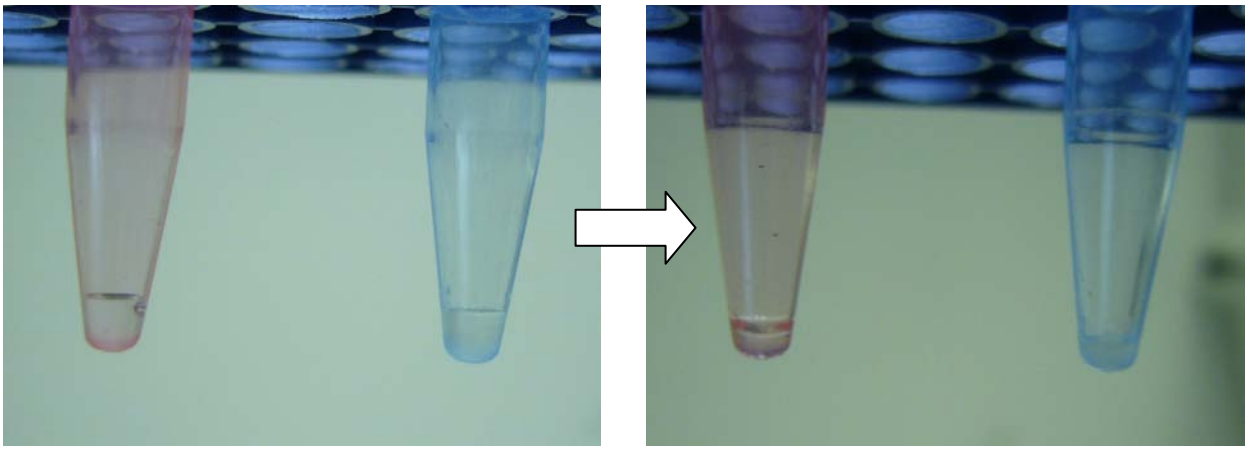

Figure A1 NASBA reagent and enzyme master-mixtures before (left) and after gelification (right). Mixtures were prepared and placed into sterile, RNase-free tubes as 10 µL aliquots. Gelification was completed after 60-minute incubations at 30ºC and 30 mbar. Red tube contains enzyme mastermix and blue tube contains reagent mastermix.

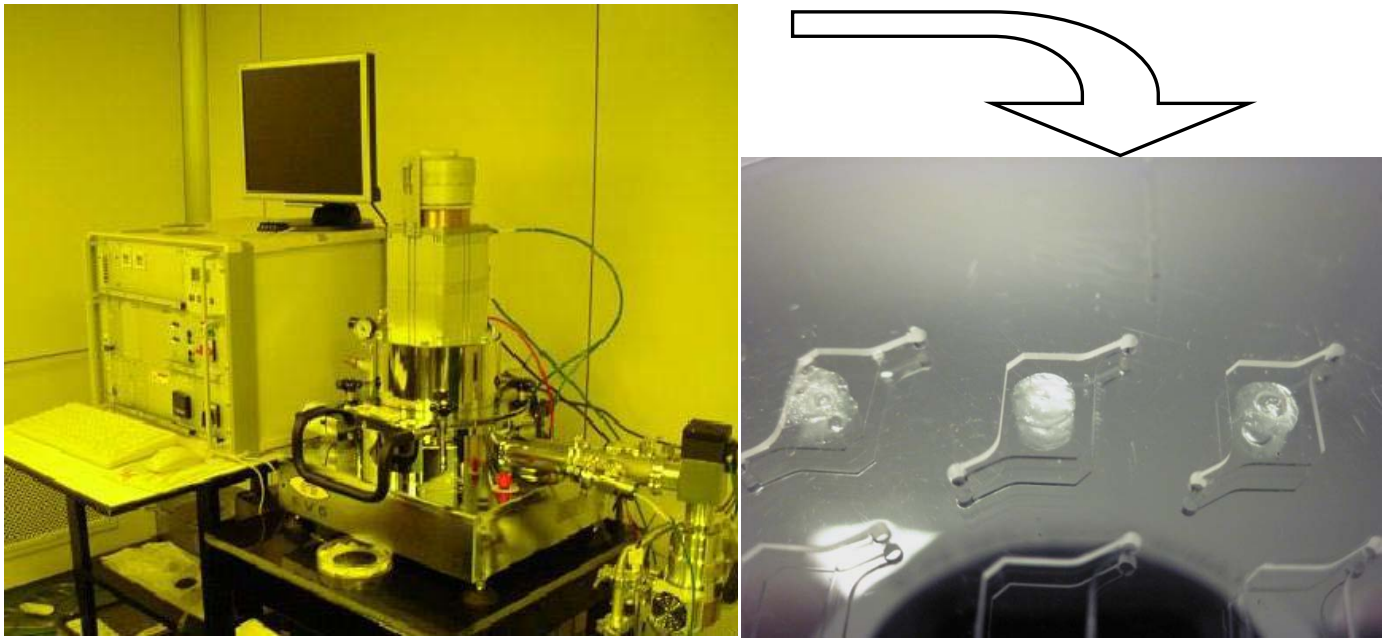

Figure A2 Illustrated are (left) an EVG501 bonding chamber used for NASBA reagent mastermix gelification on-chip, during experiments at EVGroup (Schärding Austria); (right) gelified NASBA reagent mastermix droplets (6.3 µL) in multiple on-chip chambers, after incubation in the EVG501 bonder at 35ºC, and 30 mbar, for 20 minutes.

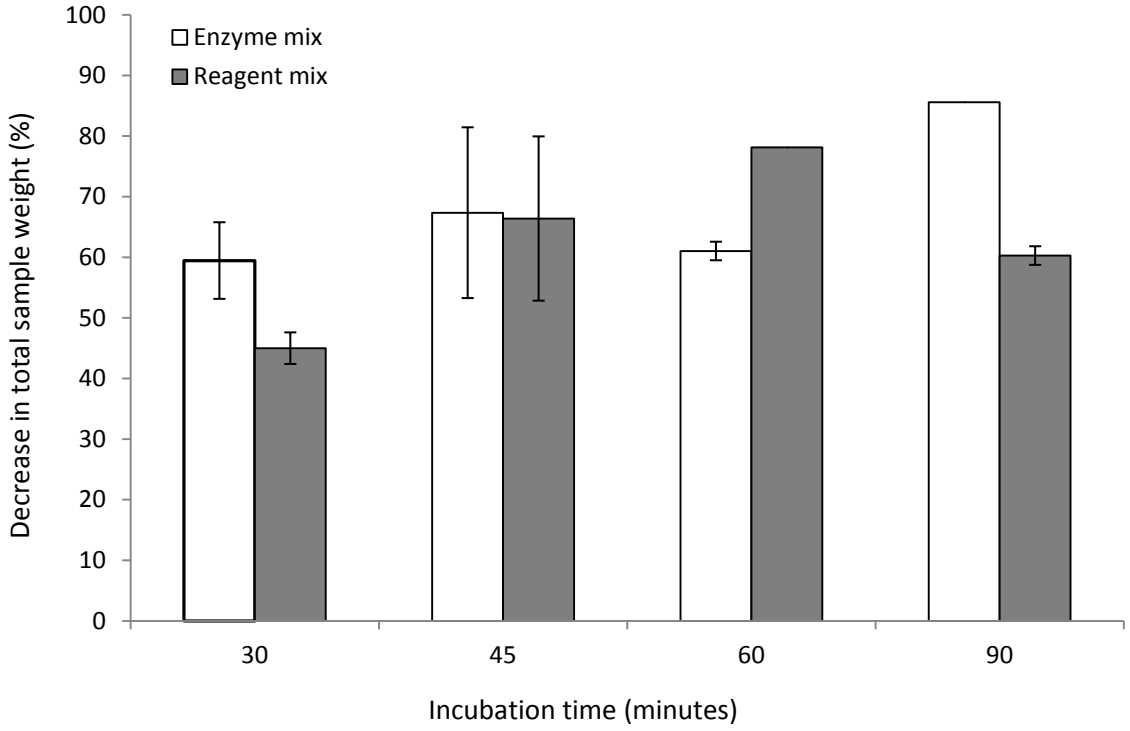

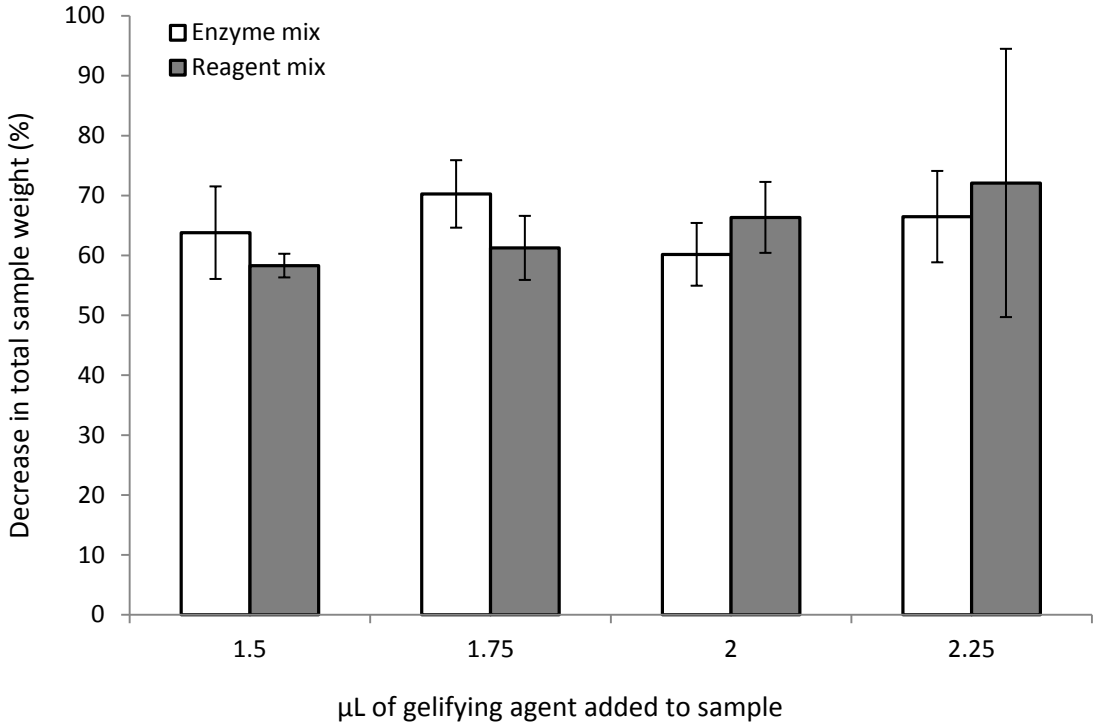

Figure A3 Presented are (top) weight loss percentages of 10 µL NASBA master-mixtures after gelification at different incubation times, at 30ºC, 30 mbar, and containing 1.5 µL gelifying agent; (bottom) weight loss percentages of 10 µL NASBA master-mixtures containing different volumes of gelifying agent, after gelification over 60 minutes at 30ºC and 30 mbar. White bars represent gelified enzyme master-mixtures and grey bars represent gelified reagent master-mixtures. Error bars denote one standard deviation of triplicate samples.

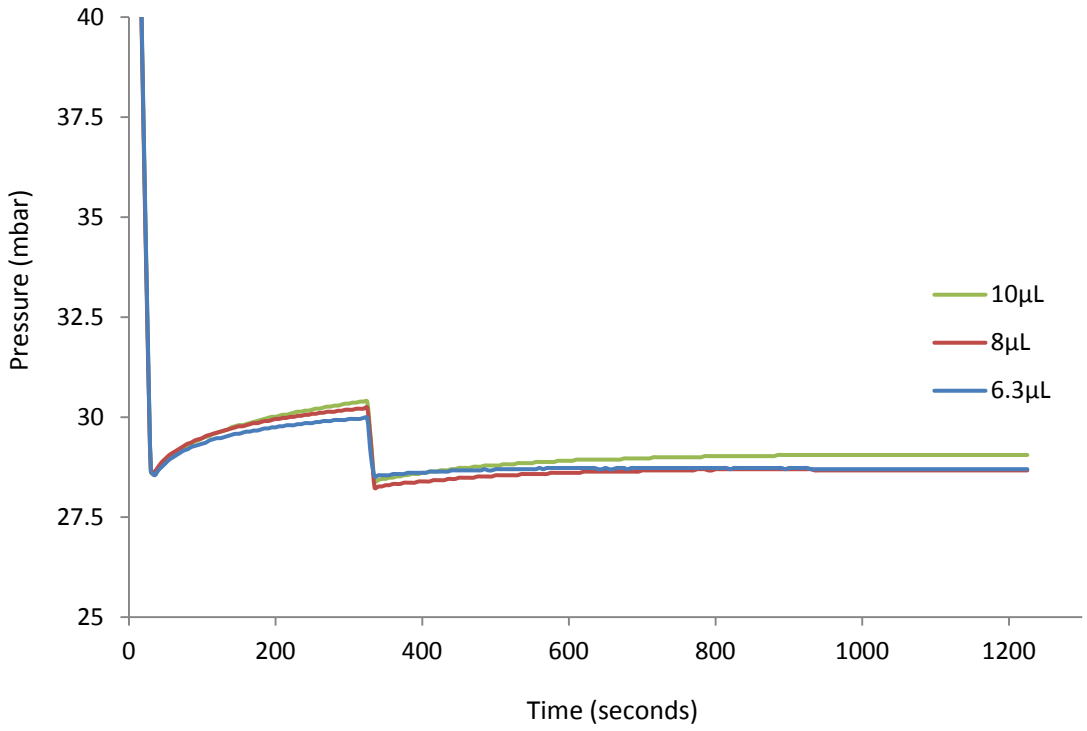

Figure A4 Changes in pressure during gelification of NASBA reagent master-mixtures at different original sample volumes, as measured within an EVG501 bonding chamber. Separate incubation runs were made using reagent mastermix droplets with volumes of 6.3 µL, 8 µL, and 10 µL. Droplets were dehydrated for 20 minutes, at 35ºC, and 30 mbar. As soon as pressure surpassed 30 mbar (due to sample dehydration) the EVG501 bonder vacuum pump was activated automatically, to restore target vacuum conditions.

Appendix B

Presented in this section are supplementary figures as taken from:

"Tsaloglou, M.N., Laouenan, F., Loukas, C.M., Monsalve, L.G., Thanner, C., Morgan, H., Ruano-López, J.M. and Mowlem, M.C., 2013. Real-time isothermal RNA amplification of toxic marine microalgae using preserved reagents on an integrated microfluidic platform. *Analyst*, 138(2), pp.593-602."

These figures where partially produced using data from early on-chip experiments, which formed a part of this PhD work.

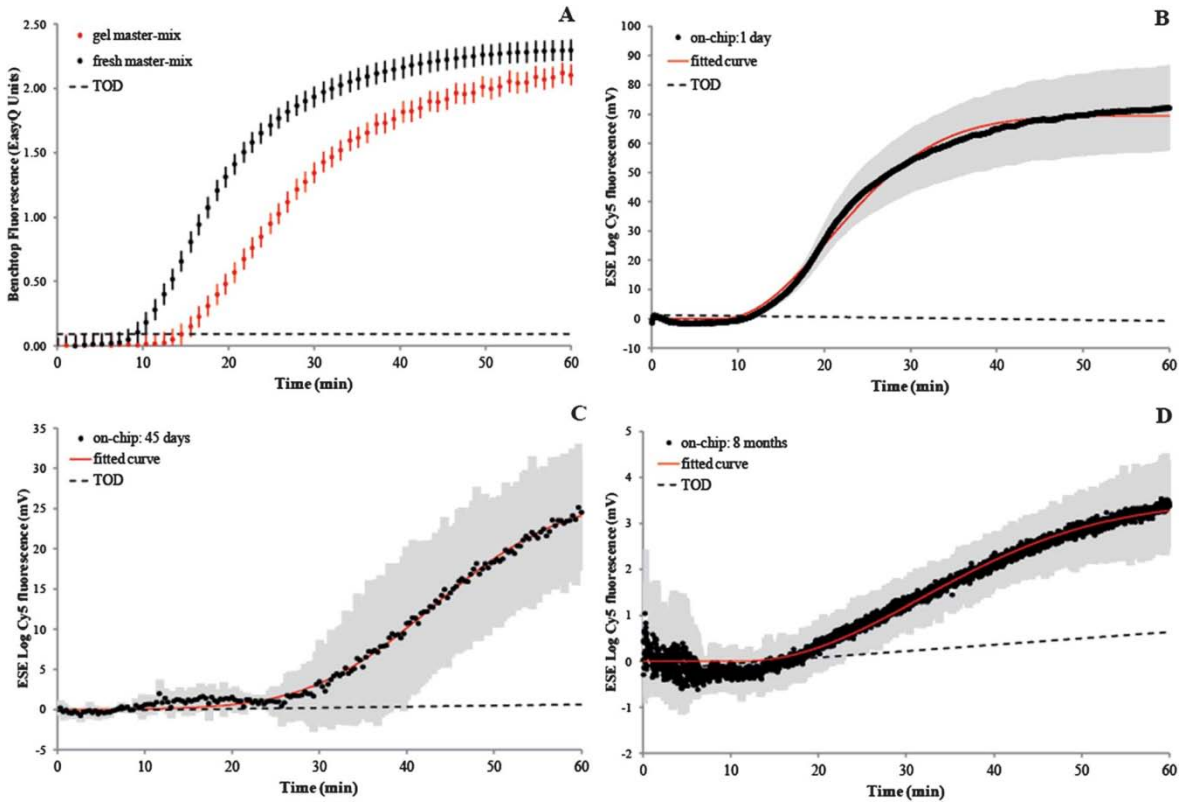

Fig. 7 NASBA results for 500 cell equivalents of K. brevis. (A) Bench-top NASBA showing the effect of gelation on the reaction kinetics. Black points show amplification using a fresh non-preserved reagent master-mix. Red points show amplification with the addition of gelator to the mix. Error bars denote one standard deviation of triplicate experiments (n = 3). The TOD (dashed line) was estimated as the average fluorescence of eight negative control amplification curves. (B) On-chip NASBA using preserved reagents one hour old (black line). The grey area represents one standard deviation of triplicate experiments (n = 3). The red line shows the fit from eqn (1), with ln(k1a1a2 2) = -5.032. The TOD (dashed line) indicates an on-chip NASBA negative control reaction. (C) On-chip NASBA using reagents preserved for 45 days (black points). The grey area represents one standard deviation of triplicate experiments (n ¼ 3). The red line shows the fit from eqn (1) with ln(k1a1a2 2) = -5.437. The TOD (dashed line) indicates an on-chip NASBA negative control reaction. (D) The same experiment with reagents preserved for 8 months (black line). The grey area represents one standard deviation of four replicate experiments (n ¼ 4). The red line shows the fit from eqn (1) with ln(k1a1a2 2) = -6.024. The TOD (dashed line) indicates an on-chip NASBA negative control reaction (Tsaloglou et al. 2013)

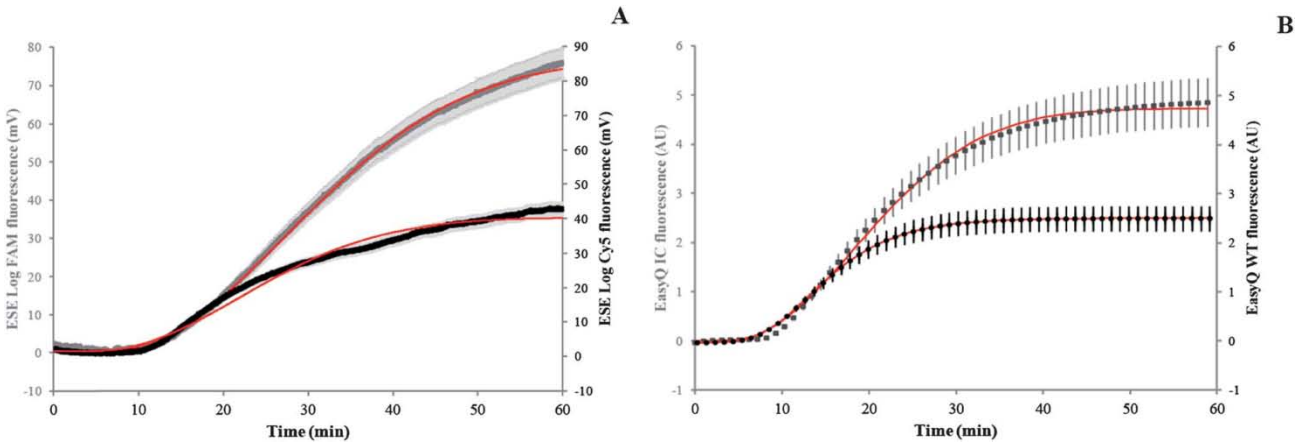

Fig. 8 NASBA results for 500 K. brevis cells and 400 IC copies (A) On-chip where the grey and black lines correspond to IC and K. brevis (WT) fluorescence amplification curves respectively. The grey shadow denotes 5 percent coefficient of variance. The red line is the fitted fluorescence curve. (B) The bench-top where the grey and black lines correspond to IC and K. brevis (WT) fluorescence amplification curves respectively. The error bars denote 10 percent coefficient of variance. The red line is the fitted fluorescence curve (Tsaloglou et al. 2013)

Appendix C

Presented in this section are the results of NASBA on filtered *K. brevis* samples (Chapter 5). Wild-type curves experienced an increase in fluorescence at approximately nine minutes before IC curves at 10^6 cells L^{-1}. The temporal gap decreased as cell concentration decreased, until at 10^4 cells L^{-1} amplification occurred at the same time. At lower concentrations, the wild-type and IC curve relationship was reversed, and the former became less prominent. Wild-type overall signal was at its lowest for the 10 cells L^{-1} samples and never surpassed 0.42 RFUs. Control samples followed a similar trend, however wild-type curve signal appeared to be stronger compared to filtered equivalents excluding control samples for 10^4 cells L^{-1} and 10^3 cells L^{-1}.

For instance, when plotting the IC-NASBA results of samples containing 10^5 cells (Figure 27) it is apparent that the slope difference between WT-RNA and IC-RNA amplification is greater for the control. The filtered replicates show IC amplification approximately seven minutes after WT amplification, and IC maximum fluorescence is reached 15-20 minutes after the WT equivalent. In comparison, control replicates experience an amplification lag which is less than five minutes, and IC reaches maximum fluorescence 10-15 minutes after the WT.

Initial NASBA results are indicative of a trend, where the relationship between wild-type and IC curves may reflect *K. brevis* concentration in filtered samples. Control samples agreed with the observed trend. However, they suggest that our sample collection system may not be as effective in preserving target RNA material as traditional laboratory extraction methods.

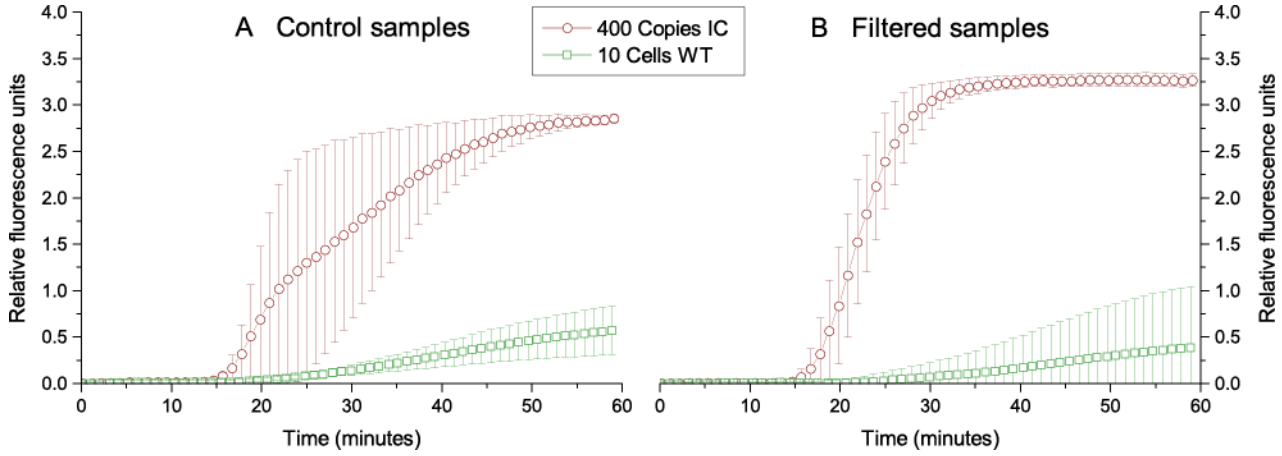

Fig C1 IC-NASBA results for 10 cell equivalents of *K. brevis* with 400 IC copies. The y-axis represents relative fluorescence units, as measured by the EasyQ benchtop incubator, and the x-axis represents time in minutes. WT-RNA amplification is shown as red squares and IC-RNA amplification is shown as green circles. Control samples are illustrated on the left whereas filtered samples are shown on the right. Error bars denote one standard deviation of triplicate samples.

Samples: (10 cells 400 IC)		Parameters						$\ln(k_1\alpha_1\alpha_2^2$ ratio)
		λ	α_2	α_3	$k_1\alpha_1$	Y_0	$k_1\alpha_1\alpha_2^2$	
Filtered sample 1	IC	6.260	0.4060	10.00	0.011920	0.631300	0.001965	-1.00292
	WT	2.980	0.2811	9.999	0.009121	0.655300	0.000721	
Filtered sample 2	IC	5.840	0.4931	10.00	0.013770	0.635900	0.003348	-0.90722
	WT	1.520	0.1574	9.999	0.054550	0.640100	0.001352	
Filtered sample 3	IC	6.240	1.2830	10.00	0.011060	0.565700	0.018206	-2.75922
	WT	2.610	0.4492	9.999	0.005715	0.615100	0.001153	
Control sample 1	IC	5940	1.3920	10.00	0.011080	0.000425	0.021469	-0.82766
	WT	10340	1.6630	10.00	0.003393	0.000148	0.009384	
Control sample 2	IC	8664	1.8010	9.999	0.003647	0.000292	0.011829	-1.17979
	WT	3972	0.5477	9.457	0.012120	0.000361	0.003636	
Control sample 3	IC	15860	2.1140	9.999	0.001605	0.000142	0.007173	-1.55819
	WT	3765	0.7612	7.489	0.002606	0.000294	0.001510	

Table C1 Fitting parameters from MATLAB curve fitting tool for the IC-NASBA curves, for the 10 cells per litre samples shown in figure B1.

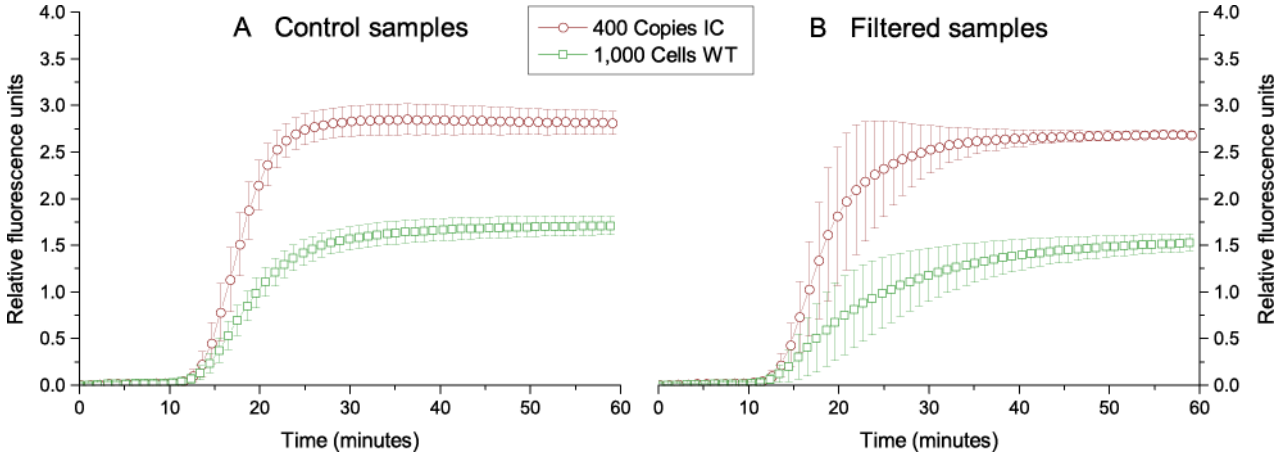

Fig C2 IC-NASBA results for 1000 cell equivalents of *K. brevis* with 400 IC copies. The y-axis represents relative fluorescence units, as measured by the EasyQ benchtop incubator, and the x-axis represents time in minutes. WT-RNA amplification is shown as red squares and IC-RNA amplification is shown as green circles. Control samples are illustrated on the left whereas filtered samples are shown on the right. Error bars denote one standard deviation of triplicate samples.

Samples: (10^3 cells 400 IC)		Parameters						ln($k_1\alpha_1\alpha_2^2$ ratio)
		λ	α_2	α_3	$k_1\alpha_1$	Y_0	$k_1\alpha_1\alpha_2^2$	
Filtered sample 1	IC	281.50	0.4993	6.2990	0.02353	0.00945	0.005866	0.086349
	WT	453.20	0.2212	8.0280	0.13070	0.003184	0.006395	
Filtered sample 2	IC	369.00	0.7066	6.3100	0.03067	0.00734	0.015313	0.030323
	WT	175.70	1.163	7.7840	0.01167	0.008983	0.015784	
Filtered sample 3	IC	365.70	0.5854	6.1090	0.03727	0.007464	0.012772	-0.983622
	WT	44.01	0.9396	9.2370	0.00541	0.03233	0.004776	
Control sample 1	IC	359.50	0.5458	5.9690	0.03689	0.008155	0.010989	0.141806
	WT	286.90	0.8774	8.4400	0.01645	0.005967	0.012664	
Control sample 2	IC	348.90	0.6378	6.2450	0.03638	0.008444	0.014799	-0.091057
	WT	409.50	0.2561	8.0740	0.20600	0.004265	0.013511	
Control sample 3	IC	375.30	0.5529	6.0860	0.03757	375.3	0.011485	0.162982
	WT	61.13	1.3380	9.2920	0.007551	0.02581	0.013518	

Table C2 Fitting parameters from MATLAB curve fitting tool for the IC-NASBA curves for the 1000 cells per litre samples shown in figure B2.

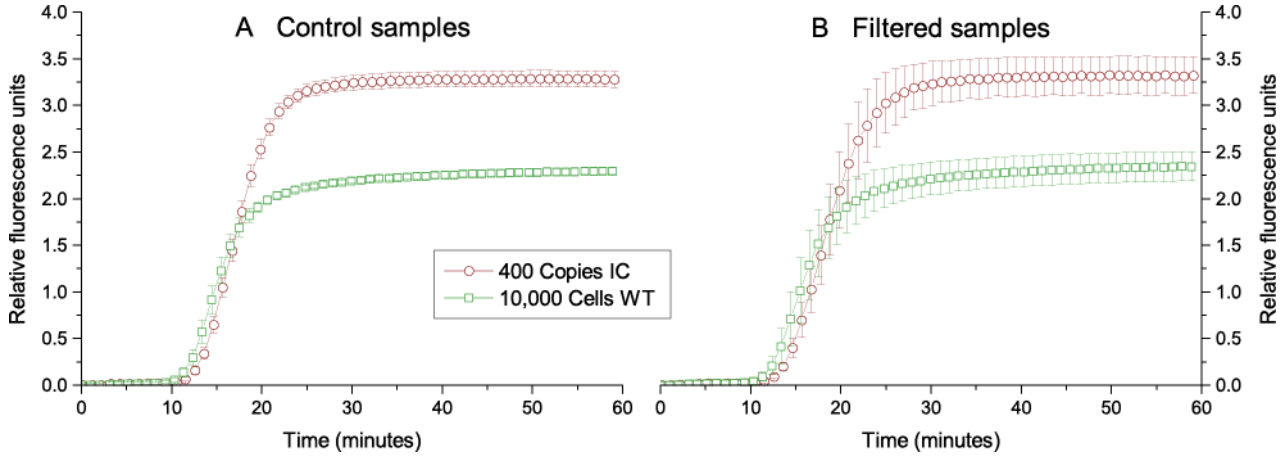

Fig C3 IC-NASBA results for 10^4 cell equivalents of *K. brevis* with 400 IC copies. The y-axis represents relative fluorescence units, as measured by the EasyQ benchtop incubator, and the x-axis represents time in minutes. WT-RNA amplification is shown as red squares and IC-RNA amplification is shown as green circles. Control samples are illustrated on the left whereas filtered samples are shown on the right. Error bars denote one standard deviation of triplicate samples.

Samples: (10^4 cells 400 IC)		Parameters						ln($k_1\alpha_1\alpha_2^2$ ratio)
		λ	α_2	α_3	$k_1\alpha_1$	Y_0	$k_1\alpha_1\alpha_2^2$	
Filtered sample 1	IC	404.90	0.5180	5.3090	0.03861	0.008185	0.01036	0.460322
	WT	379.50	0.6784	5.5260	0.03567	0.006078	0.016416	
Filtered sample 2	IC	364.40	0.5043	5.7280	0.03733	0.006078	0.009494	0.170938
	WT	381.80	0.5549	5.0770	0.03658	0.006393	0.011263	
Filtered sample 3	IC	278.10	0.7360	8.4010	0.02194	0.01136	0.011885	-0.26619
	WT	349.90	0.5931	5.1530	0.02589	0.006278	0.009107	
Control sample 1	IC	322.40	0.7337	6.7110	0.02664	0.01048	0.014341	-0.07121
	WT	289.40	0.7566	5.4980	0.02333	0.007886	0.013355	
Control sample 2	IC	385.80	0.5787	5.8420	0.03756	0.008457	0.012579	0.34479
	WT	332.50	0.7614	5.7510	0.03063	0.006802	0.017757	
Control sample 3	IC	520.30	0.5379	5.2980	0.03658	0.006322	0.010584	0.321254
	WT	407.70	0.6632	5.5100	0.03318	0.005513	0.014594	

Table C3 Fitting parameters from MATLAB curve fitting tool for the IC-NASBA curves, for the 10^4 cells per litre samples shown in figure B3.

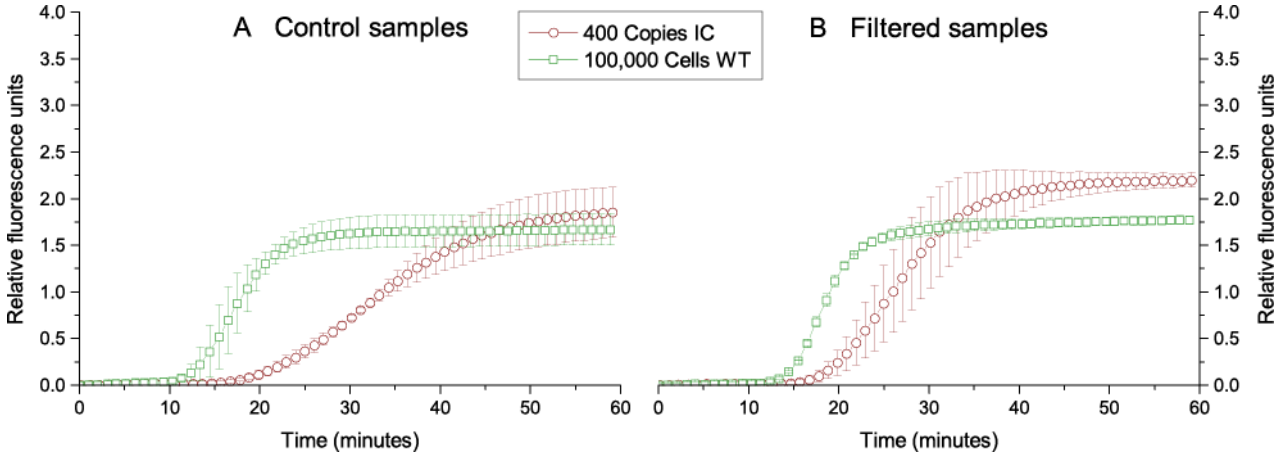

Fig C4 IC-NASBA results for 10^5 cell equivalents of *K. brevis* with 400 IC copies. The y-axis represents relative fluorescence units, as measured by the EasyQ benchtop incubator, and the x-axis represents time in minutes. WT-RNA amplification is shown as red squares and IC-RNA amplification is shown as green circles. Control samples are illustrated on the left whereas filtered samples are shown on the right. Error bars denote one standard deviation of triplicate samples.

Samples: (10^5 cells 400 IC)		Parameters						ln($k_1\alpha_1\alpha_2^2$ ratio)
		λ	α_2	α_3	$k_1\alpha_1$	Y_0	$k_1\alpha_1\alpha_2^2$	
Filtered sample 1	IC	182.30	0.4608	9.6350	0.01445	0.012410	0.003068	1.181421
	WT	589.50	0.2355	6.1260	0.18030	0.002913	0.009999	
Filtered sample 2	IC	457.10	0.3233	6.4730	0.03494	0.005127	0.003652	1.306314
	WT	332.40	0.7162	8.2660	0.02629	0.005420	0.013485	
Filtered sample 3	IC	319.50	0.5583	8.6840	0.02086	0.007078	0.006502	0.667333
	WT	259.10	0.7717	7.8750	0.02128	0.006723	0.012673	
Control sample 1	IC	747.40	0.2840	7.8630	0.02228	0.003127	0.001797	2.297944
	WT	250.50	1.0180	9.3160	0.01726	0.007209	0.017887	
Control sample 2	IC	499.10	0.3162	7.9250	0.02093	0.004294	0.002093	1.804174
	WT	169.90	0.7366	7.8300	0.02343	0.009628	0.012713	
Control sample 3	IC	649.80	0.3560	6.0370	0.01694	0.002569	0.002147	2.022114
	WT	462.60	0.2338	5.2200	0.29670	0.003335	0.016218	

Table C4 Fitting parameters from MATLAB curve fitting tool for the IC-NASBA curves, for the 10^5 cells per litre samples shown in figure B4.

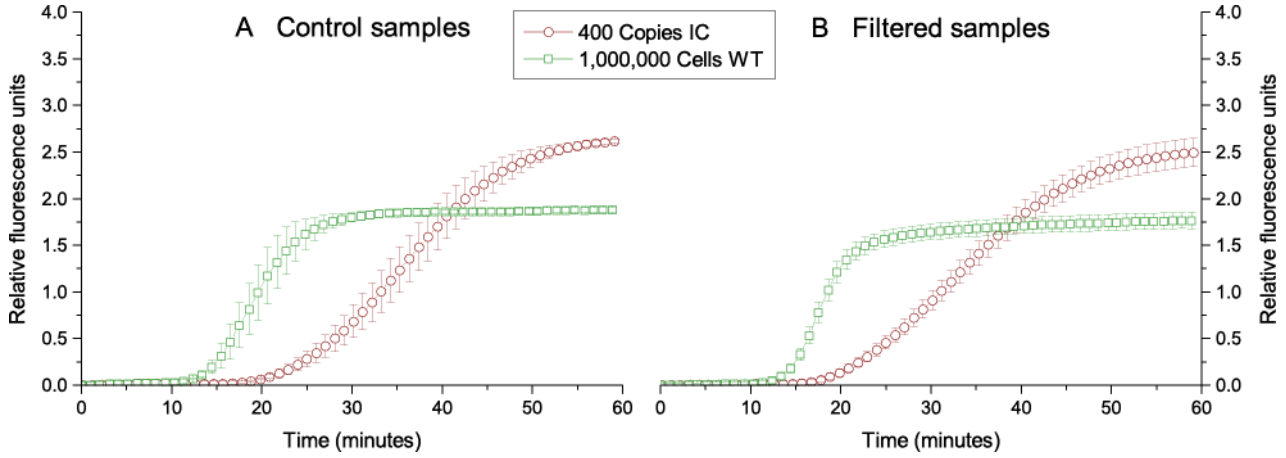

Fig C5 IC-NASBA results for 10^6 cell equivalents of *K. brevis* with 400 IC copies. The y-axis represents relative fluorescence units, as measured by the EasyQ benchtop incubator, and the x-axis represents time in minutes. WT-RNA amplification is shown as red squares and IC-RNA amplification is shown as green circles. Control samples are illustrated on the left whereas filtered samples are shown on the right. Error bars denote one standard deviation of triplicate samples.

Samples: (10^6 cells 400 IC)		Parameters						$\ln(k_1\alpha_1\alpha_2^2$ ratio)
		λ	α_2	α_3	$k_1\alpha_1$	Y_0	$k_1\alpha_1\alpha_2^2$	
Filtered sample 1	IC	728.70	0.3213	7.7470	0.01568	0.004295	0.001619	1.615885
	WT	521.70	0.4551	4.3650	0.03933	0.003502	0.008146	
Filtered sample 2	IC	1180.0	0.2517	5.4080	0.02655	0.002400	0.001682	1.940101
	WT	348.30	0.6181	6.7320	0.03064	0.004876	0.011706	
Filtered sample 3	IC	1988.0	0.3124	7.9890	0.01518	0.001479	0.001481	1.847718
	WT	333.10	0.5625	5.9550	0.02971	0.005112	0.009400	
Control sample 1	IC	101.20	0.3795	9.3570	0.01345	0.030770	0.001937	1.81542
	WT	452.10	0.6594	7.1420	0.02737	0.004193	0.011901	
Control sample 2	IC	1322.0	0.2766	8.5780	0.01636	0.002704	0.001252	2.188127
	WT	439.70	0.5606	6.7830	0.03552	0.004379	0.011163	
Control sample 3	IC	1115.0	0.3089	9.6020	0.01182	0.003244	0.001128	1.968202
	WT	354.10	0.5508	7.7520	0.02661	0.005178	0.008073	

Table C5 Fitting parameters from MATLAB curve fitting tool for the IC-NASBA curves, for the 10^6 cells per litre samples shown in figure B5.

List of References

Ahlford, Annika, et al. (2010), 'Dried reagents for multiplex genotyping by tag-array minisequencing to be used in microfluidic devices', *Analyst,* 135 (9), 2377-85.

Alberts, Bruce, et al. (2013), *Essential cell biology* (4 edn.: Garland Science).

Andersen, Morten Ø., et al. (2008), 'Delivery of siRNA from lyophilized polymeric surfaces', *Biomaterials,* 29 (4), 506-12.

Anderson, Donald M. (1998), 'Physiology and bloom dynamics of toxic *Alexandrium* species with emphasis on life cycle transitions', *Physiological Ecology of Harmful Algal Blooms*.

Anderson, Donald M., Glibert, Patricia M., and Burkholder, Joann M. (2002), 'Harmful algal blooms and eutrophication: Nutrient sources, composition, and consequences', *Estuaries,* 25 (4), 704-26.

Anderson, Donald M., Cembella, Allan D., and Hallegraeff, Gustaaf M. (2012a), 'Progress in understanding harmful algal blooms: Paradigm shifts and new technologies for research, monitoring, and management', *Annual Review of Marine Science,* 4 (1), 143-76.

Anderson, Donald M., et al. (2012b), 'The globally distributed genus *Alexandrium*: Multifaceted roles in marine ecosystems and impacts on human health', *Harmful Algae,* 14, 10-35.

Andrinolo, Darío, Michea, Luis F., and Lagos, Néstor (1999), 'Toxic effects, pharmacokinetics and clearance of saxitoxin, a component of paralytic shellfish poison (PSP), in cats', *Toxicon,* 37 (3), 447-64.

Arakawa, Tsutomu, et al. (2001), 'Factors affecting short-term and long-term stabilities of proteins', *Advanced Drug Delivery Reviews,* 46 (1-3), 307-26.

Arff, Johanne and Martin-Miguez, Belen (2016), 'Marine microalgae and harmful algal blooms: A European perspective', in Maria-Nefeli Tsaloglou (ed.), *Microaglae: Current Research and Applications* (1: Caister Academic Press).

Arya, Manit, et al. (2005), 'Basic principles of real-time quantitative PCR', *Expert Review of Molecular Diagnostics,* 5 (2), 209-19.

Ashworth, Justin, et al. (2013), 'Genome-wide diel growth state transitions in the diatom *Thalassiosira pseudonana*', *Proceedings of the National Academy of Sciences,* 110 (18), 7518-23.

Astrid, Tischler, Margit, Egg, and Leopold, Füreder (2015), 'Ethanol: A simple and effective RNA-preservation for freshwater insects living in remote habitats', *Limnology and Oceanography: Methods*, 186–95.

Backer, Lorraine C., et al. (2015), 'Cyanobacteria and algae blooms: Review of health and environmental data from the Harmful Algal Bloom-Related Illness Surveillance System (HABISS) 2007–2011', *Toxins,* 7 (4), 1048-64.

Baden, Daniel G. and Mende, Thomas J. (1978), 'Glucose transport and metabolism in *Gymnodinium breve*', *Phytochemistry,* 17 (9), 1553-58.

Bean, Judy A., et al. (2011), 'Florida red tide toxins (brevetoxins) and longitudinal respiratory effects in asthmatics', *Harmful Algae,* 10 (6), 744-48.

Beaton, Alexander D., et al. (2012), 'Lab-on-chip measurement of nitrate and nitrite for *in situ* analysis of natural waters', *Environmental Science and Technology,* 46 (17), 9548-56.

Berensmeier, Sonja (2006), 'Magnetic particles for the separation and purification of nucleic acids', *Applied Microbiology and Biotechnology,* 73 (3), 495-504.

Berg, Brandon, et al. (2015), 'Cellphone-based hand-held microplate reader for point-of-care testing of enzyme-linked immunosorbent assays', *ACS Nano,* 9 (8), 7857-66.

Berrade, Luis, Garcia, Angie, and Camarero, Julio (2011), 'Protein microarrays: Novel developments and applications', *Pharmaceutical Research,* 28 (7), 1480-99.

Blondeau-Patissier, David, et al. (2014), 'A review of ocean color remote sensing methods and statistical techniques for the detection, mapping and analysis of phytoplankton blooms in coastal and open oceans', *Progress In Oceanography,* 123, 123-44.

Bonnin, R. A. and Bouloc, Philippe (2015), 'RNA degradation in *Staphylococcus aureus*: Diversity of ribonucleases and their impact', *International Journal of Genomics,* 2015, 12.

Boom, R., et al. (1990), 'Rapid and simple method for purification of nucleic acids', *Journal of Clinical Microbiology,* 28 (3), 495-503.

Brenier-Pinchart, M. P., et al. (2014), 'Usefulness of pan-fungal NASBA test for surveillance of environmental fungal contamination in a protected hematology unit', *Medical Mycology,* 52 (4), 433-37.

Bricelj, V. M., et al. (2012), 'Trophic transfer of brevetoxins to the benthic macrofaunal community during a bloom of the harmful dinoflagellate *Karenia brevis* in Sarasota Bay, Florida', *Harmful Algae,* 16 (0), 27-34.

Brody, J. P. and Yager, P. (1997), 'Diffusion-based extraction in a microfabricated device', *Sensors and Actuators A: Physical,* 58 (1), 13-18.

Brooks, Elizabeth M., Sheflin, Lowell G., and Spaulding, Stephen W. (1995), 'Secondary structure in the 3'UTR of EGF and the choice of reverse transcriptases affect the detection of message diversity by RT-PCR', *Biotechniques,* 19 (5), 806-12, 14-5.

Burton, R. S. (1996), 'Molecular tools in marine ecology', *Journal of Experimental Marine Biology and Ecology,* 200 (1-2), 85-101.

Bustin, S. A. (2000), 'Absolute quantification of mRNA using real-time reverse transcription polymerase chain reaction assays', *Journal of Molecular Endocrinology,* 25 (2), 169-93.

Carpenter, John F., et al. (1997), 'Rational design of stable lyophilized protein formulations: Some practical advice', *Pharmaceutical Research,* 14 (8), 969-75.

Carvalho, Gustavo A., et al. (2010), 'Satellite remote sensing of harmful algal blooms: A new multi-algorithm method for detecting the Florida red tide (Karenia brevis)', *Harmful Algae,* 9 (5), 440-48.

Casper, Erica T., et al. (2004), 'Detection and quantification of the red tide dinoflagellate *Karenia brevis* by real-time Nucleic Acid Sequence-Based Amplification', *Applied and Environmental Microbiology,* 70 (8), 4727-32.

Casper, Erica T., et al. (2005), 'Development and evaluation of a method to detect and quantify enteroviruses using NASBA and internal control RNA (IC-NASBA)', *Journal of Virological Methods,* 124 (1-2), 149-55.

Casper, Erica T., et al. (2007), 'A handheld NASBA analyzer for the field detection and quantification of *Karenia brevis*', *Harmful Algae,* 6 (1), 112-18.

Cembella, Allan D. and Rafuse, Cheryl (2010), 'Chapter 7 The filter—transfer—freeze method for quantitative phytoplankton analysis', *Microscopic and Molecular Methods for Quantitative Phytoplankton Analysis* (55: Intergovernmental Oceanographic Commission UNESCO), 41-46.

Cheung, Timothy K. W., et al. (2010), 'Evaluation of novel H1N1-specific primer-probe sets using commercial RT-PCR mixtures and a premixed reaction stored in a lyophilized format', *Journal of Virological Methods,* 165 (2), 302-04.

Chuprina, VP, et al. (1991), 'Molecular dynamics simulation of the hydration shell of a B-DNA decamer reveals two main types of minor-groove hydration depending on groove width', *Proceedings of the National Academy of Sciences,* 88 (2), 593-97.

Clark, D.P. (2005), *Molecular biology* (Elsevier Academic Press) 784.

Compton, J. (1991), 'Nucleic acid sequence-based amplification', *Nature,* 350, 91-92.

Costa, Rodrigo, et al. (2004), 'An optmized protocol for simultaneous extraction of DNA and RNA from soils', *Brazilian Journal of Microbiology,* 35, 230-34.

Croft, Martin T., Warren, Martin J., and Smith, Alison G. (2006), 'Algae need their vitamins', *Eukaryotic Cell,* 5 (8), 1175-83.

Crowe, John H., Carpenter, John F., and Crowe, Lois M. (1998), 'The role of vitrification in anhydrobiosis', *Annual Review of Physiology,* 60 (1), 73-103.

Davidson, Keith, Tett, Paul, and Gowen, Richard (2011), 'Chapter 4 Harmful Algal Blooms', *Marine Pollution and Human Health* (The Royal Society of Chemistry), 95-127.

de la Rosa, Laura A., et al. (2001), 'Modulation of cytosolic calcium levels of human lymphocytes by yessotoxin, a novel marine phycotoxin', *Biochemical Pharmacology,* 61 (7), 827-33.

De Regge, N., et al. (2012), 'Detection of Schmallenberg virus in different *Culicoides* spp. by real-time RT-PCR', *Transboundary and Emerging Diseases,* 59 (6), 471-75.

Deguo, Wang, et al. (2008), 'Drawback of loop-mediated isothermal amplification', *African Journal of Food Science,* 2, 083-86.

Deiman, Birgit, van Aarle, Pierre, and Sillekens, Peter (2002), 'Characteristics and applications of nucleic acid sequence-based amplification (NASBA)', *Molecular Biotechnology,* 20 (2), 163-79.

Deiman, Birgit, et al. (2008), 'Efficient amplification with NASBA of hepatitis B virus, herpes simplex virus and methicillin resistant *Staphylococcus aureus* DNA', *Journal of Virological Methods,* 151 (2), 283-93.

Delaney, Jennifer A., Ulrich, Robert M., and Paul, John H. (2011), 'Detection of the toxic marine diatom *Pseudo-nitzschia* multiseries using the RuBisCO small subunit (*rbcS*) gene in two real-time RNA amplification formats', *Harmful Algae,* 11 (0), 54-64.

Delattre, Cyril, et al. (2012), 'Macro to microfluidics system for biological environmental monitoring', *Biosensors and Bioelectronics,* 36 (1), 230-35.

DeLong, Edward F., Wickham, Gene S., and Pace, Norman R. (1989), 'Phylogenetic stains: Ribosomal RNA-based probes for the identification of single cells', *Science,* 243 (4896), 1360-63.

Dimov, Ivan K., et al. (2011), 'Integrated microfluidic array plate (iMAP) for cellular and molecular analysis', *Lab on a Chip,* 11 (16), 2701-10.

Dimov, Ivan K., et al. (2008), 'Integrated microfluidic tmRNA purification and real-time NASBA device for molecular diagnostics', *Lab on a Chip,* 8 (12), 2071-78.

Dooms, Stefania, et al. (2007), 'Denaturing gradient gel electrophoresis (DGGE) as a tool for the characterisation of *Brachionus* sp. strains', *Aquaculture,* 262 (1), 29-40.

Doucette, Gregory J., et al. (2009), 'Remote, subsurface detection of the algal toxin domoic acid onboard the Environmental Sample Processor: Assay development and field trials', *Harmful Algae,* 8 (6), 880-88.

Eckert, Catherine, et al. (2014), 'Molecular test based on isothermal helicase-dependent amplification for detection of the *Clostridium difficile* toxin A gene', *Journal of Clinical Microbiology,* 52 (7), 2386-89.

Edler, Lars and Elbrächter, Malte (2010), 'Chapter 2 The Utermöhl method for quantitative phytoplankton analysis', *Microscopic and Molecular Methods for Quantitative Phytoplankton Analysis* (55: Intergovernmental Oceanographic Commission UNESCO), 13-20.

Errera, Reagan M. and Campbell, Lisa (2011), 'Osmotic stress triggers toxin production by the dinoflagellate *Karenia brevis*', *Proceedings of the National Academy of Sciences,* 108 (26), 10597-601.

Fabro, Elena, et al. (2016), 'Distribution of *Dinophysis* species and their association with lipophilic phycotoxins in plankton from the Argentine Sea', *Harmful Algae,* 59, 31-41.

Fang, Wei-Feng and Lee, Abraham P. (2015), 'LCAT pump optimization for an integrated microfluidic droplet generator', *Microfluidics and Nanofluidics,* 18 (5-6), 1265-75.

Fang, Xiaohong, et al. (2002), 'Molecular beacons', *Cell Biochemistry and Biophysics,* 37 (2), 71-81.

Faron, Matthew L., et al. (2015), 'Detection of group A *Streptococcus* in pharyngeal swab specimens by use of the AmpliVue GAS isothermal helicase-dependent amplification assay', *Journal of Clinical Microbiology,* 53 (7), 2365-67.

Ferrante, Margherita, et al. (2013), 'Harmful algal blooms in the Mediterranean Sea: Effects on human health', *EuroMediterranean Biomedical Journal,* 8 (6), 25-34.

Ferre, F. (1992), 'Quantitative or semi-quantitative PCR: Reality versus myth', *Genome Research,* 2 (1), 1-9.

Flaherty, Kerry and Landsberg, Jan (2011), 'Effects of a persistent red tide (*Karenia brevis*) bloom on community structure and species-specific relative abundance of nekton in a Gulf of Mexico estuary', *Estuaries and Coasts,* 34 (2), 417-39.

Fleming, Lora E., et al. (2011), 'Review of Florida red tide and human health effects', *Harmful Algae,* 10 (2), 224-33.

Flock, Stephane, Labarbe, Rudi, and Houssier, Claude (1996), 'Dielectric constant and ionic strength effects on DNA precipitation', *Biophysical journal,* 70 (3), 1456.

Fox, Karen Celia (1995), 'Putting proteins under glass', *Science,* 267 (5206), 1922-23.

Frank, Ronald (2002), 'The SPOT-synthesis technique: Synthetic peptide arrays on membrane supports—principles and applications', *Journal of Immunological Methods,* 267 (1), 13-26.

Franks, Felix and Auffret, Tony (2008), *Freeze-drying of pharmaceuticals and biopharmaceuticals* (royal Society of Chemistry).

Freytes, D. O., et al. (2008), 'Hydrated versus lyophilized forms of porcine extracellular matrix derived from the urinary bladder', *Journal of Biomedical Materials Research Part A,* 87 (4), 862-72.

Fukuba, Tatsuhiro, et al. (2011a), 'A microfluidic *in situ* analyzer for ATP quantification in ocean environments', *Lab on a Chip*, 3508-15.

Fukuba, Tatsuhiro, et al. (2011b), 'Integrated *in situ* genetic analyzer for microbiology in extreme environments', *RSC Advances,* 1 (8), 1567-73.

FWRI 'Red Tide Current Status', *Florida Fish and Wildlife Conservation Commission* <http://myfwc.com/research/redtide/statewide/>, accessed 28 Oct 2015.

Fykse, Else M., et al. (2012), 'Real-time PCR and NASBA for rapid and sensitive detection of *Vibrio cholerae* in ballast water', *Marine Pollution Bulletin,* 64 (2), 200-06.

Gadanho, Mário and Sampaio, José Paulo (2004), 'Application of temperature gradient gel electrophoresis to the study of yeast diversity in the estuary of the Tagus river, Portugal', *FEMS Yeast Research,* 5 (3), 253-61.

Gan, NanQin, et al. (2010), 'Quantitative assessment of toxic and nontoxic *Microcystis* colonies in natural environments using fluorescence *in situ* hybridization and flow cytometry', *SCIENCE CHINA Life Sciences,* 53 (8), 973-80.

Garcia, Elena, et al. (2004), 'Controlled microfluidic reconstitution of functional protein from an anhydrous storage depot', *Lab on a Chip,* 4 (1), 78-82.

Gates, Jean A. and Wilson, William B. (1960), 'The toxicity of *Gonyaulax monilata* Howell to *Mugil cephalus*', *Limnology and Oceanography,* 5 (2), 171-74.

Gómez, F. (2012), 'A checklist and classification of living dinoflagellates (Dinoflagellata, Alveolata)', *Cicimar Oceánides,* 27 (1), 65-140.

Gonzalez, Santiago F., et al. (2004), 'Simultaneous detection of marine fish pathogens by using multiplex PCR and a DNA microarray', *Journal of Clinical Microbiology,* 42 (4), 1414-19.

Grattan, Lynn M., Holobaugh, Sailor, and Morris Jr, J. Glenn (2016), 'Harmful algal blooms and public health', *Harmful Algae,* 57, Part B, 2-8.

Gray, M., et al. (2003), 'Molecular detection and quantitation of the red tide dinoflagellate *Karenia brevis* in the marine environment', *Applied and Environmental Microbiology,* 69 (9), 5726-30.

Hallegraeff, Gustaaf M. (2010), 'Ocean climate change, phytoplankton community responses, and harmful algal blooms: A formidable predictive challenge', *Journal of Phycology,* 46 (2), 220-35.

Hallegraeff, Gustaaf M., Anderson, D. M., and Cembella, Allan D. (eds.) (2003), *Manual on harmful marine microalgae* (Monographs on Oceanographic Methodology, 33; Paris: Unesco).

Hallett, Chris S., et al. (2015), 'Effects of a harmful algal bloom on the community ecology, movements and spatial distributions of fishes in a microtidal estuary', *Hydrobiologia*, 1-18.

Hardison, D. Ransom, et al. (2013), 'Increased toxicity of *Karenia brevis* during phosphate limited growth: Ecological and evolutionary implications', *PLoS ONE,* 8 (3), e58545.

Hardison, D. Ransom, et al. (2014), 'Increased cellular brevetoxins in the red tide dinoflagellate *Karenia brevis* under CO_2 limitation of growth rate: Evolutionary implications and potential effects on bloom toxicity', *Limnology and Oceanography,* 59 (2), 560-77.

Haywood, Allison J., et al. (2004), 'Comparative morphology and molecular phylogenetic analysis of three new species of the genus *Karenia* (Dinophyceae) from New Zealand', *Journal of Phycology,* 40 (1), 165-79.

Heid, C. A., et al. (1996), 'Real time quantitative PCR', *Genome Research,* 6 (10), 986-94.

Henson, Joan M. and French, Roy C. (1993), 'The polymerase chain reaction and plant disease diagnosis', *Annual Review of Phytopathology,* 31, 81-109.

Hitzbleck, Martina and Delamarche, Emmanuel (2013), 'Reagents in microfluidics: An 'in'and 'out'challenge', *Chemical Society Reviews,* 42 (21), 8494-516.

Hoagland, P., et al. (2002), 'The economic effects of harmful algal blooms in the United States: Estimates, assessment issues, and information needs', *Estuaries,* 25 (4), 819-37.

Hoek, Ingrid, Tho, Febly, and Arnold, W. Mike (2010), 'Sodium hydroxide treatment of PDMS based microfluidic devices', *Lab on a Chip,* 10 (17), 2283-85.

Hoffmann, Jochen, et al. (2010), 'Pre-storage of liquid reagents in glass ampoules for DNA extraction on a fully integrated lab-on-a-chip cartridge', *Lab on a Chip,* 10 (11), 1480-84.

Hofmann, Martin A. and Mader, Markus (2015), 'Comparison of various commercial products for phenol-guanidine-based classical swine fever virus RNA extraction', *African Journal of Biotechnology,* 13 (42), 4100-04.

Holinger, Eric P., et al. (2014), 'Molecular analysis of point-of-use municipal drinking water microbiology', *Water Research,* 49 (0), 225-35.

Holland, P. M., et al. (1991), 'Detection of specific polymerase chain reaction product by utilizing the 5'----3' exonuclease activity of *Thermus aquaticus* DNA polymerase', *Proceedings of the National Academy of Sciences of the United States of America,* 88 (16), 7276-80.

Hsu, Chung C., et al. (1995), 'Surface denaturation at solid-void interface—a possible pathway by which opalescent participates form during the storage of lyophilized tissue-type plasminogen activator at high temperatures', *Pharmaceutical Research,* 12 (1), 69-77.

Huang, Yushi, et al. (2015), 'Integrated microfluidic technology for sub-lethal and behavioral marine ecotoxicity biotests', *SPIE Microtechnologies* (International Society for Optics and Photonics), 95180F-80F-10.

Humbert, J., Quiblier, C., and Gugger, M. (2010), 'Molecular approaches for monitoring potentially toxic marine and freshwater phytoplankton species', *Analytical and Bioanalytical Chemistry,* 397 (5), 1723-32.

Ishida, Ken-ichiro and Green, Beverley R. (2002), 'Second-and third-hand chloroplasts in dinoflagellates: Phylogeny of oxygen-evolving enhancer 1 (PsbO) protein reveals

replacement of a nuclear-encoded plastid gene by that of a haptophyte tertiary endosymbiont', *Proceedings of the National Academy of Sciences,* 99 (14), 9294-99.

Jellema, L. C., et al. (2009), 'Charge-based particle separation in microfluidic devices using combined hydrodynamic and electrokinetic effects', *Lab on a Chip,* 9 (13), 1914-25.

Jensen, Maria Hastrup and Daugbjerg, Niels (2009), 'Molecular phylogeny of selected species of the order Dinophysiales (Dinophyceae) - testing the hypothesis of a Dinophysioid radiation', *Journal of Phycology,* 45 (5), 1136-52.

Jeon, Hyeong Kyu, Kim, Kyu Heon, and Eom, Keeseon S. (2010), 'Molecular identification of *Taenia* specimens after long-term preservation in formalin', *Parasitology International,* 60 (2), 203-05.

Jeong, Heon-Ho, et al. (2014), 'Effect of temperature on biofilm formation by Antarctic marine bacteria in a microfluidic device', *Analytical Biochemistry,* 446, 90-95.

Jing, Hongmei, et al. (2010), 'Impact of mesozooplankton grazing on the microbial community revealed by denaturing gradient gel electrophoresis (DGGE)', *Journal of Experimental Marine Biology and Ecology,* 383 (1), 39-47.

Johnson, Zackary I. and Martiny, Adam C. (2015), 'Techniques for quantifying phytoplankton biodiversity', *Annual Review of Marine Science,* 7 (1), 299-324.

Jowhar, Dawit, et al. (2010), 'Open access microfluidic device for the study of cell migration during chemotaxis', *Integrative Biology,* 2 (11-12), 648-58.

Kadoya, Saori, et al. (2010), 'Freeze-drying of proteins with glass-forming oligosaccharide-derived sugar alcohols', *International Journal of Pharmaceutics,* 389 (1-2), 107-13.

Karlson, Bengt, et al. (2010), 'Chapter 1 Introduction to methods for quantitative phytoplankton analysis', *Microscopic and Molecular Methods for Quantitative Phytoplankton Analysis* (55: Intergovernmental Oceanographic Commission UNESCO), 5-12.

Kasper, Julia Christina and Friess, Wolfgang (2011), 'The freezing step in lyophilization: Physico-chemical fundamentals, freezing methods and consequences on process performance and quality attributes of biopharmaceuticals', *European Journal of Pharmaceutics and Biopharmaceutics,* 78 (2), 248-63.

Keeling, Patrick J., et al. (2014), 'The Marine Microbial Eukaryote Transcriptome Sequencing Project (MMETSP): Illuminating the functional diversity of eukaryotic life in the oceans through transcriptome sequencing', *PLoS Biology,* 12 (6), e1001889.

Kitagawa, Masanari, et al. (2006), 'Complete set of ORF clones of *Escherichia coli* ASKA library (a complete set of *E. coli* K-12 ORF archive): Unique resources for biological research', *DNA Research,* 12 (5), 291-99.

Kjeldsen, Kasper Urup, et al. (2010), 'Two types of endosymbiotic bacteria in the enigmatic marine worm *Xenoturbella*', *Applied and Environmental Microbiology*, AEM.01092-09.

Klamer, Morten, et al. (2002), 'Influence of elevated CO_2 on the fungal community in a coastal scrub oak forest soil investigated with terminal-restriction fragment length polymorphism analysis', *Applied and Environmental Microbiology,* 68 (9), 4370-76.

Kochzius, M., et al. (2008), 'DNA microarrays for identifying fishes', *Marine Biotechnology,* 10 (2), 207-17.

Kodadek, Thomas (2001), 'Protein microarrays: Prospects and problems', *Chemistry and Biology,* 8 (2), 105-15.

Kohli, Gurjeet S., et al. (2015), 'Polyketide synthesis genes associated with toxin production in two species of *Gambierdiscus* (Dinophyceae)', *BMC Genomics,* 16 (1), 410.

Koseki, Taihei, Kitabatake, Naofumi, and Doi, Etsushiro (1990), 'Freezing denaturation of ovalbumin at acid pH', *Journal of Biochemistry,* 107 (3), 389-94.

Kubista, Mikael, et al. (2009), 'The real-time polymerase chain reaction', *Molecular Aspects of Medicine,* 27 (2-3), 95-125.

Kudela, R. M., et al. (2010), 'Using the molecular toolbox to compare harmful algal blooms in upwelling systems', *Progress In Oceanography,* 85 (1-2), 108-21.

Kwon, Hyuck-Jin, et al. (2010), 'Lab-on-a-chip for field *Escherichia coli* assays: long-term stability of reagents and automatic sampling system', *Journal of the Association for Laboratory Automation,* 15 (3), 216-23.

LABONFOIL (2016), 'LABONFOIL Integrated Project', <http://www.labonfoil.eu/>, accessed 9 Feb.

Landsberg, J. H., Flewelling, L. J., and Naar, J. (2009), '*Karenia brevis* red tides, brevetoxins in the food web, and impacts on natural resources: Decadal advancements', *Harmful Algae,* 8 (4), 598-607.

LeBowitz, J. H. and McMacken, R. (1986), 'The *Escherichia coli* dnaB replication protein is a DNA helicase', *Journal of Biological Chemistry,* 261 (10), 4738-48.

Lee, Joung-Hyun, Kaplan, Jeffrey, and Lee, Woo (2008), 'Microfluidic devices for studying growth and detachment of *Staphylococcus epidermidis* biofilms', *Biomedical Microdevices,* 10 (4), 489-98.

Lee, Min Hwa, Cheon, Doo-Sung, and Choi, Changsun (2009), 'Molecular genotyping of *Anisakis* species from Korean sea fish by polymerase chain reaction-restriction fragment length polymorphism (PCR-RFLP)', *Food Control,* 20 (7), 623-26.

LeGresley, Murielle and McDermott, Georgina (2010), 'Chapter 4 Counting chamber methods for quantitative phytoplankton analysis—haemocytometer, Palmer-Maloney cell and Sedgewick-Rafter cell', *Microscopic and Molecular Methods for Quantitative Phytoplankton Analysis* (55: Intergovernmental Oceanographic Commission UNESCO), 25-30.

Lekan, Danelle K. and Tomas, Carmelo R. (2010), 'The brevetoxin and brevenal composition of three *Karenia brevis* clones at different salinities and nutrient conditions', *Harmful Algae,* 9 (1), 39-47.

Leone, Gionata, et al. (1998), 'Molecular beacon probes combined with amplification by NASBA enable homogeneous, real-time detection of RNA', *Nucleic Acids Research,* 26 (9), 2150-55.

Lewitus, Alan J., et al. (2012), 'Harmful algal blooms along the North American west coast region: History, trends, causes, and impacts', *Harmful Algae,* 19 (0), 133-59.

Ligler, Frances S., et al. (2007), 'The array biosensor: Portable, automated systems', *Analytical Sciences,* 23 (1), 5-10.

Lin, Zhang, et al. (2009), 'In-situ measurement of cellular microenvironments in a microfluidic device', *Lab on a Chip,* 9 (2), 257-62.

Liu, F., et al. (2014), 'A lab-on-chip cell-based biosensor for label-free sensing of water toxicants', *Lab on a Chip,* 14 (7), 1270-80.

Liu, Lusan, et al. (2013), 'Temporal and spatial distribution of red tide outbreaks in the Yangtze River Estuary and adjacent waters, China', *Marine Pollution Bulletin,* 72 (1), 213-21.

López-Legentil, Susanna, et al. (2010), 'Characterization and localization of a hybrid non-ribosomal peptide synthetase and polyketide synthase gene from the toxic dinoflagellate *Karenia brevis*', *Marine Biotechnology,* 12 (1), 32-41.

Lou, Jerry J., et al. (2014), 'A review of room temperature storage of biospecimen tissue and nucleic acids for anatomic pathology laboratories and biorepositories', *Clinical biochemistry,* 47 (4), 267-73.

Luna, Gian, et al. (2009), 'Archaeal diversity in deep-sea sediments estimated by means of different terminal-restriction fragment length polymorphisms (T-RFLP) protocols', *Current Microbiology,* 59 (3), 356-61.

Lutz, Sascha, et al. (2010), 'Microfluidic lab-on-a-foil for nucleic acid analysis based on isothermal recombinase polymerase amplification (RPA)', *Lab on a Chip,* 10 (7), 887-93.

MacBeath, Gavin (2002), 'Protein microarrays and proteomics', *Nature Genetics,* 32, 536-32.

MacBeath, Gavin and Schreiber, Stuart L. (2000), 'Printing proteins as microarrays for high-throughput function determination', *Science,* 289 (5485), 1760-63.

Madejon, A., Limones, G., and Carcelen, N. (2005), 'Gelification technology, an innovative approach to Real Time DNA amplifications, facilitating ease of use and automisation in research and diagnostics.', (Biotools B&M Labs, S.A. (Spain)).

Maerkl, Sebastian J. (2011), 'Next generation microfluidic platforms for high-throughput protein biochemistry', *Current Opinion in Biotechnology,* 22 (1), 59-65.

Magaña, Hugo A., Contreras, Cindy, and Villareal, Tracy A. (2003), 'A historical assessment of *Karenia brevis* in the western Gulf of Mexico', *Harmful Algae,* 2 (3), 163-71.

Mallmann, C., et al. (2010), 'Fluorescence *in situ* hybridization to improve the diagnosis of endocarditis: A pilot study', *Clinical Microbiology and Infection,* 16 (6), 767-73.

Mauk, Michael G., et al. (2015), 'Integrated microfluidic nucleic acid isolation, isothermal amplification, and amplicon quantification', *Microarrays,* 4 (4), 474-89.

Medina-Pons, F., Terrados, J., and Rosselló-Móra, R. (2008), 'Application of temperature gradient gel electrophoresis technique to monitor changes in the structure of the eukaryotic leaf-epiphytic community of *Posidonia oceanica*', *Marine Biology,* 155 (4), 451-60.

Medina-Pons, F., et al. (2009), 'Evaluation of the 18S rRNA clone library approach to study the diversity of the macroeukaryotic leaf-epiphytic community of the seagrass *Posidonia oceanica* (L.) Delile', *Marine Biology,* 156 (9), 1963-76.

Medlin, Linda (2013), 'Molecular tools for monitoring harmful algal blooms', *Environmental Science and Pollution Research,* 20 (10), 6683-85.

Melzak, Kathryn A., et al. (1996), 'Driving forces for DNA adsorption to silica in perchlorate solutions', *Journal of Colloid and Interface Science,* 181 (2), 635-44.

Milani, Ambra, et al. (2015), 'Development and application of a microfluidic *in situ* analyzer for dissolved Fe and Mn in natural waters', *Talanta,* 136, 15-22.

Miles, Christopher O., et al. (2005), 'Evidence for numerous analogs of yessotoxin in *Protoceratium reticulatum*', *Harmful Algae,* 4 (6), 1075-91.

Millet, Larry J., et al. (2007), 'Microfluidic devices for culturing primary mammalian neurons at low densities', *Lab on a Chip,* 7 (8), 987-94.

Moeseneder, Markus M., et al. (1999), 'Optimization of terminal-restriction fragment length polymorphism analysis for complex marine bacterioplankton communities and comparison with denaturing gradient gel electrophoresis', *Applied and Environmental Microbiology,* 65 (8), 3518-25.

Mollasalehi, H. and Yazdanparast, R. (2013), 'An improved non-crosslinking gold nanoprobe-NASBA based on 16S rRNA for rapid discriminative bio-sensing of major salmonellosis pathogens', *Biosensors and Bioelectronics,* 47, 231-36.

Monroe, Emily A., et al. (2010), 'Characterization and expression of nuclear-encoded polyketide synthases in brevetoxin-producing dinoflagellate *Karenia brevis*', *Journal of Phycology,* 46 (3), 541-52.

Moore, Melissa J. (2005), 'From birth to death: The complex lives of eukaryotic mRNAs', *Science,* 309 (5740), 1514-18.

Morel, F. M. M., et al. (1979), 'Aquil: A chemically defined phytoplankton culture medium for trace metal studies', *Journal of Phycology,* 15 (2), 135-41.

Morey, Jeanine, et al. (2011), 'Transcriptomic response of the red tide dinoflagellate, *Karenia brevis*, to nitrogen and phosphorus depletion and addition', *BMC Genomics,* 12 (1), 346.

Moter, Annette and Göbel, Ulf B. (2000), 'Fluorescence *in situ* hybridization (FISH) for direct visualization of microorganisms', *Journal of Microbiological Methods,* 41 (2), 85-112.

Motré, Aurélie, Kong, Richard, and Li, Ying (2011), 'Improving isothermal DNA amplification speed for the rapid detection of *Mycobacterium tuberculosis*', *Journal of Microbiological Methods,* 84 (2), 343-45.

Muller-McNicoll, Michaela and Neugebauer, Karla M. (2013), 'How cells get the message: Dynamic assembly and function of mRNA-protein complexes', *Nature Reviews Genetics,* 14 (4), 275-87.

Murata, Michio, et al. (1987), 'Isolation and structure of yessotoxin, a novel polyether compound implicated in diarrhetic shellfish poisoning', *Tetrahedron Letters,* 28 (47), 5869-72.

Muyzer, Gerard (1999), 'DGGE/TGGE a method for identifying genes from natural ecosystems', *Current Opinion in Microbiology,* 2 (3), 317-22.

Muyzer, Gerard and Smalla, Kornelia (1998), 'Application of denaturing gradient gel electrophoresis (DGGE) and temperature gradient gel electrophoresis (TGGE) in microbial ecology', *Antonie van Leeuwenhoek,* 73 (1), 127-41.

Nagy, Zoltán (2010), 'A hands-on overview of tissue preservation methods for molecular genetic analyses', *Organisms Diversity and Evolution,* 10 (1), 91-105.

Nightingale, Adrian M., Beaton, Alexander D., and Mowlem, Matthew C. (2015), 'Trends in microfluidic systems for *in situ* chemical analysis of natural waters', *Sensors and Actuators B: Chemical,* 221, 1398-405.

Nocker, Andreas, Burr, Mark, and Camper, Anne (2007), 'Genotypic microbial community profiling: A critical technical review', *Microbial Ecology,* 54 (2), 276-89.

Notomi, Tsugunori, et al. (2015), 'Loop-mediated isothermal amplification (LAMP): Principle, features, and future prospects', *Journal of Microbiology,* 53 (1), 1-5.

Notomi, Tsugunori, et al. (2000), 'Loop-mediated isothermal amplification of DNA', *Nucleic Acids Research,* 28 (12), e63.

Nubel, U., et al. (1996), 'Sequence heterogeneities of genes encoding 16S rRNAs in *Paenibacillus polymyxa* detected by temperature gradient gel electrophoresis', *Journal of Bacteriology,* 178 (19), 5636-43.

Nuwaysir, Emile F., et al. (2002), 'Gene expression analysis using oligonucleotide arrays produced by maskless photolithography', *Genome Research,* 12 (11), 1749-55.

Ogilvie, I. R. G., et al. (2010), 'Reduction of surface roughness for optical quality microfluidic devices in PMMA and COC', *Journal of Micromechanics and Microengineering,* 20 (6), 065016.

Okamura, Kei, et al. (2013), 'Development of a 128-channel multi-water-sampling system for underwater platforms and its application to chemical and biological monitoring', *Methods in Oceanography,* 8, 75-90.

Olsen, Gary J., et al. (1986), 'Microbial ecology and evolution: A ribosomal RNA approach', *Annual Reviews in Microbiology,* 40 (1), 337-65.

Ottesen, Elizabeth A., et al. (2014), 'Multispecies diel transcriptional oscillations in open ocean heterotrophic bacterial assemblages', *Science,* 345 (6193), 207-12.

Patist, Alex and Zoerb, Hans (2005), 'Preservation mechanisms of trehalose in food and biosystems', *Colloids and Surfaces B: Biointerfaces,* 40 (2), 107-13.

Patterson, Stacey S., et al. (2005), 'Increased precision of microbial RNA quantification using NASBA with an internal control', *Journal of Microbiological Methods,* 60 (3), 343-52.

Paz, Beatriz, et al. (2004), 'Production and release of yessotoxins by the dinoflagellates *Protoceratium reticulatum* and *Lingulodinium polyedrum* in culture', *Toxicon,* 44 (3), 251-58.

Paz, Beatriz, et al. (2008), 'Yessotoxins, a group of marine polyether toxins: An overview', *Marine Drugs,* 6 (2), 73.

Peers, Graham and Price, Neil M. (2006), 'Copper-containing plastocyanin used for electron transport by an oceanic diatom', *Nature,* 441 (7091), 341-44.

Peplies, Jörg, et al. (2004), 'Application and validation of DNA microarrays for the 16S rRNA-based analysis of marine bacterioplankton', *Environmental Microbiology,* 6 (6), 638-45.

Perlin, David S. and Zhao, Yanan (2009), 'Molecular diagnostic platforms for detecting *Aspergillus*', *Medical Mycology,* 47 (s1), S223-S32.

Pichard, Scott L, Frischer, Marc E, and Paul, John H (1993), 'Ribulose-bisphosphate carboxylase gene expression in subtropical marine phytoplankton populations', *Marine Ecology-Progress Series,* 101, 55-65.

Pichard, Scott L., et al. (1996), 'Regulation of ribulose bisphosphate carboxylase gene expression in natural phytoplankton communities. 1. Diel rhythms', *Marine Ecology-Progress Series,* 139, 257.

Pierce, Richard H. and Kirkpatrick, Gary J. (2001), 'Innovative techniques for harmful algal toxin analysis', *Environmental Toxicology and Chemistry,* 20 (1), 107-14.

Pierce, Richard H. and Henry, M. (2008), 'Harmful algal toxins of the Florida red tide (*Karenia brevis*): Natural chemical stressors in South Florida coastal ecosystems', *Ecotoxicology,* 17 (7), 623-31.

Polanyi, M. and Szabo, A. L. (1934), 'On the mechanism of hydrolysis. The alkaline saponifications of amyl acetate', *Transactions of the Faraday Society,* 30, 508-12.

Polstra, Abeltje, Goudsmit, J., and Cornelissen, M. (2002), 'Development of real-time NASBA assays with molecular beacon detection to quantify mRNA coding for HHV-8 lytic and latent genes', *BMC Infectious Diseases,* 2 (1), 18.

Price, Neil M., et al. (1989), 'Preparation and chemistry of the artificial algal culture medium Aquil', *Biological Oceanography,* 6 (5-6), 443-61.

Primrose, S. B. (1998), *Principles of genome analysis* (Blackwell Science).

Provasoli, L., McLaughlin, J. J. A., and Droop, M. R. (1957), 'The development of artificial media for marine algae', *Archives of Microbiology,* 25 (4), 392-428.

Rasmussen, Silas Anselm, et al. (2016), 'Chemical diversity, origin, and analysis of phycotoxins', *Journal of Natural Products,* 79 (3), 662-73.

Reguera, Beatriz, et al. (2012), 'Harmful *Dinophysis* species: A review', *Harmful Algae,* 14, 87-106.

Reich, Andrew, et al. (2015), 'Assessing the impact of shellfish harvesting area closures on neurotoxic shellfish poisoning (NSP) incidence during red tide (*Karenia brevis*) blooms', *Harmful Algae,* 43 (0), 13-19.

Ren, Ling, et al. (2009), 'Nutrient limitation on phytoplankton growth in the upper Barataria basin, Louisiana: Microcosm bioassays', *Estuaries and Coasts,* 32 (5), 958-74.

Rhodes, L., et al. (2006), 'Trace metal effects on the production of biotoxins by microalgae', *African Journal of Marine Science,* 28 (2), 393-97.

Rich, Virginia I., et al. (2011), 'Time-series analyses of Monterey Bay coastal microbial picoplankton using a 'genome proxy' microarray', *Environmental Microbiology,* 13 (1), 116-34.

Rolland, Jason P., et al. (2004), 'Solvent-resistant photocurable "liquid teflon" for microfluidic device fabrication', *Journal of the American Chemical Society,* 126 (8), 2322-23.

Root, David E., et al. (2006), 'Genome-scale loss-of-function screening with a lentiviral RNAi library', *Nature Methods,* 3 (9), 715-19.

Rosado, F.D.E.S., et al. (2002), 'Method for preparing stabilised reaction mixtures, whicha re totally or partially dried, comprising at least one enzyme, reaction mixtures and kits containing said mixtures', (WO Patent 2,002,072,002).

Saunders, J. B. deC. M. and Rice, A. H. (1944), 'A practical technique for preserving surgical and anatomical dissections', *The Journal of Bone & Joint Surgery,* 26 (1), 185-88.

Scala, David J. and Kerkhof, Lee J. (2000), 'Horizontal heterogeneity of denitrifying bacterial communities in marine sediments by terminal restriction fragment length polymorphism analysis', *Applied and Environmental Microbiology,* 66 (5), 1980-86.

Schochetman, Gerald, Ou, Chin-Yih, and Jones, Wanda K. (1988), 'Polymerase chain reaction', *The Journal of Infectious Diseases,* 158 (6), 1154-57.

Schofield, Oscar, Glenn, Scott, and Moline, Mark (2013), 'The robot ocean network', *American Scientist,* 101 (6), 434-41.

Scholin, C., et al. (2006), 'The Environmental Sample Processor (ESP) - an autonomous robotic device for detecting microorganisms remotely using molecular probe technology', *OCEANS 2006*, 1-4.

Schonhuber, W., et al. (1997), 'Improved sensitivity of whole-cell hybridization by the combination of horseradish peroxidase-labeled oligonucleotides and tyramide signal amplification', *Applied and Environmental Microbiology,* 63 (8), 3268-73.

Schumacher, Soeren, et al. (2012), 'Highly-integrated lab-on-chip system for point-of-care multiparameter analysis', *Lab on a Chip,* 12 (3), 464-73.

Schuppler, Markus, et al. (1998), '*In situ* identification of nocardioform actinomycetes in activated sludge using fluorescent rRNA-targeted oligonucleotide probes', *Microbiology,* 144 (1), 249-59.

Schütte, Ursel, et al. (2008), 'Advances in the use of terminal restriction fragment length polymorphism (T-RFLP) analysis of 16S rRNA genes to characterize microbial communities', *Applied Microbiology and Biotechnology,* 80 (3), 365-80.

Shepherd, N. S., et al. (1994), 'Preparation and screening of an arrayed human genomic library generated with the P1 cloning system', *Proceedings of the National Academy of Sciences,* 91 (7), 2629-33.

Shi, Xinguo, Zhang, Huan, and Lin, Senjie (2013), 'Tandem repeats, high copy number and remarkable diel expression rhythm of form II RuBisCO in *Prorocentrum donghaiense* (Dinophyceae)', *PLoS ONE,* 8 (8), e71232.

Sidoti, Francesca, et al. (2012), 'Development of a quantitative real-time Nucleic Acid Sequence-Based Amplification assay with an Internal Control using molecular beacon probes for selective and sensitive detection of human rhinovirus serotypes', *Molecular Biotechnology,* 50 (3), 221-28.

Simister, Rachel L., Schmitt, Susanne, and Taylor, Michael W. (2011), 'Evaluating methods for the preservation and extraction of DNA and RNA for analysis of microbial communities in marine sponges', *Journal of Experimental Marine Biology and Ecology,* 397 (1), 38-43.

Simms, D., Cizdziel, P.E., and Chomczynski, P. (1993), 'TRIzol: A new reagent for optimal single-step isolation of RNA', *Focus,* 15 (4), 99-102.

Siswanto, Eko, et al. (2013), 'Detection of harmful algal blooms of *Karenia mikimotoi* using MODIS measurements: A case study of Seto-Inland Sea, Japan', *Remote Sensing of Environment,* 129 (0), 185-96.

Smith, Alison G., et al. (2007), 'Plants need their vitamins too', *Current Opinion in Plant Biology,* 10 (3), 266-75.

Smith, E. Lester (1956), 'Vitamin B12', *British Medical Bulletin,* 12 (1), 52-56.

Smythe-Wright, Denise, et al. (2010), 'Spatio-temporal changes in the distribution of phytopigments and phytoplanktonic groups at the Porcupine Abyssal Plain (PAP) site', *Deep Sea Research Part II: Topical Studies in Oceanography,* 57 (15), 1324-35.

Spear, Russell N., et al. (1999), 'Quantitative imaging and statistical analysis of fluorescence *in situ* hybridization (FISH) of *Aureobasidium pullulans*', *Journal of Microbiological Methods,* 35 (2), 101-10.

Spreitzer, Robert J. and Salvucci, Michael E. (2002), 'RuBisCO: Structure, regulatory interactions, and possibilities for a better enzyme', *Annual Review of Plant Biology,* 53 (1), 449-75.

Stevens, Dean Y., et al. (2008), 'Enabling a microfluidic immunoassay for the developing world by integration of on-card dry reagent storage', *Lab on a Chip,* 8 (12), 2038-45.

Stewart, Peter R., Letham, D. S., and Adams, John Milton (1977), *The ribonucleic acids* (Springer).

Stoecker, Kilian, et al. (2010), 'Double labeling of oligonucleotide probes for fluorescence *in situ* hybridization (DOPE-FISH) improves signal intensity and increases rRNA accessibility', *Applied and Environmental Microbiology,* 76 (3), 922-26.

Streit, W. R. and Entcheva, P. (2003), 'Biotin in microbes, the genes involved in its biosynthesis, its biochemical role and perspectives for biotechnological production', *Applied Microbiology and Biotechnology,* 61 (1), 21-31.

Sugiyama, Akio, Nishiya, Yoshiaki, and Kawakami, Bunsei (2009), 'RNA polymerase mutants with increased thermostability', in Biomerieus B.V. (ed.), (US7507567 B2: Google Patents).

Suikkanen, Sanna, et al. (2013), 'Paralytic shellfish toxins or spirolides? The role of environmental and genetic factors in toxin production of the *Alexandrium ostenfeldii* complex', *Harmful Algae,* 26, 52-59.

Sun, Yi, et al. (2013), 'Pre-storage of gelified reagents in a lab-on-a-foil system for rapid nucleic acid analysis', *Lab on a Chip,* 13 (8), 1509-14.

Sunda, William G. and Huntsman, Susan A. (1995), 'Iron uptake and growth limitation in oceanic and coastal phytoplankton', *Marine Chemistry,* 50 (1-4), 189-206.

Sunda, William G., Price, Neil M., and Morel, F. M. M. (2005), 'Trace metal ion buffers and their use in culture studies', in R.A. Andersen (ed.), *Algal Culturing Techniques* (Amsterdam: Acad. Press/Elsevier).

Takishita, Kiyotaka, Nakano, Kouichirou, and Uchida, Aritsune (2000), 'Origin of the plastid in the anomalously pigmented dinoflagellate *Gymnodinium mikimotoi* (Gymnodiniales, Dinophyta) as inferred from phylogenetic analysis based on the gene encoding the large subunit of form I-type RuBisCO', *Phycological Research,* 48 (2), 85-89.

Tan, Siun Chee and Yiap, Beow Chin (2009), 'DNA, RNA, and protein extraction: The past and the present', *Journal of Biomedicine and Biotechnology,* 2009, 574398-98.

Tanaka, Hiroyuki, et al. (2014), 'Electrochemical sensor with dry reagents implemented in lab-on-chip for single nucleotide polymorphism detection', *Japanese Journal of Applied Physics,* 53 (5S1), 05FS03.

Templin, Markus F., et al. (2002), 'Protein microarray technology', *Trends in Biotechnology,* 20 (4), 160-66.

Thakur, Narsinh L., et al. (2008), 'Marine molecular biology: An emerging field of biological sciences', *Biotechnology Advances,* 26 (3), 233-45.

Thakuria, Dwipendra, et al. (2009), 'Field preservation and DNA extraction methods for intestinal microbial diversity analysis in earthworms', *Journal of Microbiological Methods,* 76 (3), 226-33.

Tsaloglou, Maria-Nefeli (2016), 'Microfluidics and *in situ* sensors for microalgae', in Maria-Nefeli Tsaloglou (ed.), *Microaglae: Current Research and Applications* (1: Caister Academic Press), 133-51.

Tsaloglou, Maria-Nefeli, et al. (2011), 'On-chip real-time nucleic acid sequence-based amplification for RNA detection and amplification', *Analytical Methods,* 3 (9), 2127-33.

Tsaloglou, Maria-Nefeli, et al. (2013), 'Real-time isothermal RNA amplification of toxic marine microalgae using preserved reagents on an integrated microfluidic platform', *Analyst,* 138 (2), 593-602.

Tsopela, A., et al. (2016), 'Development of a lab-on-chip electrochemical biosensor for water quality analysis based on microalgal photosynthesis', *Biosensors and Bioelectronics,* 79, 568-73.

Tubaro, A, et al. (1998), 'Occurrence of yessotoxin-like toxins in phytoplankton and mussels from northern Adriatic Sea', *Harmful Algae*, 470-72.

Tyagi, S. and Kramer, F.R. (1996), 'Molecular beacons: Probes that fluoresce upon hybridization', *Biotechnology,* 14 (3), pp. 303-08.

Ulrich, Robert M., et al. (2010), 'Detection and quantification of *Karenia mikimotoi* using real-time nucleic acid sequence-based amplification with internal control RNA (IC-NASBA)', *Harmful Algae,* 9 (1), 116-22.

Umar, L., Alexander, F. A., and Wiest, J. (2015), 'Application of algae-biosensor for environmental monitoring', *Engineering in Medicine and Biology Society (EMBC), 2015 37th Annual International Conference of the IEEE*, 7099-102.

Ussler III, William, et al. (2013), 'Autonomous application of quantitative PCR in the deep sea: *In situ* surveys of aerobic methanotrophs using the deep-sea environmental sample processor', *Environmental Science and Technology,* 47 (16), 9339-46.

Valiadi, Martha, et al. (2014), 'Molecular detection of bioluminescent dinoflagellates in surface waters of the Patagonian Shelf during early austral summer 2008', *PLoS ONE,* 9 (6), e98849.

Vallaeys, Tatiana, et al. (1997), 'Evaluation of denaturing gradient gel electrophoresis in the detection of 16S rDNA sequence variation in *Rhizobia* and methanotrophs', *FEMS Microbiology Ecology,* 24 (3), 279-85.

Valledor, Luis, et al. (2014), 'A universal protocol for the combined isolation of metabolites, DNA, long RNAs, small RNAs, and proteins from plants and microorganisms', *The Plant Journal,* 79 (1), 173-80.

Vallee, Bert L. and Auld, David S. (1990), 'Zinc coordination, function, and structure of zinc enzymes and other proteins', *Biochemistry,* 29 (24), 5647-59.

van Dam, Govert J., et al. (2013), 'A robust dry reagent lateral flow assay for diagnosis of active schistosomiasis by detection of *Schistosoma* circulating anodic antigen', *Experimental Parasitology,* 135 (2), 274-82.

van Dolah, Frances M., et al. (2007), 'Microarray analysis of diurnal- and circadian-regulated genes in the Florida red-tide dinoflagellate *Karenia brevis* (dinophyceae)', *Journal of Phycology,* 43 (4), 741-52.

Vargo, Gabriel A. (2009), 'A brief summary of the physiology and ecology of *Karenia brevis* Davis (G. Hansen and Moestrup comb. nov.) red tides on the West Florida Shelf and of hypotheses posed for their initiation, growth, maintenance, and termination', *Harmful Algae,* 8 (4), 573-84.

Vargo, Gabriel A., et al. (2008), 'Nutrient availability in support of *Karenia brevis* blooms on the central West Florida Shelf: What keeps *Karenia* blooming', *Continental Shelf Research,* 28 (1), 73-98.

Velve-Casquillas, Guilhem, et al. (2010), 'Microfluidic tools for cell biological research', *Nano Today,* 5 (1), 28-47.

Vincent, Myriam, Xu, Yan, and Kong, Huimin (2004), 'Helicase-dependent isothermal DNA amplification', *EMBO Rep,* 5 (8), 795-800.

Walker, John M., et al. (2005), 'Nucleic acid sequence-based amplification', *Medical Biomethods Handbook* (Humana Press), 273-91.

Wang, Da-Zhi (2008), 'Neurotoxins from marine dinoflagellates: A brief review', *Marine Drugs,* 6 (2), 349-71.

Wang, Wei (2000), 'Lyophilization and development of solid protein pharmaceuticals', *International Journal of Pharmaceutics,* 203 (1-2), 1-60.

Weis, John H., et al. (1992), 'Detection of rare mRNAs via quantitative RT-PCR', *Trends in Genetics,* 8 (8), 263-64.

Wendeberg, Annelie (2010), 'Fluorescence *in situ* hybridization for the identification of environmental microbes', *Cold Spring Harbor Protocols,* 2010 (1), pdb.prot5366.

Weusten, Jos J. A. M., et al. (2002), 'Principles of quantitation of viral loads using nucleic acid sequence-based amplification in combination with homogeneous detection using molecular beacons', *Nucleic Acids Research,* 30 (6), e26.

Whitesides, George M. (2006), 'The origins and the future of microfluidics', *Nature,* 442 (7101), 368-73.

Wu, Liyou, et al. (2008), 'Microarray-based characterization of microbial community functional structure and heterogeneity in marine sediments from the Gulf of Mexico', *Applied and Environmental Microbiology,* 74 (14), 4516-29.

Wu, Qing, et al. (2010), 'Fluorescence *in situ* hybridization rapidly detects three different pathogenic bacteria in urinary tract infection samples', *Journal of Microbiological Methods,* 83 (2), 175-78.

Wyman, Michael, et al. (2005), 'Dynamics of ribulose 1,5-bisphosphate carboxylase/oxygenase gene expression in the coccolithophorid *Coccolithus pelagicus* during a tracer release experiment in the Northeast Atlantic', *Applied and Environmental Microbiology,* 71 (3), 1659-61.

Yamahara, K. M., et al. (2015), 'Simultaneous monitoring of faecal indicators and harmful algae using an in-situ autonomous sensor', *Letters in Applied Microbiology,* 61 (2), 130-38.

Yasumoto, T., et al. (1985), 'Diarrhetic shellfish toxins', *Tetrahedron,* 41 (6), 1019-25.

Yoon, Jeong-Yeol and Kim, Bumsang (2012), 'Lab-on-a-chip pathogen sensors for food safety', *Sensors,* 12 (8), 10713-41.

Yu, Jr-Kai, et al. (2008), 'A cDNA resource for the cephalochordate amphioxus *Branchiostoma floridae*', *Development Genes and Evolution,* 218 (11), 723-27.

Zehr, J. P., Hewson, I., and Moisander, P. H. (2008), 'Molecular biology techniques and applications for ocean sensing', *Ocean Science,* 5 (2), 101-13.

Zhang, Baoyu, et al. (2010), 'Identification of two *Skeletonema costatum*-like diatoms by fluorescence *in situ* hybridization', *Chinese Journal of Oceanology and Limnology,* 28 (2), 310-14.

Zhao, Xinyan, et al. (2012), 'Compatible immuno-NASBA LOC device for quantitative detection of waterborne pathogens: Design and validation', *Lab on a Chip,* 12 (3), 602-12.

Zheng, Guo-xia, et al. (2014), 'Marine phytoplankton motility sensor integrated into a microfluidic chip for high-throughput pollutant toxicity assessment', *Marine Pollution Bulletin,* 84 (1), 147-54.

Zinser, Erik R., et al. (2009), 'Choreography of the transcriptome, photophysiology, and cell cycle of a minimal photoautotroph, *Prochlorococcus*', *PLoS ONE,* 4 (4), e5135.